Non-Equilibrium Master Equations

Vorlesung gehalten im Rahmen des GRK 1558
Wintersemester 2014/2015
Technische Universität Berlin

Dr. Gernot Schaller

February 12, 2015

Contents

This lecture aims at providing graduate students in physics and neighboring sciences with a heuristic approach to master equations. Although the focus of the lecture is on rate equations, their derivation will be based on quantum-mechanical principles, such that basic knowledge of quantum theory is mandatory. The lecture will try to be as self-contained as possible and aims at providing rather recipes than proofs.

As successful learning requires practice, a number of exercises will be given during the lecture, the solution to these exercises may be turned in in the next lecture (computer algebra may be used if applicable), for which students may earn points. Students having earned 50 % of the points at the end of the lecture are entitled to three ECTS credit points.

This script will be made available online at

http://wwwitp.physik.tu-berlin.de/~ schaller/.

In any first draft errors are quite likely, such that corrections and suggestions should be addressed to

gernot.schaller@tu-berlin.de.

I thank the many colleagues that have given valuable feedback to improve the notes, in particular Dr. Malte Vogl, Dr. Christian Nietner, and Prof. Dr. Enrico Arrigoni.

literature:

[1] Michael A. Nielsen and Isaac L. Chuang, *Quantum Computation and Quantum Information*, Cambridge University Press, Cambridge (2000).

[2] H.-P. Breuer and F. Petruccione, *The Theory of Open Quantum Systems*, Oxford University Press, Oxford (2002).

[3] H. M. Wiseman and G. J. Milburn, *Quantum Measurement and Control*, Cambridge University Press, Cambridge (2010).

[4] G. Lindblad, Communications in Mathematical Physics **48**, 119 (1976).

[5] G. Schaller, C. Emary, G. Kiesslich, and T. Brandes, Physical Review B **84**, 085418 (2011).

[6] G. Schaller and T. Brandes, Physical Review A **78**, 022106, (2008); G. Schaller, P. Zedler, and T. Brandes, *ibid.* A **79**, 032110, (2009).

[7] G. Schaller, *Open Quantum Systems Far from Equilibrium* Springer Lecture Notes in Physics **881**, Springer (2014).

Chapter 1

An introduction to Master Equations

1.1 Master Equations – A Definition

Many processes in nature are stochastic. In classical physics, this may be due to our incomplete knowledge of the system. Due to the unknown microstate of e.g. a gas in a box, the collisions of gas particles with the domain wall will appear random. In quantum theory, the evolution equations themselves involve amplitudes rather than observables in the lowest level, such that a stochastic evolution is intrinsic. In order to understand such processes in great detail, a description should include such random events via a probabilistic description. If the master equation is a system of linear ODEs $\dot{\boldsymbol{P}} = A\boldsymbol{P}$, we will call it **rate equation**.

Box 1 (Rate Equation) *A rate equation is a first order differential equation describing the time evolution of probabilities, e.g. for discrete events*

$$\frac{dP_k}{dt} = \sum_\ell \left[T_{k\ell}P_\ell - T_{\ell k}P_k\right] , \qquad \dot{\boldsymbol{P}} = T\boldsymbol{P} , \tag{1.1}$$

where the $T_{k\ell} > 0$ are transition rates between events ℓ and k. In matrix representation, this implies

$$T = \begin{pmatrix} -\sum_{i\neq 1} T_{i1} & T_{12} & \dots & T_{1N} \\ T_{21} & -\sum_{i\neq 2} T_{i2} & & T_{2N} \\ \vdots & & \ddots & \vdots \\ T_{N1} & \dots & \dots & -\sum_{i\neq N} T_{iN} \end{pmatrix} \tag{1.2}$$

The rate equation is said to satisfy **detailed balance**, when for the stationary state $T\bar{\boldsymbol{P}} = 0$ the equality $T_{k\ell}\bar{P}_\ell = T_{\ell k}\bar{P}_k$ holds for all pairs (k, ℓ) separately.

Furthermore, when the transition matrix $T_{k\ell}$ is symmetric, all processes are reversible at the level of the rate equation description.

Here, we will use the term **master equation** in more general terms describing any system of coupled ODEs for probabilities. This is more general than a rate equation, since, for example, the

Markovian quantum master equation does in general not only involve probabilities (diagonals of the density matrix) but also coherences (off-diagonals).

It is straightforward to show that rate equations conserve the total probability

$$\sum_k \frac{dP_k}{dt} = \sum_{k\ell} \left(T_{k\ell} P_\ell - T_{\ell k} P_k\right) = \sum_{k\ell} \left(T_{\ell k} P_k - T_{\ell k} P_k\right) = 0\,. \tag{1.3}$$

Beyond this, all probabilities must remain positive, which is also respected by a normal rate equation: Evidently, the solution of a rate equation is continuous, such that when initialized with valid probabilities $0 \leq P_i(0) \leq 1$ all probabilities are non-negative initially. Let us assume that after some time, the probability P_k it the first to approach zero (such that all others are non-negative). Its time-derivative is then always non-negative

$$\left.\frac{dP_k}{dt}\right|_{P_k=0} = +\sum_\ell T_{k\ell} P_\ell \geq 0\,, \tag{1.4}$$

which implies that $P_k = 0$ is repulsive, and negative probabilities are prohibited.

Finally, the probabilities must remain smaller than one throughout the evolution. This however follows immediately from $\sum_k P_k = 1$ and $P_k \geq 0$ by contradiction.

In conclusion, a rate equation of the form (1.1) automatically preserves the sum of probabilities and also keeps $0 \leq P_i(t) \leq 1$ – a valid initialization provided. That is, under the evolution of a rate equation, probabilities remain probabilities.

1.1.1 Example 1: Fluctuating two-level system

Let us consider a system of two possible events, to which we associate the time-dependent probabilities $P_0(t)$ and $P_1(t)$. These events could for example be the two conformations of a molecule, the configurations of a spin, the two states of an excitable atom, etc. To introduce some dynamics, let the transition rate from $0 \to 1$ be denoted by $T_{10} > 0$ and the inverse transition rate $1 \to 0$ be denoted by $T_{01} > 0$. The associated master equation is then given by

$$\frac{d}{dt}\begin{pmatrix} P_0 \\ P_1 \end{pmatrix} = \begin{pmatrix} -T_{10} & +T_{01} \\ +T_{10} & -T_{01} \end{pmatrix}\begin{pmatrix} P_0 \\ P_1 \end{pmatrix} \tag{1.5}$$

Exercise 1 (Temporal Dynamics of a two-level system) *(1 point)*
Calculate the solution of Eq. (1.5). What is the stationary state?

1.1.2 Example 2: Interacting quantum dots

Imagine a double quantum dot, where the Coulomb interaction energy is so large that the doubly occupied state can be omitted from the considerations. In essence, only three states remain. Let $|0\rangle$ denote the empty, $|L\rangle$ the left-occupied, and $|R\rangle$ the right-occupied states, respectively. Now assume the two quantum dots to be tunnel-coupled to adjacent reservoirs but not among themselves, such that particle transport between the dots is prohibited. The occupation of a dot tunnel-coupled to a junction with bare tunneling rate Γ will fluctuate depending on the Fermi level of the junction, see Fig. 1.1. In particular, if at time t the dot was empty, the probability to find

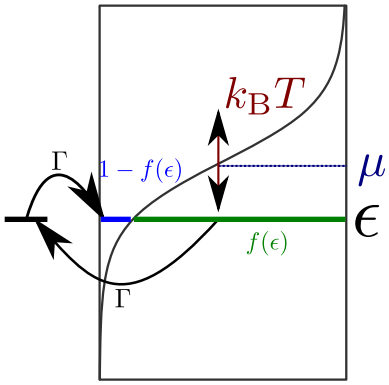

Figure 1.1: A single quantum dot coupled to a single junction, where the electronic occupation of energy levels is well approximated by a Fermi distribution.

an electron in the dot at time $t+\Delta t$ is roughly given by $\Gamma\Delta t f(\epsilon)$ with the Fermi function defined as

$$f(\omega) = \frac{1}{e^{\beta(\omega-\mu)}+1}, \tag{1.6}$$

where β denotes the inverse temperature and μ the chemical potential of the junction. The transition rate is thus given by the tunneling rate Γ multiplied by the probability to have an electron in the junction at the required energy ϵ ready to jump into the system. The inverse probability to find an initially filled dot empty reads $\Gamma\Delta t\,[1-f(\epsilon)]$, i.e., here one has to muliply the bare tunneling rate with the probability to have a free slot at energy ϵ in the junction. Applying this recipe to every dot separately we obtain for the total rate matrix

$$T = \Gamma_L \begin{pmatrix} -f_L & 1-f_L & 0 \\ +f_L & -(1-f_L) & 0 \\ 0 & 0 & 0 \end{pmatrix} + \Gamma_R \begin{pmatrix} -f_R & 0 & 1-f_R \\ 0 & 0 & 0 \\ +f_R & 0 & -(1-f_R) \end{pmatrix}. \tag{1.7}$$

In fact, a microscopic derivation can be used to confirm the above-mentioned assumptions, and the parameters f_α become the Fermi functions

$$f_\alpha = \frac{1}{e^{\beta_\alpha(\epsilon_\alpha-\mu_\alpha)}+1} \tag{1.8}$$

with inverse temperature β_α, chemical potentials μ_α, and dot level energy ϵ_α.

Exercise 2 (Detailed balance) *Determine whether the rate matrix (1.7) obeys detailed balance.*

1.1.3 Example 3: Diffusion Equation

Consider an infinite chain of coupled compartments as displayed in Fig. 1.2. Now suppose that along the chain, a molecule may move from one compartment to another with a transition rate T that is unbiased, i.e., symmetric in all directions. The evolution of probabilities obeys the

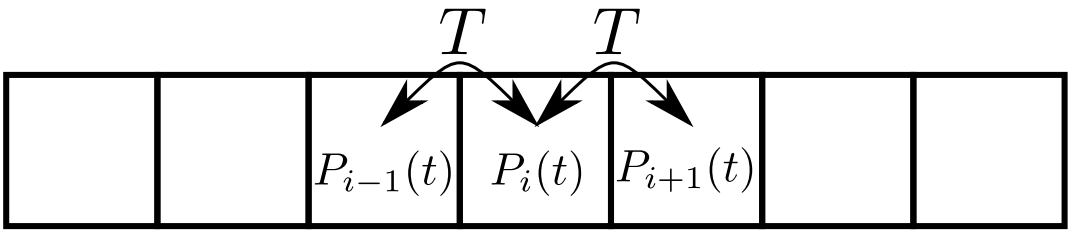

Figure 1.2: Linear chain of compartments coupled with a transition rate T, where only next neighbors are coupled to each other symmetrically.

infinite-size master equation

$$\begin{aligned} \dot{P}_i(t) &= TP_{i-1}(t) + TP_{i+1}(t) - 2TP_i(t) \\ &= T\Delta x^2 \frac{P_{i-1}(t) + P_{i+1}(t) - 2P_i(t)}{\Delta x^2} \,. \end{aligned} \tag{1.9}$$

We can introduce the probability density $\rho(x_i, t) = P_i(t)/\Delta x$, such that as $\Delta x \to 0$ and $T \to \infty$ in a way that $D = T\Delta x^2$ remains constant, we obtain the partial differential equation

$$\frac{\partial \rho(x,t)}{\partial t} = D\frac{\partial^2 \rho(x,t)}{\partial x^2} \qquad \text{with} \qquad D = T\Delta x^2 \,. \tag{1.10}$$

We note here that while the $P_i(t)$ describe (dimensionless) probabilities, $\rho(x,t)$ describes a time-dependent probability density (with dimension of inverse length).

Such diffusion equations are used to describe the distribution of chemicals in a soluble in the highly diluted limit, the kinetic dynamics of bacteria and further undirected transport processes. From our analysis of master equations, we can immediately conclude that the diffusion equation preserves positivity and total norm, i.e., $\rho(x,t) \geq 0$ and $\int_{-\infty}^{+\infty} \rho(x,t)dx = 1$. Note that it is straightforward to generalize the mapping between master equations and the diffusion equation to the higher-dimensional case.

One can now think of microscopic models where the hopping rates in different directions are not equal (drift) and may also depend on the position (spatially-dependent diffusion coefficient). A corresponding model (in next-neighbor approximation) would be given by

$$\dot{P}_i = T_{i,i-1}P_{i-1}(t) + T_{i,i+1}P_{i+1}(t) - (T_{i-1,i} + T_{i+1,i})P_i(t) \,, \tag{1.11}$$

where $T_{a,b}$ denotes the rate of jumping from b to a. An educated guess is given by the ansatz

$$\begin{aligned} \frac{\partial P}{\partial t} &= \frac{\partial^2}{\partial x^2}\left[A(x)P(x,t)\right] + \frac{\partial}{\partial x}\left[B(x)P(x,t)\right] \\ &\equiv \frac{A_{i-1}P_{i-1} - 2A_iP_i + A_{i+1}P_{i+1}}{\Delta x^2} + \frac{B_{i+1}P_{i+1} - B_{i-1}P_{i-1}}{2\Delta x} \\ &= \left[\frac{A_{i-1}}{\Delta x^2} - \frac{B_{i-1}}{2\Delta x}\right]P_{i-1} - \frac{2A_i}{\Delta x^2}P_i + \left[\frac{A_{i+1}}{\Delta x^2} + \frac{B_{i+1}}{2\Delta x}\right]P_{i+1} \,, \end{aligned} \tag{1.12}$$

which is equivalent to our master equation when

$$A_i = \frac{\Delta x^2}{2}\left[T_{i-1,i} + T_{i+1,i}\right] \,, \qquad B_i = \Delta x\left[T_{i-1,i} - T_{i+1,i}\right] \,. \tag{1.13}$$

We conclude that the Fokker-Planck equation

$$\frac{\partial \rho}{\partial t} = \frac{\partial^2}{\partial x^2}\left[A(x)\rho(x,t)\right] + \frac{\partial}{\partial x}\left[B(x)\rho(x,t)\right] \tag{1.14}$$

with $A(x) \geq 0$ preserves norm and positivity of the probability distribution $\rho(x,t)$.

Exercise 3 (Reaction-Diffusion Equation) *(1 point)*
Along a linear chain of compartments consider the master equation for two species

$$\begin{aligned} \dot{P}_i &= T\left[P_{i-1}(t) + P_{i+1}(t) - 2P_i(t)\right] - \gamma P_i(t)\,, \\ \dot{p}_i &= \tau\left[p_{i-1}(t) + p_{i+1}(t) - 2p_i(t)\right] + \gamma P_i(t), \end{aligned}$$

where $P_i(t)$ may denote the concentration of a molecule that irreversibly reacts with chemicals in the soluble to an inert form characterized by $p_i(t)$. To which partial differential equation does the master equation map?

In some cases, the probabilities may not only depend on the probabilities themselves, but also on external parameters, which appear then in the master equation. Here, we will use the term master equation for any equation describing the time evolution of probabilities, i.e., auxiliary variables may appear in the master equation.

1.2 Density Matrix Formalism

1.2.1 Density Matrix

Suppose one wants to describe a quantum system, where the system state is not exactly known. That is, there is an ensemble of known normalized states $\{|\Phi_i\rangle\}$, but there is uncertainty in which of these states the system is. Such systems can be conveniently described by the density matrix.

Box 2 (Density Matrix) *The density matrix can be written as*

$$\rho = \sum_i p_i \left|\Phi_i\right\rangle \left\langle\Phi_i\right|\,, \tag{1.15}$$

where $0 \leq p_i \leq 1$ denote the probabilities to be in the state $|\Phi_i\rangle$ with $\sum_i p_i = 1$. Note that we require the states to be normalized ($\langle\Phi_i|\Phi_i\rangle = 1$) but not generally orthogonal ($\langle\Phi_i|\Phi_j\rangle \neq \delta_{ij}$ is allowed).

Formally, any matrix fulfilling the properties

- *self-adjointness:* $\rho^\dagger = \rho$
- *normalization:* $\mathrm{Tr}\{\rho\} = 1$
- *positivity:* $\langle\Psi|\,\rho\,|\Psi\rangle \geq 0$ *for all vectors* Ψ

can be interpreted as a valid density matrix.

For a pure state one has $p_{\bar{i}} = 1$ and thereby $\rho = |\Phi_{\bar{i}}\rangle \langle \Phi_{\bar{i}}|$. Evidently, a density matrix is pure if and only if $\rho = \rho^2$.

The expectation value of an operator for a known state $|\Psi\rangle$

$$\langle A \rangle = \langle \Psi | A | \Psi \rangle \tag{1.16}$$

can be obtained conveniently from the corresponding pure density matrix $\rho = |\Psi\rangle \langle \Psi|$ by simply computing the trace

$$\begin{aligned} \langle A \rangle &\equiv \mathrm{Tr}\{A\rho\} = \mathrm{Tr}\{\rho A\} = \mathrm{Tr}\{A |\Psi\rangle \langle \Psi|\} \\ &= \sum_n \langle n | A | \Psi \rangle \langle \Psi | n \rangle = \langle \Psi | \left(\sum_n |n\rangle \langle n| \right) A | \Psi \rangle \\ &= \langle \Psi | A | \Psi \rangle \ . \end{aligned} \tag{1.17}$$

When the state is not exactly known but its probability distribution, the expectation value is obtained by computing the weighted average

$$\langle A \rangle = \sum_i P_i \langle \Phi_i | A | \Phi_i \rangle \ , \tag{1.18}$$

where P_i denotes the probability to be in state $|\Phi_i\rangle$. The definition of obtaining expectation values by calculating traces of operators with the density matrix is also consistent with mixed states

$$\begin{aligned} \langle A \rangle &\equiv \mathrm{Tr}\{A\rho\} = \mathrm{Tr}\left\{ A \sum_i p_i |\Phi_i\rangle \langle \Phi_i| \right\} = \sum_i p_i \mathrm{Tr}\{A |\Phi_i\rangle \langle \Phi_i|\} \\ &= \sum_i p_i \sum_n \langle n | A | \Phi_i \rangle \langle \Phi_i | n \rangle = \sum_i p_i \langle \Phi_i | \left(\sum_n |n\rangle \langle n| \right) A | \Phi_i \rangle \\ &= \sum_i p_i \langle \Phi_i | A | \Phi_i \rangle \ . \end{aligned} \tag{1.19}$$

Exercise 4 (Superposition vs Localized States) *(1 point)*
Calculate the density matrix for a statistical mixture in the states $|0\rangle$ *and* $|1\rangle$ *with probability* $p_0 = 3/4$ *and* $p_1 = 1/4$. *What is the density matrix for a statistical mixture of the superposition states* $|\Psi_a\rangle = \sqrt{3/4}\,|0\rangle + \sqrt{1/4}\,|1\rangle$ *and* $|\Psi_b\rangle = \sqrt{3/4}\,|0\rangle - \sqrt{1/4}\,|1\rangle$ *with probabilities* $p_a = p_b = 1/2$.

1.2.2 Dynamical Evolution in a closed system

The evolution of a pure state vector in a closed quantum system is described by the evolution operator $U(t)$, as e.g. for the Schrödinger equation

$$\left| \dot{\Psi}(t) \right\rangle = -\mathrm{i} H(t) |\Psi(t)\rangle \tag{1.20}$$

the time evolution operator

$$U(t) = \hat{\tau} \exp\left\{ -\mathrm{i} \int_0^t H(t')dt' \right\} \tag{1.21}$$

may be defined as the solution to the operator equation

$$\dot{U}(t) = -\mathrm{i}H(t)U(t)\,. \tag{1.22}$$

For constant $H(0) = H$, we simply have the solution $U(t) = e^{-\mathrm{i}Ht}$. Similarly, a pure-state density matrix $\rho = |\Psi\rangle\langle\Psi|$ would evolve according to the von-Neumann equation

$$\dot{\rho} = -\mathrm{i}\,[H(t), \rho(t)] \tag{1.23}$$

with the formal solution $\rho(t) = U(t)\rho(0)U^\dagger(t)$, compare Eq. (1.21).

When we simply apply this evolution equation to a density matrix that is not pure, we obtain

$$\rho(t) = \sum_i p_i U(t)\,|\Phi_i\rangle\langle\Phi_i|\,U^\dagger(t)\,, \tag{1.24}$$

i.e., transitions between the (now time-dependent) state vectors $|\Phi_i(t)\rangle = U(t)\,|\Phi_i\rangle$ are impossible with unitary evolution. This means that the von-Neumann evolution equation does yield the same dynamics as the Schrödinger equation if it is restarted on different initial states.

Exercise 5 (Preservation of density matrix properties by unitary evolution) *(1 point) Show that the von-Neumann (1.23) equation preserves self-adjointness, trace, and positivity of the density matrix.*

Also the Measurement process can be generalized similarly. For a quantum state $|\Psi\rangle$, measurements are described by a set of measurement operators $\{M_m\}$, each corresponding to a certain measurement outcome, and with the completeness relation $\sum_m M_m^\dagger M_m = \mathbf{1}$. The probability of obtaining result m is given by

$$p_m = \langle\Psi|\,M_m^\dagger M_m\,|\Psi\rangle \tag{1.25}$$

and after the measurement with outcome m, the quantum state is collapsed

$$|\Psi\rangle \xrightarrow{m} \frac{M_m\,|\Psi\rangle}{\sqrt{\langle\Psi|\,M_m^\dagger M_m\,|\Psi\rangle}}\,. \tag{1.26}$$

The projective measurement is just a special case of that with $M_m = |m\rangle\langle m|$.

Box 3 (Measurements with density matrix) *For a set of measurement operators $\{M_m\}$ corresponding to different outcomes m and obeying the completeness relation $\sum_m M_m^\dagger M_m = \mathbf{1}$, the probability to obtain result m is given by*

$$p_m = \mathrm{Tr}\left\{M_m^\dagger M_m \rho\right\} \tag{1.27}$$

and action of measurement on the density matrix – provided that result m was obtained – can be summarized as

$$\rho \xrightarrow{m} \rho' = \frac{M_m \rho M_m^\dagger}{\mathrm{Tr}\left\{M_m^\dagger M_m \rho\right\}} \tag{1.28}$$

It is therefore straightforward to see that description by Schrödinger equation or von-Neumann equation with the respective measurement postulates are equivalent. The density matrix formalism conveniently includes statistical mixtures in the description but at the cost of quadratically increasing the number of state variables.

Exercise 6 (Preservation of density matrix properties by measurement) *(1 point)*
Show that the measurement postulate preserves self-adjointness, trace, and positivity of the density matrix.

1.2.3 Most general evolution

Finally, we mention here that the most general evolution preserving all the nice properties of a density matrix is the so-called Kraus map. A density matrix ρ (hermitian, positive definite, and with trace one) can be mapped to another density matrix ρ' via

$$\rho' = \sum_{\alpha\beta} \gamma_{\alpha\beta} A_\alpha \rho A_\beta^\dagger \,, \qquad \text{with} \qquad \sum_{\alpha\beta} \gamma_{\alpha\beta} A_\beta^\dagger A_\alpha = \mathbf{1} \,, \tag{1.29}$$

where the prefactors $\gamma_{\alpha\beta}$ form a hermitian ($\gamma_{\alpha\beta} = \gamma^*_{\beta\alpha}$) and positive definite ($\sum_{\alpha\beta} x^*_\alpha \gamma_{\alpha\beta} x_\beta \geq 0$ or equivalently all eigenvalues of $(\gamma_{\alpha\beta})$ are non-negative) matrix. It is straightforward to see that the above map preserves trace and hermiticity of the density matrix. In addition, ρ' also inherits the positivity from $\rho = \sum_n P_n \left|n\right\rangle \left\langle n\right|$

$$\begin{aligned} \left\langle \Psi \right| \rho' \left| \Psi \right\rangle &= \sum_{\alpha\beta} \gamma_{\alpha\beta} \left\langle \Psi \right| A_\alpha \rho A_\beta^\dagger \left| \Psi \right\rangle = \sum_n P_n \sum_{\alpha\beta} \gamma_{\alpha\beta} \left\langle \Psi \right| A_\alpha \left| n \right\rangle \left\langle n \right| A_\beta^\dagger \left| \Psi \right\rangle \\ &= \sum_n \underbrace{P_n}_{\geq 0} \underbrace{\sum_{\alpha\beta} \left(\left\langle n \right| A_\alpha^\dagger \left| \Psi \right\rangle \right)^* \gamma_{\alpha\beta} \left\langle n \right| A_\beta^\dagger \left| \Psi \right\rangle}_{\geq 0} \geq 0 \,. \end{aligned} \tag{1.30}$$

Since the matrix $\gamma_{\alpha\beta}$ is hermitian, it can be diagonalized by a suitable unitary transformation, and we introduce the new operators $A_\alpha = \sum_{\alpha'} U_{\alpha\alpha'} \bar{K}_{\alpha'}$

$$\begin{aligned} \rho' &= \sum_{\alpha\beta} \sum_{\alpha'\beta'} \gamma_{\alpha\beta} U_{\alpha\alpha'} \bar{K}_{\alpha'} \rho U^*_{\beta\beta'} K^\dagger_{\beta'} = \sum_{\alpha'\beta'} \bar{K}_{\alpha'} \rho \bar{K}^\dagger_{\beta'} \underbrace{\sum_{\alpha\beta} U_{\alpha\alpha'} \gamma_{\alpha\beta} U^*_{\beta\beta'}}_{\gamma_{\alpha'} \delta_{\alpha'\beta'}} \\ &= \sum_\alpha \gamma_\alpha \bar{K}_\alpha \rho \bar{K}^\dagger_\alpha \,, \end{aligned} \tag{1.31}$$

where $\gamma_\alpha \geq 0$ represent the eigenvalues of the matrix $(\gamma_{\alpha\beta})$. Since these are by construction positive, we introduce further new operators $K_\alpha = \sqrt{\gamma_\alpha} \bar{K}_\alpha$ to obtain the simplest representation of a Kraus map.

Box 4 (Kraus map) *The map*

$$\rho(t + \Delta t) = \sum_\alpha K_\alpha(t, \Delta t) \rho(t) K^\dagger_\alpha(t, \Delta t) \tag{1.32}$$

with Kraus operators $K_\alpha(t, \Delta t)$ obeying the relation $\sum_\alpha K_\alpha^\dagger(t, \Delta t) K_\alpha(t, \Delta t) = \mathbf{1}$ preserves hermiticity, trace, and positivity of the density matrix.

Obviously, both unitary evolution and evolution under measurement are just special cases of a Kraus map. Though Kraus maps are heavily used in quantum information, they are not often very easy to interpret. For example, it is not straightforward to identify the unitary and the non-unitary part induced the Kraus map.

1.2.4 Lindblad master equation

Any dynamical evolution equation for the density matrix should (at least in some approximate sense) preserve its interpretation as density matrix, i.e., trace, hermiticity, and positivity must be preserved. By construction, the measurement postulate and unitary evolution preserve these properties. However, more general evolutions are conceivable. If we constrain ourselves to master equations that are local in time and have constant coefficients, the most general evolution that preserves trace, self-adjointness, and positivity of the density matrix is given by a Lindblad form.

Box 5 (Lindblad form) *In an N-dimensional system Hilbert space, a master equation of Lindblad form has the structure*

$$\dot{\rho} = \mathcal{L}\rho = -\mathrm{i}\,[H, \rho] + \sum_{\alpha,\beta=1}^{N^2-1} \gamma_{\alpha\beta} \left(A_\alpha \rho A_\beta^\dagger - \frac{1}{2} \left\{ A_\beta^\dagger A_\alpha, \rho \right\} \right) , \tag{1.33}$$

where the hermitian operator $H = H^\dagger$ can be interpreted as an effective Hamiltonian and $\gamma_{\alpha\beta} = \gamma_{\beta\alpha}^*$ is a positive semidefinite matrix, i.e., it fulfills $\sum_{\alpha\beta} x_\alpha^* \gamma_{\alpha\beta} x_\beta \geq 0$ for all vectors x (or, equivalently that all eigenvalues of $(\gamma_{\alpha\beta})$ are non-negative $\lambda_i \geq 0$).

Exercise 7 (Trace and Hermiticity preservation by Lindblad forms) *(1 points)*
Show that the Lindblad form master equation preserves trace and hermiticity of the density matrix.

The Lindblad type master equation can be written in simpler form: As the dampening matrix γ is hermitian, it can be diagonalized by a suitable unitary transformation U, such that $\sum_{\alpha\beta} U_{\alpha'\alpha} \gamma_{\alpha\beta} (U^\dagger)_{\beta\beta'} = \delta_{\alpha'\beta'} \gamma_{\alpha'}$ with $\gamma_\alpha \geq 0$ representing its non-negative eigenvalues. Using this unitary operation, a new set of operators can be defined via $A_\alpha = \sum_{\alpha'} U_{\alpha'\alpha} L_{\alpha'}$. Inserting this

decomposition in the master equation, we obtain

$$\begin{aligned}\dot{\rho} &= -\mathrm{i}\,[H,\rho] + \sum_{\alpha,\beta=1}^{N^2-1} \gamma_{\alpha\beta}\left(A_\alpha \rho A_\beta^\dagger - \frac{1}{2}\left\{A_\beta^\dagger A_\alpha, \rho\right\}\right) \\ &= -\mathrm{i}\,[H,\rho] + \sum_{\alpha',\beta'}\left[\sum_{\alpha\beta}\gamma_{\alpha\beta}U_{\alpha'\alpha}U^*_{\beta'\beta}\right]\left(L_{\alpha'}\rho L_{\beta'}^\dagger - \frac{1}{2}\left\{L_{\beta'}^\dagger L_{\alpha'}, \rho\right\}\right) \\ &= -\mathrm{i}\,[H,\rho] + \sum_\alpha \gamma_\alpha\left(L_\alpha \rho L_\alpha^\dagger - \frac{1}{2}\left\{L_\alpha^\dagger L_\alpha, \rho\right\}\right)\,, \end{aligned} \tag{1.34}$$

where γ_α denote the N^2-1 non-negative eigenvalues of the dampening matrix. Furthermore, we can in principle absorb the γ_α in the Lindblad operators $\bar{L}_\alpha = \sqrt{\gamma_\alpha}L_\alpha$, such that another form of a Lindblad master equation would be

$$\dot{\rho} = -\mathrm{i}\,[H,\rho] + \sum_\alpha\left(\bar{L}_\alpha \rho \bar{L}_\alpha^\dagger - \frac{1}{2}\left\{\bar{L}_\alpha^\dagger \bar{L}_\alpha, \rho\right\}\right)\,. \tag{1.35}$$

Evidently, the representation of a master equation is not unique.

Any other unitary operation would lead to a different non-diagonal form of $\gamma_{\alpha\beta}$ which however describes the same master equation. In addition, we note here that the master equation is not only invariant to unitary transformations of the operators A_α, but in the diagonal representation also to inhomogeneous transformations of the form

$$\begin{aligned} L_\alpha &\to L'_\alpha = L_\alpha + a_\alpha \\ H &\to H' = H + \frac{1}{2\mathrm{i}}\sum_\alpha \gamma_\alpha\left(a_\alpha^* L_\alpha - a_\alpha L_\alpha^\dagger\right) + b\,, \end{aligned} \tag{1.36}$$

with complex numbers a_α and a real number b. The numbers a_α can be chosen such that the Lindblad operators are traceless $\mathrm{Tr}\,\{L_\alpha\} = 0$, which is a popular convention. Choosing b simply corresponds to gauging the energy of the system.

Exercise 8 (Shift invariance) *(1 points)*
Show the invariance of the diagonal representation of a Lindblad form master equation (1.34) with respect to the transformation (1.36).

We would like to demonstrate the preservation of positivity here. Since preservation of hermiticity follows directly from the Lindblad form, we can – at any time – formally write the density matrix in its spectral representation

$$\rho(t) = \sum_j P_j(t)\,|\Psi_j(t)\rangle\,\langle\Psi_j(t)| \tag{1.37}$$

with probabilities $P_j(t) \in \mathbb{R}$ (we still have to show that these remain positive) and time-dependent orthonormal eigenstates obeying unitary evolution

$$\left|\dot{\Psi}_j(t)\right\rangle = -\mathrm{i}K(t)\,|\Psi_j(t)\rangle\,, \qquad K(t) = K^\dagger(t)\,. \tag{1.38}$$

Exercise 9 (Evolution of Eigenstates is Unitary) *Show that orthonormality of time-dependent eigenstates implies unitary evolution, i.e., a hermitian operator $K(t)$.*

The hermitian conjugate equation also implies that $\left\langle \dot{\Psi}_j \right| = +\mathrm{i} \left\langle \Psi_j \right| K$. Therefore, its time-derivative becomes

$$\dot{\rho} = \sum_j \left[\dot{P}_j \left|\Psi_j\right\rangle \left\langle\Psi_j\right| - \mathrm{i} P_j K \left|\Psi_j\right\rangle \left\langle\Psi_j\right| + \mathrm{i} P_j \left|\Psi_j\right\rangle \left\langle\Psi_j\right| K \right] , \tag{1.39}$$

and sandwiching the density matrix yields to the cancellation of two terms, such that $\langle\Psi_j(t)| \dot{\rho} |\Psi_j(t)\rangle = \dot{P}_j(t)$. On the other hand, we can also use the Lindblad equation to obtain

$$\begin{aligned} \dot{P}_j &= -\mathrm{i} \left\langle\Psi_j\right| H \left|\Psi_j\right\rangle P_j + \mathrm{i} P_j \left\langle\Psi_j\right| H \left|\Psi_j\right\rangle \\ &\quad + \sum_\alpha \gamma_\alpha \left[\left\langle\Psi_j\right| L_\alpha (\sum_k P_k \left|\Psi_k\right\rangle \left\langle\Psi_k\right|) L_\alpha^\dagger \left|\Psi_j\right\rangle - \left\langle\Psi_j\right| L_\alpha^\dagger L_\alpha \left|\Psi_j\right\rangle P_j \right] \\ &= \left(\sum_k \sum_\alpha \gamma_\alpha |\left\langle\Psi_j\right| L_\alpha \left|\Psi_k\right\rangle|^2 P_k \right) - \left(\sum_\alpha \gamma_\alpha \left\langle\Psi_j\right| L_\alpha^\dagger L_\alpha \left|\Psi_j\right\rangle \right) P_j \, . \end{aligned} \tag{1.40}$$

This is nothing but a rate equation with positive but time-dependent transition rates

$$R_{k\to j}(t) = \sum_\alpha \gamma_\alpha |\langle\Psi_j(t)| L_\alpha |\Psi_k(t)\rangle|^2 \geq 0 \, , \tag{1.41}$$

and with our arguments from Sec. 1.1 it follows that the positivity of the eigenvalues $P_j(t)$ is granted, a valid initialization provided. Unfortunately, the basis within which this simple rate equation holds is time-dependent and also only known after solving the master equation and diagonalizing the solution. It is therefore not very practical in most occasions.

1.2.5 Example: Master Equation for a cavity in a thermal bath

Consider the Lindblad form master equation

$$\begin{aligned} \dot{\rho} &= -\mathrm{i} \left[\Omega a^\dagger a, \rho \right] + \Gamma(1+n_B) \left[a\rho a^\dagger - \frac{1}{2} a^\dagger a \rho - \frac{1}{2} \rho a^\dagger a \right] \\ &\quad + \Gamma n_B \left[a^\dagger \rho a - \frac{1}{2} a a^\dagger \rho - \frac{1}{2} \rho a a^\dagger \right] , \end{aligned} \tag{1.42}$$

with bosonic operators $\left[a, a^\dagger\right] = \mathbf{1}$ and Bose-Einstein bath occupation $n_B = \left[e^{\beta\Omega} - 1\right]^{-1}$ and cavity frequency Ω. In Fock-space representation, these operators act as $a^\dagger |n\rangle = \sqrt{n+1}\,|n+1\rangle$ (where $0 \leq n < \infty$), such that the above master equation couples only the diagonals of the density matrix $\rho_n = \langle n| \rho |n\rangle$ to each other. This is directly visible by sandwhiching the master equation with $\langle n| \ldots |n\rangle$

$$\begin{aligned} \dot{\rho_n} &= \Gamma(1+n_B) \left[(n+1)\rho_{n+1} - n\rho_n \right] + \Gamma n_B \left[n\rho_{n-1} - (n+1)\rho_n \right] \\ &= \Gamma n_B n \rho_{n-1} - \Gamma \left[n + (2n+1) n_B \right] \rho_n + \Gamma(1+n_B)(n+1)\rho_{n+1} \, , \end{aligned} \tag{1.43}$$

which shows that the rate equation arising for the diagonals even has a simple tri-diagonal form. That makes it particularly easy to calculate its stationary state recursively, since the boundary solution $n_B\bar{\rho}_0 = (1+n_B)\bar{\rho}_1$ implies for all n the relation

$$\frac{\bar{\rho}_{n+1}}{\bar{\rho}_n} = \frac{n_B}{1+n_B} = e^{-\beta\Omega}\,, \tag{1.44}$$

i.e., the stationary state is a thermalized Gibbs state with the same temperature as the reservoir.

Exercise 10 (Moments) *(1 points)*
Calculate the expectation value of the number operator $n = a^\dagger a$ and its square $n^2 = a^\dagger a a^\dagger a$ in the stationary state of the master equation (1.42).

In general, the matrix elements of the density matrix $\rho_{nm} = \langle n|\,\rho\,|m\rangle$ will obey

$$\begin{aligned}
\dot{\rho}_{nm} &= -\mathrm{i}\Omega(n-m)\rho_{nm} + \Gamma(1+n_B)\left[\sqrt{(n+1)(m+1)}\rho_{n+1,m+1} - \frac{n+m}{2}\rho_{nm}\right] \\
&\quad +\Gamma n_B\left[\sqrt{nm}\rho_{n-1,m-1} - \frac{n+1+m+1}{2}\rho_{nm}\right] \\
&= \left[-\mathrm{i}\Omega(n-m) - \Gamma\frac{(1+n_B)(n+m)+n_B(n+1+m+1)}{2}\right]\rho_{nm} \\
&\quad +\Gamma(1+n_B)\sqrt{(n+1)(m+1)}\rho_{n+1,m+1} + \Gamma n_B\sqrt{nm}\rho_{n-1,m-1}\,,
\end{aligned} \tag{1.45}$$

and it is straightforward to see that vanishing coherences (off-diagonal matrix elements) $\bar{\rho}_{n\neq m} = 0$ are a valid steady-state solution. Not being aware of the Lindblad form we may nevertheless ask whether there are other solutions. The above equation shows that among the coherences, only few couple, and by arranging them in a favorable form we can write these equations in matrix form with infinite-dimensional tri-diagonal matrices (for brevity we use $\gamma = \Gamma n_B$ and $\bar{\gamma} = \Gamma(1+n_B)$)

$$W = \begin{pmatrix}
 & \vdots & & \\
\ddots & +\bar{\gamma}\sqrt{nm} & 0 & \\
\ldots\ +\gamma\sqrt{nm} & \left[-\mathrm{i}\Omega(n-m) - \bar{\gamma}\frac{n+m}{2} - \gamma\frac{n+1+m+1}{2}\right] & +\bar{\gamma}\sqrt{(n+1)(m+1)} & \ldots \\
0 & +\gamma\sqrt{(n+1)(m+1)} & \ddots & \\
 & \vdots & &
\end{pmatrix}. \tag{1.46}$$

By examining every column in detail, we see that the real part of the diagonal entries has always larger magnitude than the sum of the off-diagonal entries

$$\bar{\gamma}\frac{n+m}{2} + \gamma\frac{n+1+m+1}{2} \geq +\bar{\gamma}\sqrt{nm} + \gamma\sqrt{(n+1)(m+1)}\,, \tag{1.47}$$

where equality actually only holds for the diagonal elements ($n = m$). From Gershgorins circle theorem, we can therefore conclude that all the eigenvalues of the matrix W have for $n \neq m$ a negative real part. Consequently, the coherences must decay and the stationary state only contains populations in the Fock space representation.

1.2.6 Master Equation for a driven cavity

When the cavity is driven with a laser and simultaneously coupled to a vaccuum bath $n_B = 0$, one often uses the master equation

$$\dot{\rho_{\mathrm{S}}} = -\mathrm{i}\left[\Omega a^\dagger a + \frac{P}{2}e^{+i\omega t}a + \frac{P^*}{2}e^{-i\omega t}a^\dagger, \rho_{\mathrm{S}}\right] + \gamma\left[a\rho_{\mathrm{S}}a^\dagger - \frac{1}{2}a^\dagger a\rho_{\mathrm{S}} - \frac{1}{2}\rho_{\mathrm{S}}a^\dagger a\right] \tag{1.48}$$

with the Laser frequency ω and amplitude P. The transformation $\rho = e^{+\mathrm{i}\omega a^\dagger at}\rho_{\mathrm{S}}e^{-\mathrm{i}\omega a^\dagger at}$ maps to a time-independent master equation

$$\dot{\rho} = -\mathrm{i}\left[(\Omega-\omega)a^\dagger a + \frac{P}{2}a + \frac{P^*}{2}a^\dagger, \rho\right] + \gamma\left[a\rho a^\dagger - \frac{1}{2}a^\dagger a\rho - \frac{1}{2}\rho a^\dagger a\right] . \tag{1.49}$$

This equation couples coherences and populations in the Fock space representation, and in the long-term limit we will also observe non-vanishing coherences. Nevertheless, it is possible to solve for the evolution of expectation values by just making use of the bosonic commutation relations. Here, the basic idea is to obtain a closed set of differential equations for observables

$$\left\langle \dot{O}_\alpha \right\rangle = \mathrm{Tr}\left\{O_\alpha\dot{\rho}\right\} = \mathrm{Tr}\left\{O_\alpha\mathcal{L}\rho\right\} = \sum_{\alpha\beta}\Gamma_{\alpha\beta}\left\langle O_\beta\right\rangle , \tag{1.50}$$

where the coefficients $\Gamma_{\alpha\beta}$ have to be obtained from

Exercise 11 (Coherent state) *(1 points)*
Using the driven cavity master equation, show that the stationary expectation value of the cavity occupation fulfils

$$\lim_{t\to\infty}\left\langle a^\dagger a\right\rangle = \frac{|P|^2}{\gamma^2 + 4(\Omega-\omega)^2}$$

Chapter 2

Obtaining a Master Equation

2.1 Mathematical Prerequisites

Master equations are often used to describe the dynamics of systems interacting with one or many large reservoirs (baths). To derive them from microscopic models – including the Hamiltonian of the full system – requires to review some basic mathematical concepts.

2.1.1 Tensor Product

The greatest advantage of the density matrix formalism is visible when quantum systems composed of several subsystems are considered. Roughly speaking, the tensor product represents a way to construct a larger vector space from two (or more) smaller vector spaces.

Box 6 (Tensor Product) *Let V and W be Hilbert spaces (vector spaces with scalar product) of dimension m and n with basis vectors $\{|v\rangle\}$ and $\{|w\rangle\}$, respectively. Then $V \otimes W$ is a Hilbert space of dimension $m \cdot n$, and a basis is spanned by $\{|v\rangle \otimes |w\rangle\}$, which is a set combining every basis vector of V with every basis vector of W.*

Mathematical properties

- *Bilinearity* $(z_1 |v_1\rangle + z_2 |v_2\rangle) \otimes |w\rangle = z_1 |v_1\rangle \otimes |w\rangle + z_2 |v_2\rangle \otimes |w\rangle$
- *operators acting on the combined Hilbert space* $A \otimes B$ *act on the basis states as* $(A \otimes B)(|v\rangle \otimes |w\rangle) = (A |v\rangle) \otimes (B |w\rangle)$
- *any linear operator on* $V \otimes W$ *can be decomposed as* $C = \sum_i c_i A_i \otimes B_i$
- *the scalar product is inherited in the natural way, i.e., one has for* $|a\rangle = \sum_{ij} a_{ij} |v_i\rangle \otimes |w_j\rangle$ *and* $|b\rangle = \sum_{k\ell} b_{k\ell} |v_k\rangle \otimes |w_\ell\rangle$ *the scalar product* $\langle a|b\rangle = \sum_{ijk\ell} a^*_{ij} b_{k\ell} \langle v_i|v_k\rangle \langle w_j|w_\ell\rangle = \sum_{ij} a^*_{ij} b_{ij}$

If more than just two vector spaces are combined to form a larger vector space, the dimension of the joint vector space grows rapidly, as e.g. exemplified by the case of a qubit: Its Hilbert space is just spanned by two vectors $|0\rangle$ and $|1\rangle$. The joint Hilbert space of two qubits is four-dimensional, of three qubits 8-dimensional, and of n qubits 2^n-dimensional. Eventually, this exponential growth of the Hilbert space dimension for composite quantum systems is at the heart of quantum computing.

Exercise 12 (Tensor Products of Operators) *(1 points)*
Let $\boldsymbol{\sigma}$ denote the Pauli matrices, i.e.,

$$\sigma^1 = \begin{pmatrix} 0 & +1 \\ +1 & 0 \end{pmatrix} \qquad \sigma^2 = \begin{pmatrix} 0 & -\mathrm{i} \\ +\mathrm{i} & 0 \end{pmatrix} \qquad \sigma^3 = \begin{pmatrix} +1 & 0 \\ 0 & -1 \end{pmatrix}$$

Compute the trace of the operator

$$\Sigma = a\mathbf{1} \otimes \mathbf{1} + \sum_{i=1}^{3} \alpha_i \sigma^i \otimes \mathbf{1} + \sum_{j=1}^{3} \beta_j \mathbf{1} \otimes \sigma^j + \sum_{i,j=1}^{3} a_{ij} \sigma^i \otimes \sigma^j \,.$$

Since the scalar product is inherited, this typically enables a convenient calculation of the trace in case of a few operator decomposition, e.g., for just two operators

$$\begin{aligned} \mathrm{Tr}\left\{A \otimes B\right\} &= \sum_{n_A, n_B} \langle n_A, n_B| \, A \otimes B \, |n_A, n_B\rangle \\ &= \left[\sum_{n_A} \langle n_A| \, A \, |n_A\rangle\right] \left[\sum_{n_B} \langle n_B| \, B \, |n_B\rangle\right] \\ &= \mathrm{Tr}_A\{A\}\mathrm{Tr}_B\{B\} \,, \end{aligned} \tag{2.1}$$

where $\mathrm{Tr}_{A/B}$ denote the trace in the Hilbert space of A and B, respectively.

2.1.2 The partial trace

For composite systems, it is usually not necessary to keep all information of the complete system in the density matrix. Rather, one would like to have a density matrix that encodes all the information on a particular subsystem only. Obviously, the map $\rho \to \mathrm{Tr_B}\left\{\rho\right\}$ to such a reduced density matrix should leave all expectation values of observables A acting only on the considered subsystem invariant, i.e.,

$$\mathrm{Tr}\left\{A \otimes \mathbf{1}\rho\right\} = \mathrm{Tr}\left\{A\mathrm{Tr_B}\left\{\rho\right\}\right\} \,. \tag{2.2}$$

If this basic condition was not fulfilled, there would be no point in defining such a thing as a reduced density matrix: Measurement would yield different results depending on the Hilbert space of the experimenters feeling.

Box 7 (Partial Trace) *Let $|a_1\rangle$ and $|a_2\rangle$ be vectors of state space A and $|b_1\rangle$ and $|b_2\rangle$ vectors of state space B. Then, the partial trace over state space B is defined via*

$$\mathrm{Tr_B}\left\{|a_1\rangle\langle a_2| \otimes |b_1\rangle\langle b_2|\right\} = |a_1\rangle\langle a_2| \, \mathrm{Tr}\left\{|b_1\rangle\langle b_2|\right\} \,. \tag{2.3}$$

The partial trace is linear, such that the partial trace of arbitrary operators is calculated similarly. By choosing the $|a_\alpha\rangle$ and $|b_\gamma\rangle$ as an orthonormal basis in the respective Hilbert space,

one may therefore calculate the most general partial trace via

$$\begin{aligned}
\mathrm{Tr_B}\left\{C\right\} &= \mathrm{Tr_B}\left\{\sum_{\alpha\beta\gamma\delta} c_{\alpha\beta\gamma\delta}\left|a_\alpha\right\rangle\left\langle a_\beta\right| \otimes \left|b_\gamma\right\rangle\left\langle b_\delta\right|\right\} \\
&= \sum_{\alpha\beta\gamma\delta} c_{\alpha\beta\gamma\delta}\mathrm{Tr_B}\left\{\left|a_\alpha\right\rangle\left\langle a_\beta\right| \otimes \left|b_\gamma\right\rangle\left\langle b_\delta\right|\right\} \\
&= \sum_{\alpha\beta\gamma\delta} c_{\alpha\beta\gamma\delta}\left|a_\alpha\right\rangle\left\langle a_\beta\right| \mathrm{Tr}\left\{\left|b_\gamma\right\rangle\left\langle b_\delta\right|\right\} \\
&= \sum_{\alpha\beta\gamma\delta} c_{\alpha\beta\gamma\delta}\left|a_\alpha\right\rangle\left\langle a_\beta\right| \sum_\epsilon \left\langle b_\epsilon|b_\gamma\right\rangle\left\langle b_\delta|b_\epsilon\right\rangle \\
&= \sum_{\alpha\beta}\left[\sum_\gamma c_{\alpha\beta\gamma\gamma}\right]\left|a_\alpha\right\rangle\left\langle a_\beta\right| . \qquad (2.4)
\end{aligned}$$

The definition 7 is the only linear map that respects the invariance of expectation values.

Exercise 13 (Partial Trace) *(1 points)*
Compute the partial trace of a pure density matrix $\rho = |\Psi\rangle\langle\Psi|$ *in the bipartite state*

$$|\Psi\rangle = \frac{1}{\sqrt{2}}\left(|01\rangle + |10\rangle\right) \equiv \frac{1}{\sqrt{2}}\left(|0\rangle \otimes |1\rangle + |1\rangle \otimes |0\rangle\right)$$

2.2 Derivations for Open Quantum Systems

In some cases, it is possible to derive a master equation rigorously based only on a few assumptions. Open quantum systems for example are mostly treated as part of a much larger closed quantum system (the union of system and bath), where the partial trace is used to eliminate the unwanted (typically many) degrees of freedom of the bath, see Fig. 2.1. Technically speaking, we will consider

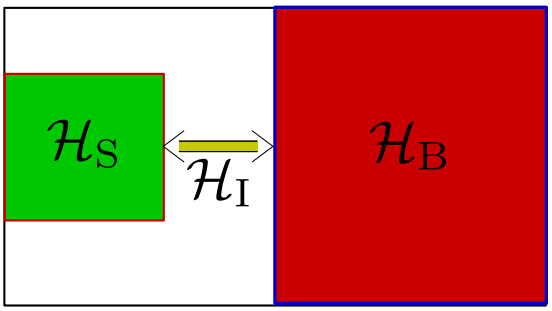

Figure 2.1: An open quantum system can be conceived as being part of a larger closed quantum system, where the system part ($\mathcal{H}_\mathrm{S}$) is coupled to the bath ($\mathcal{H}_\mathrm{B}$) via the interaction Hamiltonian $\mathcal{H}_\mathrm{I}$.

Hamiltonians of the form

$$H = \mathcal{H}_\mathrm{S} \otimes \mathbf{1} + \mathbf{1} \otimes \mathcal{H}_\mathrm{B} + \mathcal{H}_\mathrm{I}\,, \qquad (2.5)$$

where the system and bath Hamiltonians act only on the system and bath Hilbert space, respectively. In contrast, the interaction Hamiltonian acts on both Hilbert spaces

$$\mathcal{H}_{\rm I} = \sum_\alpha A_\alpha \otimes B_\alpha \,, \tag{2.6}$$

where the summation boundaries are in the worst case limited by the dimension of the system Hilbert space. As we consider physical observables here, it is required that all Hamiltonians are self-adjoint.

Exercise 14 (Hermiticity of Couplings) *(1 points)*
Show that it is always possible to choose hermitian coupling operators $A_\alpha = A_\alpha^\dagger$ and $B_\alpha = B_\alpha^\dagger$ using that $\mathcal{H}_{\rm I} = \mathcal{H}_{\rm I}^\dagger$.

2.2.1 Standard Quantum-Optical Derivation

Interaction Picture

When the interaction $\mathcal{H}_{\rm I}$ is small, it is justified to apply perturbation theory. The von-Neumann equation in the joint total quantum system

$$\dot\rho = -{\rm i}\left[\mathcal{H}_{\rm S}\otimes\mathbf{1} + \mathbf{1}\otimes\mathcal{H}_{\rm B} + \mathcal{H}_{\rm I}, \rho\right] \tag{2.7}$$

describes the full evolution of the combined density matrix. This equation can be formally solved by the unitary evolution $\rho(t) = e^{-{\rm i}Ht}\rho_0 e^{+{\rm i}Ht}$, which however is impractical to compute as H involves too many degrees of freedom.

Transforming to the interaction picture

$$\boldsymbol{\rho}(t) = e^{+{\rm i}(\mathcal{H}_{\rm S}+\mathcal{H}_{\rm B})t}\rho(t)e^{-{\rm i}(\mathcal{H}_{\rm S}+\mathcal{H}_{\rm B})t}\,, \tag{2.8}$$

which will be denoted by bold symbols throughout, the von-Neumann equation transforms into

$$\dot{\boldsymbol{\rho}} = -{\rm i}\left[\boldsymbol{\mathcal{H}_{\rm I}}(t), \boldsymbol{\rho}\right]\,, \tag{2.9}$$

where the in general time-dependent interaction Hamiltonian

$$\begin{aligned}\boldsymbol{\mathcal{H}_{\rm I}}(t) &= e^{+{\rm i}(\mathcal{H}_{\rm S}+\mathcal{H}_{\rm B})t}\mathcal{H}_{\rm I}e^{-{\rm i}(\mathcal{H}_{\rm S}+\mathcal{H}_{\rm B})t} = \sum_\alpha e^{+i\mathcal{H}_{\rm S}t}A_\alpha e^{-{\rm i}\mathcal{H}_{\rm S}t}\otimes e^{+i\mathcal{H}_{\rm B}t}B_\alpha e^{-{\rm i}\mathcal{H}_{\rm B}t}\\ &= \sum_\alpha \boldsymbol{A_\alpha}(t)\otimes\boldsymbol{B_\alpha}(t)\end{aligned} \tag{2.10}$$

allows to perform perturbation theory.

Without loss of generality we will for simplicity assume here the case of hermitian coupling operators $A_\alpha = A_\alpha^\dagger$ and $B_\alpha = B_\alpha^\dagger$. One heuristic way to perform perturbation theory is to formally integrate Eq. (2.10) and to re-insert the result in the r.h.s. of Eq. (2.10). The time-derivative of the system density matrix is obtained by performing the partial trace

$$\dot{\boldsymbol{\rho}}_{\mathbf{S}} = -{\rm i}{\rm Tr}_{\rm B}\left\{\left[\boldsymbol{\mathcal{H}_{\rm I}}(\boldsymbol{t}), \rho_0\right]\right\} - \int_0^t {\rm Tr}_{\rm B}\left\{\left[\boldsymbol{\mathcal{H}_{\rm I}}(t), \left[\boldsymbol{\mathcal{H}_{\rm I}}(t'), \boldsymbol{\rho}(t')\right]\right]dt'\right\}\,. \tag{2.11}$$

This integro-differential equation is still exact but unfortunately not closed as the r.h.s. does not depend on $\rho_{\rm S}$ but the full density matrix at all previous times.

Born approximation

To close the above equation, we employ factorization of the initial density matrix

$$\rho_0 = \rho_{\mathrm{S}}^0 \otimes \bar{\rho}_{\mathrm{B}} \tag{2.12}$$

together with perturbative considerations: Assuming that $\boldsymbol{\mathcal{H}_{\mathrm{I}}}(t) = \mathcal{O}\{\lambda\}$ with λ beeing a small dimensionless perturbation parameter (solely used for bookkeeping purposes here) and that the environment is so large such that it is hardly affected by the presence of the system, we may formally expand the full density matrix

$$\boldsymbol{\rho}(t) = \boldsymbol{\rho_{\mathrm{S}}}(t) \otimes \bar{\rho}_{\mathrm{B}} + \mathcal{O}\{\lambda\}\,, \tag{2.13}$$

where the neglect of all higher orders is known as **Born approximation**. Eq. (2.11) demonstrates that the Born approximation is equivalent to a perturbation theory in the interaction Hamiltonian

$$\dot{\boldsymbol{\rho}}_{\mathbf{S}} = -\mathrm{i}\mathrm{Tr}_{\mathrm{B}}\left\{[\boldsymbol{\mathcal{H}_{\mathrm{I}}}(t), \rho_0]\right\} - \int_0^t \mathrm{Tr}_{\mathrm{B}}\left\{[\boldsymbol{\mathcal{H}_{\mathrm{I}}}(t), [\boldsymbol{\mathcal{H}_{\mathrm{I}}}(t'), \boldsymbol{\rho_{\mathrm{S}}}(t') \otimes \bar{\rho}_{\mathrm{B}}]]\, dt'\right\} + \mathcal{O}\{\lambda^3\}\,. \tag{2.14}$$

Using the decomposition of the interaction Hamiltonian (2.6), this obviously yields a closed equation for the system density matrix

$$\begin{aligned}
\dot{\boldsymbol{\rho}}_{\mathbf{S}} \;=\; & -\mathrm{i}\sum_{\alpha}\left[\boldsymbol{A_\alpha}(t)\rho_{\mathrm{S}}^0\mathrm{Tr}\left\{\boldsymbol{B_\alpha}(t)\bar{\rho}_{\mathrm{B}}\right\} - \rho_{\mathrm{S}}^0\boldsymbol{A_\alpha}(t)\mathrm{Tr}\left\{\bar{\rho}_{\mathrm{B}}\boldsymbol{B_\alpha}(t)\right\}\right] - \sum_{\alpha\beta}\int_0^t \Big[\\
& +\boldsymbol{A_\alpha}(t)\boldsymbol{A_\beta}(t')\boldsymbol{\rho_{\mathrm{S}}}(t')\mathrm{Tr}\left\{\boldsymbol{B_\alpha}(t)\boldsymbol{B_\beta}(t')\bar{\rho}_{\mathrm{B}}\right\} \\
& -\boldsymbol{A_\alpha}(t)\boldsymbol{\rho_{\mathrm{S}}}(t')\boldsymbol{A_\beta}(t')\mathrm{Tr}\left\{\boldsymbol{B_\alpha}(t)\bar{\rho}_{\mathrm{B}}\boldsymbol{B_\beta}(t')\right\} \\
& -\boldsymbol{A_\beta}(t')\boldsymbol{\rho_{\mathrm{S}}}(t')\boldsymbol{A_\alpha}(t)\mathrm{Tr}\left\{\boldsymbol{B_\beta}(t')\bar{\rho}_{\mathrm{B}}\boldsymbol{B_\alpha}(t)\right\} \\
& +\boldsymbol{\rho_{\mathrm{S}}}(t')\boldsymbol{A_\beta}(t')\boldsymbol{A_\alpha}(t)\mathrm{Tr}\left\{\bar{\rho}_{\mathrm{B}}\boldsymbol{B_\beta}(t')\boldsymbol{B_\alpha}(t)\right\}\Big]\, dt'\,.
\end{aligned} \tag{2.15}$$

Without loss of generality, we proceed by assuming that the single coupling operator expectation value vanishes

$$\mathrm{Tr}\left\{\boldsymbol{B_\alpha}(t)\bar{\rho}_{\mathrm{B}}\right\} = 0\,. \tag{2.16}$$

This situation can always be constructed by simultaneously modifying system Hamiltonian $\mathcal{H}_{\mathrm{S}}$ and coupling operators A_α, see exercise 15.

Exercise 15 (Vanishing single-operator expectation values) *(1 points)*
Show that by modifying system and interaction Hamiltonian

$$\mathcal{H}_{\mathrm{S}} \to \mathcal{H}_{\mathrm{S}} + \sum_\alpha g_\alpha A_\alpha\,, \qquad B_\alpha \to B_\alpha - g_\alpha \mathbf{1} \tag{2.17}$$

one can construct a situation where $\mathrm{Tr}\left\{\boldsymbol{B_\alpha}(t)\bar{\rho}_{\mathrm{B}}\right\} = 0$. *Determine* g_α.

Using the cyclic property of the trace, we obtain

$$\dot{\boldsymbol{\rho}}_{\mathbf{S}} = -\sum_{\alpha\beta}\int_0^t dt' \Big[C_{\alpha\beta}(t,t') \left[\boldsymbol{A}_{\boldsymbol{\alpha}}(t), \boldsymbol{A}_{\boldsymbol{\beta}}(t')\boldsymbol{\rho}_{\mathbf{S}}(t')\right] + C_{\beta\alpha}(t',t) \left[\boldsymbol{\rho}_{\mathbf{S}}(t')\boldsymbol{A}_{\boldsymbol{\beta}}(t'), \boldsymbol{A}_{\boldsymbol{\alpha}}(t)\right] \Big] \tag{2.18}$$

with the bath correlation function

$$C_{\alpha\beta}(t_1,t_2) = \mathrm{Tr}\left\{\boldsymbol{B}_{\boldsymbol{\alpha}}(t_1)\boldsymbol{B}_{\boldsymbol{\beta}}(t_2)\bar{\rho}_{\mathrm{B}}\right\} . \tag{2.19}$$

The integro-differential equation (2.18) is a **non-Markovian master equation**, as the r.h.s. depends on the value of the dynamical variable (the density matrix) at all previous times – weighted by the bath correlation functions. It does preserve trace and hermiticity of the system density matrix, but not necessarily its positivity. Such integro-differential equations can only be solved in very specific cases, e.g., when the correlation functions have a very simple decay law. Therefore, we motivate further approximations, for which we need to discuss the analytic properties of the bath correlation functions.

Markov approximation

It is quite straightforward to see that when the bath Hamiltonian commutes with the bath density matrix $[\mathcal{H}_{\mathrm{B}}, \bar{\rho}_{\mathrm{B}}] = 0$, the bath correlation functions actually only depend on the difference of their time arguments $C_{\alpha\beta}(t_1,t_2) = C_{\alpha\beta}(t_1 - t_2)$ with

$$C_{\alpha\beta}(t_1 - t_2) = \mathrm{Tr}\left\{e^{+i\mathcal{H}_{\mathrm{B}}(t_1-t_2)} B_\alpha e^{-i\mathcal{H}_{\mathrm{B}}(t_1-t_2)} B_\beta \bar{\rho}_{\mathrm{B}}\right\} . \tag{2.20}$$

Since we chose our coupling operators hermitian, we have the additional symmetry that $C_{\alpha\beta}(\tau) = C^*_{\beta\alpha}(-\tau)$. One can now evaluate several system-bath models and when the bath has a dense spectrum, the bath correlation functions are typically found to be strongly peaked around zero, see exercise 16.

Exercise 16 (Bath Correlation Function) *(1 points)*
Evaluate the Fourier transform $\gamma_{\alpha\beta}(\omega) = \int C_{\alpha\beta}(\tau) e^{+\mathrm{i}\omega\tau} d\tau$ *of the bath correlation functions for the coupling operators* $B_1 = \sum_k h_k b_k$ *and* $B_2 = \sum_k h_k^* b_k^\dagger$ *for a bosonic bath* $\mathcal{H}_{\mathrm{B}} = \sum_k \omega_k b_k^\dagger b_k$ *in the thermal equilibrium state* $\bar{\rho}_{\mathrm{B}}^0 = \frac{e^{-\beta\mathcal{H}_{\mathrm{B}}}}{\mathrm{Tr}\left\{e^{-\beta\mathcal{H}_{\mathrm{B}}}\right\}}$. *You may use the continous representation* $\Gamma(\omega) = 2\pi \sum_k |h_k|^2 \delta(\omega - \omega_k)$ *for the tunneling rates.*

In superoperator notation, one can also write the integro-differential equation (2.18) as

$$\dot{\rho}_{\mathrm{S}} = \int_0^t \mathcal{W}(t-t')\rho_{\mathrm{S}}(t')dt' , \tag{2.21}$$

where the kernel $\mathcal{W}(\tau)$ assigns a much smaller weight to density matrices far in the past than to the density matrix just an instant ago. In the most extreme case, we would approximate

$C_{\alpha\beta}(t_1, t_2) \approx \Gamma_{\alpha\beta}\delta(t_1 - t_2)$, but we will be cautious here and assume that only the density matrix varies slower than the decay time of the bath correlation functions. Therefore, we replace in the r.h.s. $\boldsymbol{\rho}_\mathbf{S}(t') \to \boldsymbol{\rho}_\mathbf{S}(t)$ (**first Markov approximation**), which yields in Eq. (2.14)

$$\dot{\boldsymbol{\rho}}_\mathbf{S} = -\int_0^t \mathrm{Tr}_\mathrm{B}\left\{[\boldsymbol{\mathcal{H}}_\mathbf{I}(t), [\boldsymbol{\mathcal{H}}_\mathbf{I}(t'), \boldsymbol{\rho}_\mathbf{S}(t) \otimes \bar{\rho}_\mathrm{B}]]\right\} dt' \tag{2.22}$$

This equation is often called **Born-Redfield** equation. It is time-local and preserves trace and hermiticity, but still has time-dependent coefficients (also when transforming back from the interaction picture). We substitute $\tau = t - t'$

$$\begin{aligned}\dot{\boldsymbol{\rho}}_\mathbf{S} &= -\int_0^t \mathrm{Tr}_\mathrm{B}\left\{[\boldsymbol{\mathcal{H}}_\mathbf{I}(t), [\boldsymbol{\mathcal{H}}_\mathbf{I}(t-\tau), \boldsymbol{\rho}_\mathbf{S}(t) \otimes \bar{\rho}_\mathrm{B}]]\right\} d\tau \qquad (2.23)\\ &= -\sum_{\alpha\beta}\int_0^t \left\{C_{\alpha\beta}(\tau)\left[\boldsymbol{A}_{\boldsymbol{\alpha}}(t), \boldsymbol{A}_{\boldsymbol{\beta}}(t-\tau)\boldsymbol{\rho}_\mathbf{S}(t)\right] + C_{\beta\alpha}(-\tau)\left[\boldsymbol{\rho}_\mathbf{S}(t)\boldsymbol{A}_{\boldsymbol{\beta}}(t-\tau), \boldsymbol{A}_{\boldsymbol{\alpha}}(t)\right]\right\} d\tau\end{aligned}$$

The problem that the r.h.s. still depends on time is removed by extending the integration bounds to infinity (**second Markov approximation**) – by the same reasoning that the bath correlation functions decay rapidly

$$\dot{\boldsymbol{\rho}}_\mathbf{S} = -\int_0^\infty \mathrm{Tr}_\mathrm{B}\left\{[\boldsymbol{\mathcal{H}}_\mathbf{I}(t), [\boldsymbol{\mathcal{H}}_\mathbf{I}(t-\tau), \boldsymbol{\rho}_\mathbf{S}(t) \otimes \bar{\rho}_\mathrm{B}]]\right\} d\tau\,. \tag{2.24}$$

This equation is called the **Markovian master equation**, which in the original Schrödinger picture

$$\begin{aligned}\dot{\rho}_\mathrm{S} &= -\mathrm{i}\left[\mathcal{H}_\mathrm{S}, \rho_\mathrm{S}(t)\right] - \sum_{\alpha\beta}\int_0^\infty C_{\alpha\beta}(\tau)\left[A_\alpha, e^{-\mathrm{i}\mathcal{H}_\mathrm{S}\tau}A_\beta e^{+\mathrm{i}\mathcal{H}_\mathrm{S}\tau}\rho_\mathrm{S}(t)\right] d\tau\\ &\quad -\sum_{\alpha\beta}\int_0^\infty C_{\beta\alpha}(-\tau)\left[\rho_\mathrm{S}(t)e^{-\mathrm{i}\mathcal{H}_\mathrm{S}\tau}A_\beta e^{+\mathrm{i}\mathcal{H}_\mathrm{S}\tau}, A_\alpha\right] d\tau \qquad (2.25)\end{aligned}$$

is time-local, preserves trace and hermiticity, and has constant coefficients – best prerequisites for treatment with established solution methods.

Exercise 17 (Properties of the Markovian Master Equation) *(1 points)*
Show that the Markovian Master equation (2.25) preserves trace and hermiticity of the density matrix.

In addition, it can be obtained easily from the coupling Hamiltonian: We have so far not used that the coupling operators should be hermitian, and the above form is therefore also valid for non-hermitian coupling operators.

There is just one problem left: In the general case, it is not of Lindblad form. Note that there are specific cases where the Markovian master equation is of Lindblad form, but these rather include simple limits. Though this is sometimes considered a rather cosmetic drawback, it may lead to unphysical results such as negative probabilities.

Secular Approximation

To generally obtain a Lindblad type master equation, a further approximation is required. The **secular approximation** involves an averaging over fast oscillating terms, but in order to identify the oscillating terms, it is necessary to at least formally calculate the interaction picture dynamics of the system coupling operators. We begin by writing Eq. (2.25) in the interaction picture again explicitly – now using the hermiticity of the coupling operators

$$\begin{aligned}
\dot{\boldsymbol{\rho}}_{\mathbf{S}} &= -\int_0^\infty \sum_{\alpha\beta} \left\{ C_{\alpha\beta}(\tau) \left[\boldsymbol{A}_{\boldsymbol{\alpha}}(t), \boldsymbol{A}_{\boldsymbol{\beta}}(t-\tau)\boldsymbol{\rho}_{\mathbf{S}}(t) \right] + \text{h.c.} \right\} d\tau \\
&= +\int_0^\infty \sum_{\alpha\beta} C_{\alpha\beta}(\tau) \sum_{a,b,c,d} \Big\{ |a\rangle \langle a| \boldsymbol{A}_{\boldsymbol{\beta}}(t-\tau) |b\rangle \langle b| \boldsymbol{\rho}_{\mathbf{S}}(t) |d\rangle \langle d| \boldsymbol{A}_{\boldsymbol{\alpha}}(t) |c\rangle \langle c| \\
&\quad - |d\rangle \langle d| \boldsymbol{A}_{\boldsymbol{\alpha}}(t) |c\rangle \langle c| |a\rangle \langle a| \boldsymbol{A}_{\boldsymbol{\beta}}(t-\tau) |b\rangle \langle b| \boldsymbol{\rho}_{\mathbf{S}}(t) \Big\} d\tau + \text{h.c.}\,, \qquad (2.26)
\end{aligned}$$

where we have introduced the system energy eigenbasis

$$\mathcal{H}_{\mathrm{S}} |a\rangle = E_a |a\rangle \ . \qquad (2.27)$$

We can use this eigenbasis to make the time-dependence of the coupling operators in the interaction picture explicit. To reduce the notational effort, we abbreviate $A_\alpha^{ab} = \langle a| A_\alpha |b\rangle$ and $L_{ab} = |a\rangle \langle b|$. Then, the density matrix becomes

$$\begin{aligned}
\dot{\boldsymbol{\rho}}_{\mathbf{S}} &= +\int_0^\infty \sum_{\alpha\beta} C_{\alpha\beta}(\tau) \sum_{a,b,c,d} \Big\{ e^{+\mathrm{i}(E_a-E_b)(t-\tau)} e^{+\mathrm{i}(E_d-E_c)t} A_\beta^{ab} A_\alpha^{dc} L_{ab} \boldsymbol{\rho}_{\mathbf{S}}(t) L_{cd}^\dagger \\
&\quad - e^{+\mathrm{i}(E_a-E_b)(t-\tau)} e^{+\mathrm{i}(E_d-E_c)t} A_\beta^{ab} A_\alpha^{dc} L_{cd}^\dagger L_{ab} \boldsymbol{\rho}_{\mathbf{S}}(t) \Big\} d\tau + \text{h.c.}\,, \\
&= \sum_{\alpha\beta} \sum_{a,b,c,d} \int_0^\infty C_{\alpha\beta}(\tau) e^{+\mathrm{i}(E_b-E_a)\tau} d\tau e^{-\mathrm{i}(E_b-E_a-(E_d-E_c))t} A_\beta^{ab} (A_\alpha^{cd})^* \Big\{ L_{ab} \boldsymbol{\rho}_{\mathbf{S}}(t) L_{cd}^\dagger - L_{cd}^\dagger L_{ab} \boldsymbol{\rho}_{\mathbf{S}}(t) \Big\} \\
&\quad + \text{h.c.} \qquad (2.28)
\end{aligned}$$

The **secular approximation** now involves neglecting all terms that are oscillatory in time t (long-time average), i.e., we have

$$\begin{aligned}
\dot{\boldsymbol{\rho}}_{\mathbf{S}} &= \sum_{\alpha\beta} \sum_{a,b,c,d} \Gamma_{\alpha\beta}(E_b - E_a) \delta_{E_b-E_a, E_d-E_c} A_\beta^{ab} (A_\alpha^{cd})^* \Big\{ +L_{ab} \boldsymbol{\rho}_{\mathbf{S}}(t) L_{cd}^\dagger - L_{cd}^\dagger L_{ab} \boldsymbol{\rho}_{\mathbf{S}}(t) \Big\} \\
&\quad + \sum_{\alpha\beta} \sum_{a,b,c,d} \Gamma_{\alpha\beta}^*(E_b - E_a) \delta_{E_b-E_a, E_d-E_c} (A_\beta^{ab})^* A_\alpha^{cd} \Big\{ +L_{cd} \boldsymbol{\rho}_{\mathbf{S}}(t) L_{ab}^\dagger - \boldsymbol{\rho}_{\mathbf{S}}(t) L_{ab}^\dagger L_{cd} \Big\} \qquad (2.29)
\end{aligned}$$

where we have introduced the half-sided Fourier transform of the bath correlation functions

$$\Gamma_{\alpha\beta}(\omega) = \int_0^\infty C_{\alpha\beta}(\tau) e^{+i\omega\tau} d\tau \,. \qquad (2.30)$$

This equation preserves trace, hermiticity, and positivity of the density matrix and hence all desired properties, since it is of Lindblad form (which will be shown later). Unfortunately, it is typically

not so easy to obtain as it requires diagonalization of the system Hamiltonian first. By using the transformations $\alpha \leftrightarrow \beta$, $a \leftrightarrow c$, and $b \leftrightarrow d$ in the second line and also using that the δ-function is symmetric, we may rewrite the master equation as

$$\begin{aligned}\dot{\boldsymbol{\rho}}_{\mathbf{S}} &= \sum_{\alpha\beta}\sum_{a,b,c,d}\left[\Gamma_{\alpha\beta}(E_b-E_a)+\Gamma^*_{\beta\alpha}(E_b-E_a)\right]\delta_{E_b-E_a,E_d-E_c}A^{ab}_{\beta}(A^{cd}_{\alpha})^*L_{ab}\boldsymbol{\rho}_{\mathbf{S}}(t)L^\dagger_{cd}\\ &-\sum_{\alpha\beta}\sum_{a,b,c,d}\Gamma_{\alpha\beta}(E_b-E_a)\delta_{E_b-E_a,E_d-E_c}A^{ab}_{\beta}(A^{cd}_{\alpha})^*L^\dagger_{cd}L_{ab}\boldsymbol{\rho}_{\mathbf{S}}(t)\\ &-\sum_{\alpha\beta}\sum_{a,b,c,d}\Gamma^*_{\beta\alpha}(E_b-E_a)\delta_{E_b-E_a,E_d-E_c}A^{ab}_{\beta}(A^{cd}_{\alpha})^*\boldsymbol{\rho}_{\mathbf{S}}(t)L^\dagger_{cd}L_{ab}\,. \end{aligned} \tag{2.31}$$

We split the matrix-valued function $\Gamma_{\alpha\beta}(\omega)$ into hermitian and anti-hermitian parts

$$\begin{aligned}\Gamma_{\alpha\beta}(\omega) &= \frac{1}{2}\gamma_{\alpha\beta}(\omega)+\frac{1}{2}\sigma_{\alpha\beta}(\omega)\,,\\ \Gamma^*_{\beta\alpha}(\omega) &= \frac{1}{2}\gamma_{\alpha\beta}(\omega)-\frac{1}{2}\sigma_{\alpha\beta}(\omega)\,,\end{aligned} \tag{2.32}$$

with hermitian $\gamma_{\alpha\beta}(\omega)=\gamma^*_{\beta\alpha}(\omega)$ and anti-hermitian $\sigma_{\alpha\beta}(\omega)=-\sigma^*_{\beta\alpha}(\omega)$. These new functions can be interpreted as full even and odd Fourier transforms of the bath correlation functions

$$\begin{aligned}\gamma_{\alpha\beta}(\omega) &= \Gamma_{\alpha\beta}(\omega)+\Gamma^*_{\beta\alpha}(\omega)=\int_{-\infty}^{+\infty}C_{\alpha\beta}(\tau)e^{+\mathrm{i}\omega\tau}d\tau\,,\\ \sigma_{\alpha\beta}(\omega) &= \Gamma_{\alpha\beta}(\omega)-\Gamma^*_{\beta\alpha}(\omega)=\int_{-\infty}^{+\infty}C_{\alpha\beta}(\tau)\mathrm{sgn}(\tau)\mathrm{e}^{+\mathrm{i}\omega\tau}\mathrm{d}\tau\,.\end{aligned} \tag{2.33}$$

Exercise 18 (Odd Fourier Transform) *(1 points)*
Show that the odd Fourier transform $\sigma_{\alpha\beta}(\omega)$ may be obtained from the even Fourier transform $\gamma_{\alpha\beta}(\omega)$ by a Cauchy principal value integral

$$\sigma_{\alpha\beta}(\omega)=\frac{\mathrm{i}}{\pi}\mathcal{P}\int_{-\infty}^{+\infty}\frac{\gamma_{\alpha\beta}(\Omega)}{\omega-\Omega}d\Omega\,.$$

In the master equation, these replacements lead to

$$\begin{aligned}\dot{\boldsymbol{\rho}}_{\mathbf{S}} &= \sum_{\alpha\beta}\sum_{a,b,c,d}\gamma_{\alpha\beta}(E_b-E_a)\delta_{E_b-E_a,E_d-E_c}A^{ab}_{\beta}(A^{cd}_{\alpha})^*\left[L_{ab}\boldsymbol{\rho}_{\mathbf{S}}(t)L^\dagger_{cd}-\frac{1}{2}\left\{L^\dagger_{cd}L_{ab},\boldsymbol{\rho}_{\mathbf{S}}(t)\right\}\right]\\ &-\mathrm{i}\sum_{\alpha\beta}\sum_{a,b,c,d}\frac{1}{2\mathrm{i}}\sigma_{\alpha\beta}(E_b-E_a)\delta_{E_b-E_a,E_d-E_c}A^{ab}_{\beta}(A^{cd}_{\alpha})^*\left[L^\dagger_{cd}L_{ab},\boldsymbol{\rho}_{\mathbf{S}}(t)\right]\\ &= \sum_{\alpha\beta}\sum_{a,b,c,d}\gamma_{\alpha\beta}(E_b-E_a)\delta_{E_b-E_a,E_d-E_c}A^{ab}_{\beta}(A^{cd}_{\alpha})^*\left[L_{ab}\boldsymbol{\rho}_{\mathbf{S}}(t)L^\dagger_{cd}-\frac{1}{2}\left\{L^\dagger_{cd}L_{ab},\boldsymbol{\rho}_{\mathbf{S}}(t)\right\}\right]\\ &-\mathrm{i}\left[\sum_{\alpha\beta}\sum_{a,b,c}\frac{1}{2\mathrm{i}}\sigma_{\alpha\beta}(E_b-E_c)\delta_{E_b,E_a}A^{cb}_{\beta}(A^{ca}_{\alpha})^*L_{ab},\boldsymbol{\rho}_{\mathbf{S}}(t)\right]\,.\end{aligned} \tag{2.34}$$

To prove that we have a Lindblad form, it is easy to see first that the term in the commutator

$$H_{\rm LS} = \sum_{\alpha\beta}\sum_{a,b,c}\frac{1}{2{\rm i}}\sigma_{\alpha\beta}(E_b-E_c)\delta_{E_b,E_a}A^{cb}_\beta(A^{ca}_\alpha)^*\left|a\right\rangle\left\langle b\right| \tag{2.35}$$

is an effective Hamiltonian. This Hamiltonian is often called Lamb-shift Hamiltonian, since it renormalizes the system Hamiltonian due to the interaction with the reservoir. Note that we have $[\mathcal{H}_{\rm S}, H_{\rm LS}] = 0$.

Exercise 19 (Lamb-shift) *(1 points)*
Show that $H_{\rm LS} = H^\dagger_{\rm LS}$ *and* $[H_{\rm LS}, \mathcal{H}_{\rm S}] = 0$.

To show the Lindblad-form of the non-unitary evolution, we identify the Lindblad jump operator $L_\alpha = \left|a\right\rangle\left\langle b\right| = L_{(a,b)}$. For an N-dimensional system Hilbert space with N eigenvectors of $\mathcal{H}_{\rm S}$ we would have N^2 such jump operators, but the identity matrix $\mathbf{1} = \sum_a \left|a\right\rangle\left\langle a\right|$ has trivial action, which can be used to eliminate one jump operator. It remains to be shown that the matrix

$$\gamma_{(ab),(cd)} = \sum_{\alpha\beta}\gamma_{\alpha\beta}(E_b-E_a)\delta_{E_b-E_a,E_d-E_c}A^{ab}_\beta(A^{cd}_\alpha)^* \tag{2.36}$$

is non-negative, i.e., $\sum_{a,b,c,d} x^*_{ab}\gamma_{(ab),(cd)}x_{cd} \geq 0$ for all x_{ab}. We first note that for hermitian coupling operators the Fourier transform matrix at fixed ω is positive (recall that $B_\alpha = B^\dagger_\alpha$ and $[\bar\rho_{\rm B}, \mathcal{H}_{\rm B}] = 0$)

$$\begin{aligned}
\Gamma &= \sum_{\alpha\beta} x^*_\alpha\gamma_{\alpha\beta}(\omega)x_\beta \\
&= \int_{-\infty}^{+\infty} d\tau e^{+{\rm i}\omega\tau}{\rm Tr}\left\{e^{{\rm i}\mathcal{H}_{\rm S}\tau}\left[\sum_\alpha x^*_\alpha B_\alpha\right]e^{-{\rm i}\mathcal{H}_{\rm S}\tau}\left[\sum_\beta x_\beta B_\beta\right]\bar\rho_{\rm B}\right\} \\
&= \int_{-\infty}^{+\infty} d\tau e^{+{\rm i}\omega\tau}\sum_{nm} e^{+{\rm i}(E_n-E_m)\tau}\left\langle n\right|B^\dagger\left|m\right\rangle\left\langle m\right|B\bar\rho_{\rm B}\left|n\right\rangle \\
&= \sum_{nm} 2\pi\delta(\omega+E_n-E_m)|\left\langle m\right|B\left|n\right\rangle|^2\rho_n \\
&\geq 0\,.
\end{aligned} \tag{2.37}$$

Now, we replace the Kronecker symbol in the dampening coefficients by two via the introduction of an auxiliary summation

$$\begin{aligned}
\tilde\Gamma &= \sum_{abcd} x^*_{ab}\gamma_{(ab),(cd)}x_{cd} \\
&= \sum_\omega\sum_{\alpha\beta}\sum_{abcd}\gamma_{\alpha\beta}(\omega)\delta_{E_b-E_a,\omega}\delta_{E_d-E_c,\omega}x^*_{ab}\left\langle a\right|A_\beta\left|b\right\rangle x_{cd}\left\langle c\right|A_\alpha\left|d\right\rangle^* \\
&= \sum_\omega\sum_{\alpha\beta}\left[\sum_{cd} x_{cd}\left\langle c\right|A_\alpha\left|d\right\rangle^*\delta_{E_d-E_c,\omega}\right]\gamma_{\alpha\beta}(\omega)\left[\sum_{ab} x^*_{ab}\left\langle a\right|A_\beta\left|b\right\rangle\delta_{E_b-E_a,\omega}\right] \\
&= \sum_\omega\sum_{\alpha\beta} y^*_\alpha(\omega)\gamma_{\alpha\beta}(\omega)y_\beta(\omega) \geq 0\,.
\end{aligned} \tag{2.38}$$

Transforming Eq. (2.34) back to the Schrödinger picture (note that the δ-functions prohibit the occurrence of oscillatory factors), we finally obtain the Born-Markov-secular master equation.

Box 8 (BMS master equation) *In the weak coupling limit, an interaction Hamiltonian of the form* $\mathcal{H}_{\rm I} = \sum_\alpha A_\alpha \otimes B_\alpha$ *with hermitian coupling operators (*$A_\alpha = A_\alpha^\dagger$ *and* $B_\alpha = B_\alpha^\dagger$*) and* $[\mathcal{H}_{\rm B}, \bar{\rho}_{\rm B}] = 0$ *and* $\mathrm{Tr}\{B_\alpha \bar{\rho}_{\rm B}\} = 0$ *leads in the system energy eigenbasis* $\mathcal{H}_{\rm S}|a\rangle = E_a|a\rangle$ *to the Lindblad-form master equation*

$$\begin{aligned}
\dot{\rho}_{\rm S} &= -\mathrm{i}\left[\mathcal{H}_{\rm S} + \sum_{ab} \sigma_{ab} |a\rangle\langle b|, \rho_{\rm S}(t)\right] \\
&\quad + \sum_{a,b,c,d} \gamma_{ab,cd}\left[|a\rangle\langle b| \boldsymbol{\rho}_{\mathbf{S}}(t) (|c\rangle\langle d|)^\dagger - \frac{1}{2}\left\{(|c\rangle\langle d|)^\dagger |a\rangle\langle b|, \boldsymbol{\rho}_{\mathbf{S}}(t)\right\}\right], \\
\gamma_{ab,cd} &= \sum_{\alpha\beta} \gamma_{\alpha\beta}(E_b - E_a)\delta_{E_b - E_a, E_d - E_c} \langle a|A_\beta|b\rangle \langle c|A_\alpha|d\rangle^*, \qquad (2.39)
\end{aligned}$$

where the Lamb-shift Hamiltonian $H_{\rm LS} = \sum_{ab} \sigma_{ab}|a\rangle\langle b|$ *matrix elements read*

$$\sigma_{ab} = \sum_{\alpha\beta}\sum_c \frac{1}{2\mathrm{i}} \sigma_{\alpha\beta}(E_b - E_c)\delta_{E_b,E_a} \langle c|A_\beta|b\rangle \langle c|A_\alpha|a\rangle^* \qquad (2.40)$$

and the constants are given by even and odd Fourier transforms

$$\begin{aligned}
\gamma_{\alpha\beta}(\omega) &= \int_{-\infty}^{+\infty} C_{\alpha\beta}(\tau) e^{+\mathrm{i}\omega\tau} d\tau, \\
\sigma_{\alpha\beta}(\omega) &= \int_{-\infty}^{+\infty} C_{\alpha\beta}(\tau)\mathrm{sgn}(\tau)\mathrm{e}^{+\mathrm{i}\omega\tau}\mathrm{d}\tau = \frac{\mathrm{i}}{\pi}\mathcal{P}\int_{-\infty}^{+\infty} \frac{\gamma_{\alpha\beta}(\omega')}{\omega - \omega'}\mathrm{d}\omega' \qquad (2.41)
\end{aligned}$$

of the bath correlation functions

$$C_{\alpha\beta}(\tau) = \mathrm{Tr}\left\{e^{+\mathrm{i}\mathcal{H}_{\rm B}\tau} B_\alpha e^{-\mathrm{i}\mathcal{H}_{\rm B}\tau} B_\beta \bar{\rho}_{\rm B}\right\}. \qquad (2.42)$$

The above definition may serve as a recipe to derive a Lindblad type master equation in the weak-coupling limit. It is expected to yield good results in the weak coupling and Markovian limit (continuous and nearly flat bath spectral density) and when $[\bar{\rho}_{\rm B}, \mathcal{H}_{\rm B}] = 0$. It requires to rewrite the coupling operators in hermitian form, the calculation of the bath correlation function Fourier transforms, and the diagonalization of the system Hamiltonian.

In the case that the spectrum of the system Hamiltonian is non-degenerate, we have a further simplification, since the δ-functions simplify further, e.g. $\delta_{E_b,E_a} \to \delta_{ab}$. By taking matrix elements of Eq. (2.39) in the energy eigenbasis $\rho_{aa} = \langle a|\rho_{\rm S}|a\rangle$, we obtain an effective rate equation for the populations only

$$\dot{\rho}_{aa} = +\sum_b \gamma_{ab,ab}\rho_{bb} - \left[\sum_b \gamma_{ba,ba}\right]\rho_{aa}, \qquad (2.43)$$

i.e., the coherences decouple from the evolution of the populations. The transition rates from state b to state a reduce in this case to

$$\gamma_{ab,ab} = \sum_{\alpha\beta} \gamma_{\alpha\beta}(E_b - E_a) \langle a| A_\beta |b\rangle \langle a| A_\alpha |b\rangle^* \geq 0\,, \tag{2.44}$$

which – after inserting all definitions condenses basically to Fermis Golden Rule. Therefore, with such a rate equation description, open quantum systems can be described with the same complexity as closed quantum systems, since only N dynamical variables have to be evolved. The BMS master equation is problematic for near-degenerate systems: For exact degeneracies, couplings to coherences between energetically degenerate states have to be kept, but for lifted degeneracies, they are neglected. This discontinuous behaviour may map to observables and poses the question which of the two resulting equations is correct, in particular for near degeneracies. Despite such problems, the BMS master equation is heavily used since it has many favorable properties. For example, we will see later that if coupled to a single thermal bath, the quantum system generally relaxes to the Gibbs equilibrium, i.e., we obtain simply equilibration of the system temperature with the temperature of the bath.

2.2.2 Coarse-Graining

Perturbation Theory in the Interaction Picture

Although the BMS approximation respects of course the exact initial condition, we have in the derivation made several long-term approximations. For example, the Markov approximation implied that we consider timescales much larger than the decay time of the bath correlation functions. Similarly, the secular approximation implied timescales larger than the inverse minimal splitting of the system energy eigenvalues. Therefore, we can only expect the solution originating from the BMS master equation to be an asymptotically valid long-term approximation.

Coarse-graining in contrast provides a possibility to obtain valid short-time approximations of the density matrix with a generator that is of Lindblad form, see Fig. 2.2. We start with the von-Neumann equation in the interaction picture (2.9). For factorizing initial density matrices, it is formally solved by $\boldsymbol{U}(t)\rho_{\mathrm{S}}^0 \otimes \bar{\rho}_{\mathrm{B}}\boldsymbol{U}^\dagger(t)$, where the time evolution operator

$$\boldsymbol{U}(t) = \hat{\tau} \exp\left\{-\mathrm{i}\int_0^t \boldsymbol{\mathcal{H}}_{\mathbf{I}}(t')dt'\right\} \tag{2.45}$$

obeys the evolution equation

$$\dot{\boldsymbol{U}} = -\mathrm{i}\boldsymbol{\mathcal{H}}_{\mathbf{I}}(t)\boldsymbol{U}(t)\,, \tag{2.46}$$

which defines the time-ordering operator $\hat{\tau}$. Formally integrating this equation with the evident

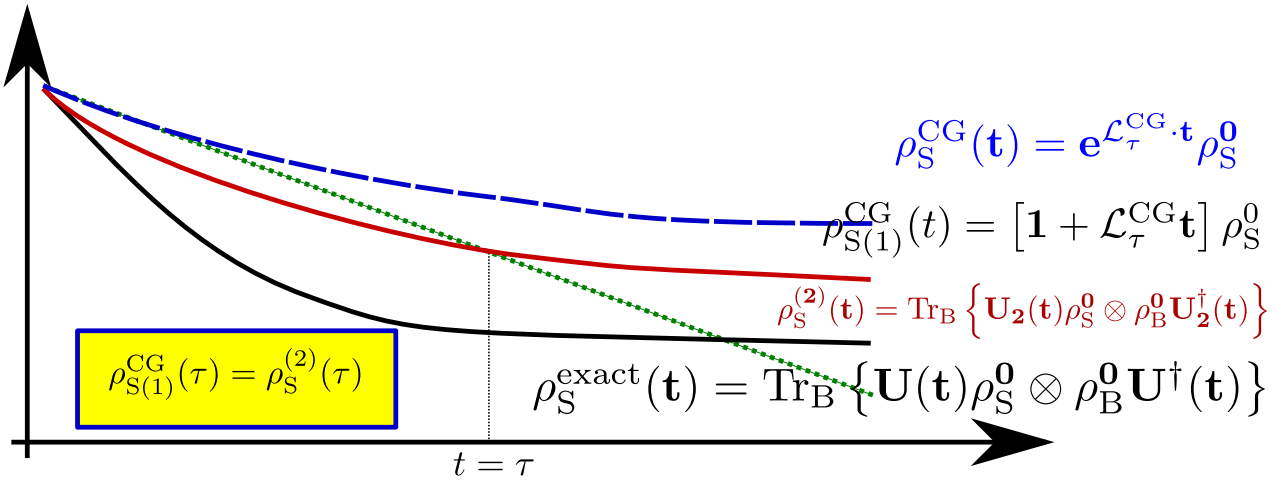

Figure 2.2: Sketch of the coarse-graining perturbation theory. Calculating the exact time evolution operator $\boldsymbol{U}(t) = \tau \exp\left\{-\mathrm{i}\int_0^t \mathcal{H}_{\mathrm{I}}(t')dt'\right\}$ in a closed form is usually prohibitive, which renders the calculation of the exact solution an impossible task (black curve). It is however possible to expand the evolution operator $\mathbf{U_2}(t) = \mathbf{1} - i\int_0^t \boldsymbol{\mathcal{H}}_{\mathbf{I}}(t')dt' - \int_0^t dt_1 dt_2 \boldsymbol{\mathcal{H}}_{\mathbf{I}}(t_1)\boldsymbol{\mathcal{H}}_{\mathbf{I}}(t_2)\Theta(t_1 - t_2)$ to second order in $\boldsymbol{\mathcal{H}}_{\mathbf{I}}$ and to obtain the corresponding reduced approximate density matrix. Calculating the matrix exponential of a constant Lindblad-type generator $\mathcal{L}_\tau^{\mathrm{CG}}$ is also usually prohibitive, but the first order approximation may be matched with $\mathbf{U_2}(t)$ at time $t = \tau$ to obtain a defining equation for $\mathcal{L}_\tau^{\mathrm{CG}}$.

initial condition $\boldsymbol{U}(0) = \mathbf{1}$ yields

$$\begin{aligned}
\boldsymbol{U}(t) &= \mathbf{1} - \mathrm{i}\int_0^t \boldsymbol{\mathcal{H}}_{\mathbf{I}}(t')\boldsymbol{U}(t')dt' \\
&= \mathbf{1} - \mathrm{i}\int_0^t \boldsymbol{\mathcal{H}}_{\mathbf{I}}(t')dt' - \int_0^t dt'\boldsymbol{\mathcal{H}}_{\mathbf{I}}(t')\left[\int_0^{t'} dt''\boldsymbol{\mathcal{H}}_{\mathbf{I}}(\boldsymbol{t''})\boldsymbol{U}(t'')\right] \\
&\approx \mathbf{1} - \mathrm{i}\int_0^t \boldsymbol{\mathcal{H}}_{\mathbf{I}}(t')dt' - \int_0^t dt_1 dt_2 \boldsymbol{\mathcal{H}}_{\mathbf{I}}(t_1)\boldsymbol{\mathcal{H}}_{\mathbf{I}}(t_2)\Theta(t_1 - t_2)\,, \qquad (2.47)
\end{aligned}$$

where the occurrence of the Heaviside function is a consequence of time-ordering. For the hermitian conjugate operator we obtain

$$\boldsymbol{U}^{\dagger}(t) \approx \mathbf{1} + \mathrm{i}\int_0^t \boldsymbol{\mathcal{H}}_{\mathbf{I}}(t')dt' - \int_0^t dt_1 dt_2 \boldsymbol{\mathcal{H}}_{\mathbf{I}}(t_1)\boldsymbol{\mathcal{H}}_{\mathbf{I}}(t_2)\Theta(t_2 - t_1)\,. \qquad (2.48)$$

To keep the discussion at a moderate level, we assume $\mathrm{Tr}\{B_\alpha \bar{\rho}_{\mathrm{B}}\} = 0$ from the beginning. The

exact solution $\boldsymbol{\rho_S(t)} = \mathrm{Tr_B}\left\{\boldsymbol{U}(t)\rho_\mathrm{S}^0 \otimes \bar{\rho}_\mathrm{B}\boldsymbol{U}^\dagger(t)\right\}$ is then approximated by

$$\begin{aligned}
\boldsymbol{\rho_S^{(2)}}(t) &\approx \mathrm{Tr_B}\Big\{ \left[\mathbf{1} - \mathrm{i}\int_0^t \boldsymbol{\mathcal{H}_I}(t_1)dt_1 - \int_0^t dt_1 dt_2 \boldsymbol{\mathcal{H}_I}(t_1)\boldsymbol{\mathcal{H}_I}(t_2)\Theta(t_1-t_2)\right]\rho_\mathrm{S}^0 \otimes \bar{\rho}_\mathrm{B} \times \\
&\quad \times \left[\mathbf{1} + \mathrm{i}\int_0^t \boldsymbol{\mathcal{H}_I}(t_1)dt_1 - \int_0^t dt_1 dt_2 \boldsymbol{\mathcal{H}_I}(t_1)\boldsymbol{\mathcal{H}_I}(t_2)\Theta(t_2-t_1)\right]\Big\} \\
&= \rho_\mathrm{S}^0 + \mathrm{Tr_B}\left\{\int_0^t dt_1 \int_0^t dt_2 \boldsymbol{\mathcal{H}_I}(t_1)\rho_\mathrm{S}^0 \otimes \bar{\rho}_\mathrm{B}\boldsymbol{\mathcal{H}_I}(t_2)\right\} \\
&\quad - \int_0^t dt_1 dt_2 \mathrm{Tr_B}\left\{\Theta(t_1-t_2)\boldsymbol{\mathcal{H}_I}(t_1)\boldsymbol{\mathcal{H}_I}(t_2)\rho_\mathrm{S}^0 \otimes \bar{\rho}_\mathrm{B} + \Theta(t_2-t_1)\rho_\mathrm{S}^0 \otimes \bar{\rho}_\mathrm{B}\boldsymbol{\mathcal{H}_I}(t_1)\boldsymbol{\mathcal{H}_I}(t_2)\right\} .
\end{aligned} \tag{2.49}$$

Again, we introduce the bath correlation functions with two time arguments as in Eq. (2.19)

$$C_{\alpha\beta}(t_1,t_2) = \mathrm{Tr}\left\{\boldsymbol{B_\alpha}(t_1)\boldsymbol{B_\beta}(t_2)\bar{\rho}_\mathrm{B}\right\} , \tag{2.50}$$

such that we have

$$\begin{aligned}
\boldsymbol{\rho_S^{(2)}}(t) &= \rho_\mathrm{S}^0 + \sum_{\alpha\beta}\int_0^t dt_1 \int_0^t dt_2 C_{\alpha\beta}(t_1,t_2)\Big[\boldsymbol{A_\beta}(t_2)\rho_\mathrm{S}^0\boldsymbol{A_\alpha}(t_1) \\
&\quad -\Theta(t_1-t_2)\boldsymbol{A_\alpha}(t_1)\boldsymbol{A_\beta}(t_2)\rho_\mathrm{S}^0 - \Theta(t_2-t_1)\rho_\mathrm{S}^0\boldsymbol{A_\alpha}(t_1)\boldsymbol{A_\beta}(t_2)\Big] .
\end{aligned} \tag{2.51}$$

Typically, in the interaction picture, the system coupling operators $\boldsymbol{A_\alpha}(t)$ will simply carry some oscillatory time dependence. In the worst case, they may remain time-independent. Therefore, the decay of the correlation function is essential for the convergence of the above integrals. In particular, we note that the truncated density matrix may remain finite even when $t \to \infty$, rendering the expansion convergent also in the long-term limit.

Coarse-Graining

The basic idea of **coarse-graining** is to match this approximate expression for the system density matrix at time $t = \tau$ with one resulting from a Markovian generator

$$\boldsymbol{\rho_S}^{\mathrm{CG}}(\tau) = e^{\mathcal{L}_\tau^{\mathrm{CG}}\cdot\tau}\rho_\mathrm{S}^0 \approx \rho_\mathrm{S}^0 + \tau\mathcal{L}_\tau^{\mathrm{CG}}\rho_\mathrm{S}^0 , \tag{2.52}$$

such that we can infer the action of the generator on an arbitrary density matrix

$$\begin{aligned}\mathcal{L}_\tau^{\rm CG}\boldsymbol{\rho_{\rm S}} &= \frac{1}{\tau}\sum_{\alpha\beta}\int_0^\tau dt_1\int_0^\tau dt_2 C_{\alpha\beta}(t_1,t_2)\Big[\boldsymbol{A_\beta}(t_2)\boldsymbol{\rho_{\rm S}}\boldsymbol{A_\alpha}(t_1)\\ &\quad -\Theta(t_1-t_2)\boldsymbol{A_\alpha}(t_1)\boldsymbol{A_\beta}(t_2)\boldsymbol{\rho_{\rm S}}-\Theta(t_2-t_1)\boldsymbol{\rho_{\rm S}}\boldsymbol{A_\alpha}(t_1)\boldsymbol{A_\beta}(t_2)\Big]\\ &= -{\rm i}\left[\frac{1}{2{\rm i}\tau}\int_0^\tau dt_1\int_0^\tau dt_2\sum_{\alpha\beta}C_{\alpha\beta}(t_1,t_2){\rm sgn}({\rm t}_1-{\rm t}_2)\boldsymbol{A_\alpha}({\rm t}_1)\boldsymbol{A_\beta}({\rm t}_2),\boldsymbol{\rho_{\rm S}}\right]\\ &\quad +\frac{1}{\tau}\int_0^\tau dt_1\int_0^\tau dt_2\sum_{\alpha\beta}C_{\alpha\beta}(t_1,t_2)\left[\boldsymbol{A_\beta}(t_2)\boldsymbol{\rho_{\rm S}}\boldsymbol{A_\alpha}(t_1)-\frac{1}{2}\left\{\boldsymbol{A_\alpha}(t_1)\boldsymbol{A_\beta}(t_2),\boldsymbol{\rho_{\rm S}}\right\}\right] \quad (2.53)\end{aligned}$$

where we have inserted $\Theta(x)=\frac{1}{2}\left[1+{\rm sgn(x)}\right]$ – in order to separate unitary and dissipative effects of the system-reservoir interaction.

Box 9 (CG Master Equation) *In the weak coupling limit, an interaction Hamiltonian of the form $\mathcal{H}_{\rm I}=\sum_\alpha A_\alpha\otimes B_\alpha$ leads to the Lindblad-form master equation in the interaction picture*

$$\begin{aligned}\dot{\boldsymbol{\rho}}_{\rm S} &= -{\rm i}\left[\frac{1}{2{\rm i}\tau}\int_0^\tau dt_1\int_0^\tau dt_2\sum_{\alpha\beta}C_{\alpha\beta}(t_1,t_2){\rm sgn}({\rm t}_1-{\rm t}_2)\boldsymbol{A_\alpha}({\rm t}_1)\boldsymbol{A_\beta}({\rm t}_2),\boldsymbol{\rho_{\rm S}}\right]\\ &\quad +\frac{1}{\tau}\int_0^\tau dt_1\int_0^\tau dt_2\sum_{\alpha\beta}C_{\alpha\beta}(t_1,t_2)\left[\boldsymbol{A_\beta}(t_2)\boldsymbol{\rho_{\rm S}}\boldsymbol{A_\alpha}(t_1)-\frac{1}{2}\left\{\boldsymbol{A_\alpha}(t_1)\boldsymbol{A_\beta}(t_2),\boldsymbol{\rho_{\rm S}}\right\}\right],\end{aligned}$$

where the bath correlation functions are given by

$$C_{\alpha\beta}(t_t,t_2) = {\rm Tr}\left\{e^{+{\rm i}\mathcal{H}_{\rm B}t_1}B_\alpha e^{-{\rm i}\mathcal{H}_{\rm B}t_1}e^{+{\rm i}\mathcal{H}_{\rm B}t_2}B_\beta e^{-{\rm i}\mathcal{H}_{\rm B}t_2}\bar{\rho}_{\rm B}\right\}. \quad (2.54)$$

We have not used hermiticity of the coupling operators nor that the bath correlation functions do typically only depend on a single argument. However, if the coupling operators were chosen hermitian, it is easy to show the Lindblad form. For completeness, we also note there that a Lindblad form is also obtained for non-hermitian couplings. Obtaining the master equation requires the calculation of bath correlation functions and the evolution of the coupling operators in the interaction picture.

Exercise 20 (Lindblad form) *(1 point)*
By assuming hermitian coupling operators $A_\alpha=A_\alpha^\dagger$, show that the CG master equation is of Lindblad form for all coarse-graining times τ.

Correspondence to the quantum-optical master equation

Let us make once more the time-dependence of the coupling operators explicit, which is most conveniently done in the system energy eigenbasis. Now, we also assume that the bath correlation functions only depend on the difference of their time arguments $C_{\alpha\beta}(t_1,t_2)=C_{\alpha\beta}(t_1-t_2)$, such that we may use the Fourier transform definitions in Eq. (2.33) to obtain

$$\begin{aligned}
\dot{\boldsymbol{\rho}}_{\mathbf{S}} &= -\mathrm{i}\left[\frac{1}{2\mathrm{i}\tau}\sum_{abc}\int_0^\tau dt_1\int_0^\tau dt_2\sum_{\alpha\beta}C_{\alpha\beta}(t_1-t_2)\mathrm{sgn}(\mathrm{t}_1-\mathrm{t}_2)\left|\mathrm{a}\right\rangle\left\langle\mathrm{a}\right|\boldsymbol{A}_{\boldsymbol{\alpha}}(\mathrm{t}_1)\left|\mathrm{c}\right\rangle\left\langle\mathrm{c}\right|\boldsymbol{A}_{\boldsymbol{\beta}}(\mathrm{t}_2)\left|\mathrm{b}\right\rangle\left\langle\mathrm{b}\right|,\boldsymbol{\rho}_{\mathbf{S}}\right]\\
&\quad+\frac{1}{\tau}\int_0^\tau dt_1\int_0^\tau dt_2\sum_{\alpha\beta}\sum_{abcd}C_{\alpha\beta}(t_1-t_2)\Big[\left|a\right\rangle\left\langle a\right|\boldsymbol{A}_{\boldsymbol{\beta}}(t_2)\left|b\right\rangle\left\langle b\right|\boldsymbol{\rho}_{\mathbf{S}}\left|d\right\rangle\left\langle d\right|\boldsymbol{A}_{\boldsymbol{\alpha}}(t_1)\left|c\right\rangle\left\langle c\right|\\
&\quad-\frac{1}{2}\left\{\left|d\right\rangle\left\langle d\right|\boldsymbol{A}_{\boldsymbol{\alpha}}(t_1)\left|c\right\rangle\left\langle c\right|\cdot\left|a\right\rangle\left\langle a\right|\boldsymbol{A}_{\boldsymbol{\beta}}(t_2)\left|b\right\rangle\left\langle b\right|,\boldsymbol{\rho}_{\mathbf{S}}\right\}\Big]\\
&= -\mathrm{i}\frac{1}{4\mathrm{i}\pi\tau}\int d\omega\sum_{abc}\int_0^\tau dt_1\int_0^\tau dt_2\sum_{\alpha\beta}\sigma_{\alpha\beta}(\omega)e^{-\mathrm{i}\omega(t_1-t_2)}e^{+\mathrm{i}(E_a-E_c)t_1}e^{+\mathrm{i}(E_c-E_b)t_2}A_\beta^{cb}A_\alpha^{ac}\left[L_{ab},\boldsymbol{\rho}_{\mathbf{S}}\right]\\
&\quad+\frac{1}{2\pi\tau}\int d\omega\int_0^\tau dt_1\int_0^\tau dt_2\sum_{\alpha\beta}\sum_{abcd}\gamma_{\alpha\beta}(\omega)e^{-\mathrm{i}\omega(t_1-t_2)}e^{+\mathrm{i}(E_a-E_b)t_2}e^{+\mathrm{i}(E_d-E_c)t_1}A_\beta^{ab}A_\alpha^{dc}\times\\
&\quad\times\left[L_{ab}\boldsymbol{\rho}_{\mathbf{S}}L_{cd}^\dagger-\frac{1}{2}\left\{L_{cd}^\dagger L_{ab},\boldsymbol{\rho}_{\mathbf{S}}\right\}\right].
\end{aligned}\tag{2.55}$$

We perform the temporal integrations by invoking

$$\int_0^\tau e^{\mathrm{i}\alpha_k t_k}dt_k=\tau e^{\mathrm{i}\alpha_k\tau/2}\mathrm{sinc}\left[\frac{\alpha_\mathrm{k}\tau}{2}\right]\tag{2.56}$$

with $\mathrm{sinc(x)}=\mathrm{sin(x)/x}$ to obtain

$$\begin{aligned}
\dot{\boldsymbol{\rho}}_{\mathbf{S}} &= -\mathrm{i}\frac{\tau}{4\mathrm{i}\pi}\int d\omega\sum_{abc}\sum_{\alpha\beta}\sigma_{\alpha\beta}(\omega)e^{\mathrm{i}\tau(E_a-E_b)/2}\mathrm{sinc}\left[\frac{\tau}{2}(\mathrm{E_a}-\mathrm{E_c}-\omega)\right]\mathrm{sinc}\left[\frac{\tau}{2}(\mathrm{E_c}-\mathrm{E_b}+\omega)\right]\times\\
&\quad\times\left\langle c\right|A_\beta\left|b\right\rangle\left\langle c\right|A_\alpha^\dagger\left|a\right\rangle^*\left[\left|a\right\rangle\left\langle b\right|,\boldsymbol{\rho}_{\mathbf{S}}\right]\\
&\quad+\frac{\tau}{2\pi}\int d\omega\sum_{\alpha\beta}\sum_{abcd}\gamma_{\alpha\beta}(\omega)e^{\mathrm{i}\tau(E_a-E_b+E_d-E_c)/2}\mathrm{sinc}\left[\frac{\tau}{2}(\mathrm{E_d}-\mathrm{E_c}-\omega)\right]\mathrm{sinc}\left[\frac{\tau}{2}(\omega+\mathrm{E_a}-\mathrm{E_b})\right]\times\\
&\quad\times\left\langle a\right|A_\beta\left|b\right\rangle\left\langle c\right|A_\alpha^\dagger\left|d\right\rangle^*\left[\left|a\right\rangle\left\langle b\right|\boldsymbol{\rho}_{\mathbf{S}}\left(\left|c\right\rangle\left\langle d\right|\right)^\dagger-\frac{1}{2}\left\{\left(\left|c\right\rangle\left\langle d\right|\right)^\dagger\left|a\right\rangle\left\langle b\right|,\boldsymbol{\rho}_{\mathbf{S}}\right\}\right].
\end{aligned}\tag{2.57}$$

Therefore, we have the same structure as before, but now with coarse-graining time dependent dampening coefficients

$$\begin{aligned}
\dot{\boldsymbol{\rho}}_{\mathbf{S}} &= -\mathrm{i}\left[\sum_{ab}\sigma_{ab}^\tau\left|a\right\rangle\left\langle b\right|,\boldsymbol{\rho}_{\mathbf{S}}\right]\\
&\quad+\sum_{abcd}\gamma_{ab,cd}^\tau\left[\left|a\right\rangle\left\langle b\right|\boldsymbol{\rho}_{\mathbf{S}}\left(\left|c\right\rangle\left\langle d\right|\right)^\dagger-\frac{1}{2}\left\{\left(\left|c\right\rangle\left\langle d\right|\right)^\dagger\left|a\right\rangle\left\langle b\right|,\boldsymbol{\rho}_{\mathbf{S}}\right\}\right]
\end{aligned}\tag{2.58}$$

with the coefficients

$$\begin{aligned}\sigma^{\tau}_{ab} &= \frac{1}{2\mathrm{i}}\int d\omega \sum_{c} e^{\mathrm{i}\tau(E_a-E_b)/2}\frac{\tau}{2\pi}\mathrm{sinc}\left[\frac{\tau}{2}(\mathrm{E_a}-\mathrm{E_c}-\omega)\right]\mathrm{sinc}\left[\frac{\tau}{2}(\mathrm{E_b}-\mathrm{E_c}-\omega)\right]\times \\ &\quad\times\left[\sum_{\alpha\beta}\sigma_{\alpha\beta}(\omega)\left\langle c\right|A_\beta\left|b\right\rangle\left\langle c\right|A^\dagger_\alpha\left|a\right\rangle^*\right], \\ \gamma^{\tau}_{ab,cd} &= \int d\omega e^{\mathrm{i}\tau(E_a-E_b+E_d-E_c)/2}\frac{\tau}{2\pi}\mathrm{sinc}\left[\frac{\tau}{2}(\mathrm{E_d}-\mathrm{E_c}-\omega)\right]\mathrm{sinc}\left[\frac{\tau}{2}(\mathrm{E_b}-\mathrm{E_a}-\omega)\right]\times \\ &\quad\times\left[\sum_{\alpha\beta}\gamma_{\alpha\beta}(\omega)\left\langle a\right|A_\beta\left|b\right\rangle\left\langle c\right|A^\dagger_\alpha\left|d\right\rangle^*\right]. \end{aligned} \tag{2.59}$$

Finally, we note that in the limit of large coarse-graining times $\tau\to\infty$ and assuming hermitian coupling operators $A_\alpha = A^\dagger_\alpha$, these dampening coefficients converge to the ones in definition 8, i.e., formally

$$\begin{aligned}\lim_{\tau\to\infty}\sigma^{\tau}_{ab} &= \sigma_{ab}\,, \\ \lim_{\tau\to\infty}\gamma^{\tau}_{ab,cd} &= \gamma_{ab,cd}\,. \end{aligned} \tag{2.60}$$

Exercise 21 (CG-BMS correspondence) *(1 points)*
Show for hermitian coupling operators that when $\tau\to\infty$, CG and BMS approximation are equivalent. You may use the identity

$$\lim_{\tau\to\infty}\tau\mathrm{sinc}\left[\frac{\tau}{2}(\Omega_\mathrm{a}-\omega)\right]\mathrm{sinc}\left[\frac{\tau}{2}(\Omega_\mathrm{b}-\omega)\right] = 2\pi\delta_{\Omega_\mathrm{a},\Omega_\mathrm{b}}\delta(\Omega_\mathrm{a}-\omega)\,.$$

This shows that coarse-graining provides an alternative derivation of the quantum-optical master equation, replacing three subsequent approximations (Born-, Markov- and secular) by just one (perturbative expansion in the interaction).

2.2.3 Thermalization

The BMS limit has beyond its relatively compact Lindblad form further appealing properties in the case of a bath that is in thermal equilibrium

$$\bar{\rho}_\mathrm{B} = \frac{e^{-\beta\mathcal{H}_\mathrm{B}}}{\mathrm{Tr}\left\{e^{-\beta\mathcal{H}_\mathrm{B}}\right\}} \tag{2.61}$$

with inverse temperature β. These root in further analytic properties of the bath correlation functions such as the Kubo-Martin-Schwinger (KMS) condition

$$C_{\alpha\beta}(\tau) = C_{\beta\alpha}(-\tau-\mathrm{i}\beta)\,. \tag{2.62}$$

Exercise 22 (KMS condition) *(1 points)*
Show the validity of the KMS condition for a thermal bath with $\bar{\rho}_\mathrm{B} = \frac{e^{-\beta\mathcal{H}_\mathrm{B}}}{\mathrm{Tr}\left\{e^{-\beta\mathcal{H}_\mathrm{B}}\right\}}$.

For the Fourier transform, this shift property implies

$$\begin{aligned}\gamma_{\alpha\beta}(-\omega) &= \int_{-\infty}^{+\infty} C_{\alpha\beta}(\tau)e^{-\mathrm{i}\omega\tau}d\tau = \int_{-\infty}^{+\infty} C_{\beta\alpha}(-\tau-\mathrm{i}\beta)e^{-\mathrm{i}\omega\tau}d\tau \\ &= \int_{+\infty-\mathrm{i}\beta}^{-\infty-\mathrm{i}\beta} C_{\beta\alpha}(\tau')e^{+\mathrm{i}\omega(\tau'+\mathrm{i}\beta)}(-)d\tau' = \int_{-\infty-\mathrm{i}\beta}^{+\infty-\mathrm{i}\beta} C_{\beta\alpha}(\tau')e^{+\mathrm{i}\omega\tau'}d\tau' e^{-\beta\omega} \\ &= \int_{-\infty}^{+\infty} C_{\beta\alpha}(\tau')e^{+\mathrm{i}\omega\tau'}d\tau' e^{-\beta\omega} = \gamma_{\beta\alpha}(+\omega)e^{-\beta\omega}\,, \end{aligned} \tag{2.63}$$

where in the last line we have used that the bath correlation functions are analytic in τ in the complex plane and vanish at infinity, such that we may safely deform the integration contour. Finally, the KMS condition can thereby be used to prove that for a reservoir with inverse temperature β, the density matrix

$$\bar{\rho_{\mathrm{S}}} = \frac{e^{-\beta\mathcal{H}_{\mathrm{S}}}}{\mathrm{Tr}\left\{e^{-\beta\mathcal{H}_{\mathrm{S}}}\right\}} \tag{2.64}$$

is one stationary state of the BMS master equation (and the $\tau\to\infty$ limit of the CG appraoch).

Exercise 23 (Thermalization) *(1 points)*
Show that $\bar{\rho_{\mathrm{S}}} = \frac{e^{-\beta\mathcal{H}_{\mathrm{S}}}}{\mathrm{Tr}\left\{e^{-\beta\mathcal{H}_{\mathrm{S}}}\right\}}$ *is a stationary state of the BMS master equation, when* $\gamma_{\alpha\beta}(-\omega) = \gamma_{\beta\alpha}(+\omega)e^{-\beta\omega}$.

When the reservoir is in the grand-canonical equilibrium state

$$\bar{\rho}_{\mathrm{B}} = \frac{e^{-\beta(\mathcal{H}_{\mathrm{B}}-\mu N_{\mathrm{B}})}}{\mathrm{Tr}\left\{e^{-\beta(\mathcal{H}_{\mathrm{B}}-\mu N_{\mathrm{B}})}\right\}}\,, \tag{2.65}$$

where $N = N_{\mathrm{S}} + N_{\mathrm{B}}$is a conserved quantity $[\mathcal{H}_{\mathrm{S}}+\mathcal{H}_{\mathrm{B}}+\mathcal{H}_{\mathrm{I}}, N_{\mathrm{S}}+N_{\mathrm{B}}] = 0$, the KMS condition is not fulfilled anymore. However, even in this case one can show that a stationary state of the BMS master equation is given by

$$\bar{\rho_{\mathrm{S}}} = \frac{e^{-\beta(\mathcal{H}_{\mathrm{S}}-\mu N_{\mathrm{S}})}}{\mathrm{Tr}\left\{e^{-\beta(\mathcal{H}_{\mathrm{S}}-\mu N_{\mathrm{S}})}\right\}}\,, \tag{2.66}$$

i.e., both temperature β and chemical potential μ equilibrate.

2.2.4 Example: Spin-Boson Model

The spin-boson model describes the interaction of a spin with a bosonic environment

$$\begin{aligned}\mathcal{H}_{\mathrm{S}} &= \Omega\sigma^z + T\sigma^x\,, \qquad \mathcal{H}_{\mathrm{B}} = \sum_k \omega_k b_k^\dagger b_k\,, \\ \mathcal{H}_{\mathrm{I}} &= \sigma^z \otimes \sum_k \left[h_k b_k + h_k^* b_k^\dagger\right]\,, \end{aligned} \tag{2.67}$$

where Ω and T denote parameters of the system Hamiltonian, σ^α the Pauli matrices, and $b^\dagger$ creates a boson with frequency ω_k in the reservoir. The model can be motivated by a variety of setups, e.g. a charge qubit (singly-charged double quantum dot) that is coupled to vibrations. We note the a priori hermitian coupling operators

$$A_1 = \sigma^z\,, \qquad B_1 = \sum_k \left[h_k b_k + h_k^* b_k^\dagger\right]\,. \tag{2.68}$$

We first diagonalize the system part of the Hamiltonian to obtain the eigenbasis $\mathcal{H}_\mathrm{S}\,|n\rangle = E_n\,|n\rangle$, where

$$E_\pm = \pm\sqrt{\Omega^2+T^2}\,, \qquad |\pm\rangle = \frac{1}{\sqrt{T^2+\left(\Omega\pm\sqrt{\Omega^2+T^2}\right)^2}}\left[\left(\Omega\pm\sqrt{\Omega^2+T^2}\right)|0\rangle + T\,|1\rangle\right]\,, \tag{2.69}$$

where $|0/1\rangle$ denote the eigenvectors of the σ^z Pauli matrix with $\sigma^z\,|i\rangle = (-1)^i\,|i\rangle$.

Exercise 24 (Eigenbasis) *(1 points)*
Confirm the validity of Eq. (2.69).

Second, we calculate the correlation function (in this case, there is just one). Transforming everything in the interaction picture we see that the annihilation operators just pick up time-dependent phases

$$\begin{aligned} C(\tau) &= \mathrm{Tr}\left\{\sum_k \left[h_k b_k e^{-\mathrm{i}\omega_k\tau} + h_k^* b_k^\dagger e^{+\mathrm{i}\omega_k\tau}\right]\sum_q \left[h_q b_q + h_q^* b_q^\dagger\right]\bar\rho_\mathrm{B}\right\} \\ &= \sum_k |h_k|^2\left[e^{-\mathrm{i}\omega_k\tau}\left(1+n_B(\omega_k)\right) + e^{+\mathrm{i}\omega_k\tau} n_B(\omega_k)\right] \\ &= \frac{1}{2\pi}\int d\omega\Gamma(\omega)\left[e^{-\mathrm{i}\omega\tau}\left(1+n_B(\omega)\right) + e^{+\mathrm{i}\omega\tau} n_B(\omega)\right]\,, \end{aligned} \tag{2.70}$$

where we have introduced the spectral coupling density $\Gamma(\omega) = 2\pi\sum_k |h_k|^2\delta(\omega-\omega_k)$ and the Bose distribution

$$n_B(\omega) = \frac{1}{e^{\beta(\omega-\mu)}-1}\,. \tag{2.71}$$

Exercise 25 (Bose distribution) *(1 points)*
Confirm the validity of Eq. (2.71), i.e., show that

$$\delta_{kq} n_B(\omega_k) = \mathrm{Tr}\left\{b_k^\dagger b_q \frac{e^{-\beta(\mathcal{H}_\mathrm{B}-\mu N_\mathrm{B})}}{Z}\right\}\,, \tag{2.72}$$

where $\mathcal{H}_\mathrm{B} = \sum_k \omega_k b_k^\dagger b_k$, $N_\mathrm{B} = \sum_k b_k^\dagger b_k$, *and* $Z = \mathrm{Tr}\left\{e^{-\beta(\mathcal{H}_\mathrm{B}-\mu N_\mathrm{B})}\right\}$.

We can directly read off the even Fourier transform of the correlation function

$$\gamma(\omega) = \Gamma(+\omega)\Theta(+\omega)[1 + n_B(+\omega)] + \Gamma(-\omega)\Theta(-\omega)n_B(-\omega)\,. \tag{2.73}$$

We note that for bosons we necessarily have $\Gamma(\omega < 0) = 0$, since all oscillator frequencies in the reservoir must be positive. We compute some relevant dampening coefficients

$$\begin{aligned}
\gamma_{-+,-+} &= \Gamma(+2\sqrt{\Omega^2 + T^2})[1 + n_B(+2\sqrt{\Omega^2 + T^2})]|\langle -|\,\sigma^z\,|+\rangle|^2\,,\\
\gamma_{+-,+-} &= \Gamma(+2\sqrt{\Omega^2 + T^2})n_B(+2\sqrt{\Omega^2 + T^2})|\langle -|\,\sigma^z\,|+\rangle|^2\,,\\
\gamma_{--,++} &= \gamma(0)\,\langle -|\,\sigma^z\,|-\rangle\,\langle +|\,\sigma^z\,|+\rangle\ .
\end{aligned} \tag{2.74}$$

The explicit calculation of the non-vanishing Lamb-shift terms σ_{--} and σ_{++} is possible but more involved. Fortunately, it can be omitted for many applications. Since the system Hamiltonian is non-degenerate, the populations evolve according to

$$\dot\rho_{--} = +\gamma_{-+,-+}\rho_{++} - \gamma_{+-,+-}\rho_{--}\,, \qquad \dot\rho_{++} = +\gamma_{+-,+-}\rho_{--} - \gamma_{-+,-+}\rho_{++}\,, \tag{2.75}$$

which is independent from the coherences

$$\dot\rho_{-+} = -\mathrm{i}\,(E_- - E_+ + \sigma_{--} - \sigma_{++})\,\rho_{-+} + \left[\gamma_{--,++} - \frac{\gamma_{-+,-+} + \gamma_{+-,+-}}{2}\right]\rho_{-+}\,. \tag{2.76}$$

Since the Lamb-shift terms σ_{ii} are purely imaginary, the quantities at hand already allow us to deduce that the coherences will decay $|\rho_{-+}|^2 = e^{-(-2\gamma_{--,++}+\gamma_{-+,-+}+\gamma_{+-,+-})t}\left|\rho^0_{-+}\right|^2$, which shows that the decoherence rate increases with temperature (finite n_B) but can also at zero temperature not be suppressed below a minimum value. A special (exactly solvable) case arises when $T = 0$: Then, the interaction commutes with the system Hamiltonian leaving the energy of the system invariant. Consistently, the eigenbasis is in this case that of σ^z and the coefficients $\gamma_{-+,-+}$ and $\gamma_{+-,+-}$ do vanish. In contrast, the coefficient $\gamma_{--,++} \to -\gamma(0)$ may remain finite. Such models are called pure dephasing models (since only their coherences decay). However, for finite T the steady state of the master equation is given by (we assume here $\mu = 0$)

$$\frac{\bar\rho_{++}}{\bar\rho_{--}} = \frac{\gamma_{+-,+-}}{\gamma_{-+,-+}} = \frac{n_B(+2\sqrt{\Omega^2 + T^2})}{1 + n_B(+2\sqrt{\Omega^2 + T^2})} = e^{-2\beta\sqrt{\Omega^2+T^2}}\,, \tag{2.77}$$

i.e., the stationary state is given by the thermalized one.

Chapter 3

Multi-Terminal Coupling : Non-Equilibrium Case I

The most obvious way to achieve non-equilibrium dynamics is to use reservoir states that are non-thermalized, i.e., states that cannot simply be characterized by just temperature and chemical potential. Since the derivation of the master equation only requires $[\bar{\rho}_{\mathrm{B}}, \mathcal{H}_{\mathrm{B}}] = 0$, this would still allow for many nontrivial models, $\langle n| \bar{\rho}_{\mathrm{B}} |n\rangle$ could e.g. follow multi-modal distributions. Alternatively, a non-equilibrium situation may be established when a system is coupled to different thermal equilibrium baths or of course when the system itself is externally driven – either unconditionally (open-loop feedback) or conditioned on the actual state of the system (closed-loop feedback).

First, we will consider the case of multiple reservoirs at different thermal equilibria that are only indirectly coupled via the system: Without the system, they would be completely independent. Since these are chosen at different equilibria, they drag the system towards different thermal states, and the resulting stationary state is in general a non-thermal one. Since the different compartments interact only indirectly via the system, we have the case of a multi-terminal system, where one can most easily derive the corresponding master equation, since each contact may be treated separately. Therefore, we do now consider multiple (K) reservoirs

$$\mathcal{H}_{\mathrm{B}} = \sum_{\ell=1}^{K} \mathcal{H}_{\mathrm{B}}^{(\ell)} \tag{3.1}$$

with commuting individual parts $\left[\mathcal{H}_{\mathrm{B}}^{(\ell)}, \mathcal{H}_{\mathrm{B}}^{(k)}\right] = 0$. These are held at different chemical potentials and different temperatures

$$\bar{\rho}_{\mathrm{B}} = \frac{e^{-\beta(\mathcal{H}_{\mathrm{B}}^{(1)} - \mu N_{\mathrm{B}}^{(1)})}}{\mathrm{Tr}\left\{e^{-\beta(\mathcal{H}_{\mathrm{B}}^{(1)} - \mu N_{\mathrm{B}}^{(1)})}\right\}} \otimes \ldots \otimes \frac{e^{-\beta(\mathcal{H}_{\mathrm{B}}^{(K)} - \mu N_{\mathrm{B}}^{(K)})}}{\mathrm{Tr}\left\{e^{-\beta(\mathcal{H}_{\mathrm{B}}^{(K)} - \mu N_{\mathrm{B}}^{(K)})}\right\}} \,. \tag{3.2}$$

To each of the reservoirs, the system is coupled via different coupling operators

$$\mathcal{H}_{\mathrm{I}} = \sum_{\alpha} A_{\alpha} \otimes \sum_{\ell=1}^{k} B_{\alpha}^{(\ell)} \,. \tag{3.3}$$

Since we assume that the first order bath correlation functions vanish $\left\langle B_{\alpha}^{\ell} \bar{\rho}_{\mathrm{B}} \right\rangle = 0$, the second-order bath correlation functions may be computed additively

$$C_{\alpha\beta}(\tau) = \sum_{\ell=1}^{K} C_{\alpha\beta}^{(\ell)}(\tau) \,. \tag{3.4}$$

Exercise 26 (Additive Reservoirs) *(1 points)*
Show with using Eqns. (3.1) and (3.2) that expectation values of coupling operators belonging to different reservoirs vanish, i.e.,

$$C_{(\alpha,\ell),(\beta,k)}(\tau) = \mathrm{Tr}\left\{\boldsymbol{B}^{(\boldsymbol{\ell})}_{\boldsymbol{\alpha}}(\tau) B^{(k)}_{\beta}\bar{\rho}_{\mathrm{B}}\right\} = \delta_{k\ell} C_{(\alpha,\ell),(\beta,\ell)}\,.$$

This obviously transfers to their Fourier transforms and thus, also to the final Liouvillian (to second order in the coupling)

$$\mathcal{L} = \mathcal{L}^{(0)} + \sum_{\ell=1}^{K} \mathcal{L}^{(\ell)}\,. \tag{3.5}$$

Here, $\mathcal{L}^{(0)}\rho \hat{=} -\mathrm{i}\,[\mathcal{H}_{\mathrm{S}}, \rho]$ describes the action of the system Hamiltonian and $\mathcal{L}^{(\ell)}$ denotes the Liouvillian resulting only from the ℓ-th reservoir. The resulting stationary state is in general a non-equilibrium one.

Let us however first identify a special case where even in a non-equilibrium setup we can determine the non-equilibrium steady state analytically. For some simple models, one obtains that the coupling structure of all Liouvillians is identical for different reservoirs

$$\mathcal{L}^{(\ell)} = \Gamma^{(\ell)}\left[\mathcal{L}_A + n^{(\ell)}\mathcal{L}_B\right]\,, \tag{3.6}$$

i.e., the reservoirs trigger exactly the same transitions within the system. Here, $n^{(\ell)}$ is a parameter encoding the thermal properties of the respective bath (e.g. a Fermi-Dirac or a Bose-Einstein distribution evaluated at one of the systems transition frequencies), and $\mathcal{L}_{A/B}$ simply label parts of the Liouvillian that are proportional to thermal characteristics (B) or not (A). Finally, $\Gamma^{(\ell)}$ represent coupling constants to the different reservoirs. For coupling to a single reservoir, the stationary state is defined via the equation

$$\mathcal{L}^{(\ell)}\bar{\rho}^{(\ell)} = \Gamma^{(\ell)}\left[\mathcal{L}_A + n^{(\ell)}\mathcal{L}_B\right]\bar{\rho}^{(\ell)} = 0 \tag{3.7}$$

and thus implicitly depends on the thermal parameter $\bar{\rho}^{(\ell)} = \bar{\rho}(n^{(\ell)})$. Obviously, the steady state will be independent of the coupling strength $\Gamma^{(\ell)}$. For the total Liouvillian, it follows that the dependence of the full stationary state on all thermal parameters simply given by the same dependence on an average thermal parameter

$$\begin{aligned}\mathcal{L}\bar{\rho} &= \sum_{\ell}\mathcal{L}^{(\ell)}\bar{\rho} = \sum_{\ell}\Gamma^{(\ell)}\left[\mathcal{L}_A + n^{(\ell)}\mathcal{L}_B\right]\bar{\rho} = \left[\sum_{\ell}\Gamma^{(\ell)}\right]\left[\mathcal{L}_A + \frac{\sum_{\ell}\Gamma^{(\ell)}n^{(\ell)}}{\sum_{\ell'}\Gamma^{(\ell')}}\mathcal{L}_B\right]\bar{\rho}\,,\\ &= \left[\sum_{\ell}\Gamma^{(\ell)}\right]\left[\mathcal{L}_A + \bar{n}\mathcal{L}_B\right]\bar{\rho}\,,\end{aligned} \tag{3.8}$$

where

$$\bar{n} = \frac{\sum_{\ell}\Gamma^{(\ell)}n^{(\ell)}}{\sum_{\ell}\Gamma^{(\ell)}} \tag{3.9}$$

represents an average thermal parameter (e.g. the average occupation). Formally, this is the same equation that determines the steady state for a single reservoir, which may now however be non-thermal.

This can be illustrated by upgrading the Liouvillian for a single resonant level coupled to a single junction

$$\mathcal{L} = \begin{pmatrix} -\Gamma f & +\Gamma(1-f) \\ +\Gamma f & -\Gamma(1-f) \end{pmatrix}, \tag{3.10}$$

where the Fermi function $f = \left[e^{\beta(\epsilon-\mu)}+1\right]^{-1}$ of the contact is evaluated at the dot level ϵ, to the Liouvillian for a single-electron transistor (SET) coupled to two (left and right) junctions

$$\mathcal{L} = \begin{pmatrix} -\Gamma_L f_L - \Gamma_R f_R & +\Gamma_L(1-f_L)+\Gamma_R(1-f_R) \\ +\Gamma_L f_L + \Gamma_R f_R & -\Gamma_L(1-f_L)-\Gamma_R(1-f_R) \end{pmatrix}. \tag{3.11}$$

Now, the system is coupled to two fermionic reservoirs, and in order to support a current, the dot level ϵ must be within the transport window, see Fig. 3.1. This also explains the name single-

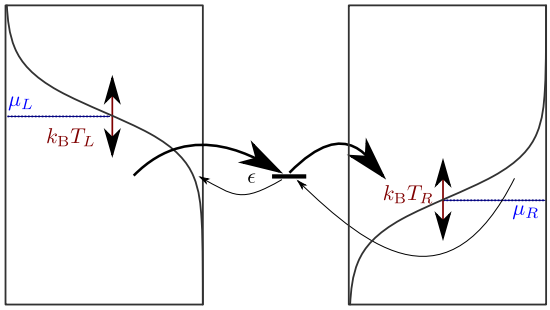

Figure 3.1: Sketch of a single resonant level (QD at energy level ϵ) coupled to two junctions with different Fermi distributions (e.g. with different chemical potentials or different temperatures. If the dot level ϵ is changed with a third gate, the device functions as a transistor, since the current through the system is exponentially suppressed when the the dot level ϵ is not within the transport window.

electron transistor, since the dot level ϵ may be tuned by a third gate, which thereby controls the current.

Exercise 27 (Pseudo-Nonequilibrium) *(1 points)*
Show that the stationary state of Eq.(3.11) is a thermal one, i.e., that

$$\frac{\bar{\rho}_{11}}{\bar{\rho}_{00}} = \frac{\bar{f}}{1-\bar{f}}.$$

Determine $\bar{f}$ in dependence of Γ_α and f_α.

3.1 Conditional Master equation from conservation laws

Suppose we have derived a QME for an open system, where the combined system obeys the conservation of some conserved quantity (e.g., the total number of particles). Then, it can be

directly concluded that a change in the system particle number by e.g. minus one must be directly accompagnied by the corresponding change of the reservoir particle number by plus one. For couplings to multiple reservoirs these terms can also be uniquely identified, since the Liouvillians are additive. Whereas its actual density matrix says little about the number of quanta that have already passed the quantum system, a full trajectory would reveal this information. In such cases, it is reasonable to discretize the master equation in time, where it can most easily be upgraded to an n-resolved (conditional) master equation. In what follows, we just track the particle number in a single attached reservoir and denote by $\rho^{(n)}(t)$ the system density matrix under the condition that n net particles have left into the monitored reservoirs, but the method may easily be generalized. Assuming that at time t, we have n particles transferred to the reservoir, we may discretize the conventional master equation $\dot{\rho} = \mathcal{L}\rho$ in time and identify terms that increase or decrease the particle number (often called jumpers)

$$\dot{\rho}^{(n)} = \mathcal{L}_0\rho^{(n)} + \mathcal{L}_+\rho^{(n-1)} + \mathcal{L}_-\rho^{(n+1)} \,. \tag{3.12}$$

Here, $\mathcal{L}_+$ increases the number of particles in the monitored reservoirs by one and $\mathcal{L}_-$ decreases it by one. All remaining processes (jumps to other reservoirs or internal transitions within the system) are contained in $\mathcal{L}_0$, such that the original Liouvillian is given by

$$\mathcal{L} = \mathcal{L}_0 + \mathcal{L}_- + \mathcal{L}_+ \,. \tag{3.13}$$

Since the total number of transferred particles is normally not constrained, this immediately yields an infinite set of equations for the conditioned system density matrix. Exploiting the translational invariance suggests to use the (discrete) Fourier transform

$$\rho(\chi, t) = \sum_n \rho^{(n)}(t) e^{+\mathrm{i}n\chi} \,, \tag{3.14}$$

which recovers the original dimension of the master equation

$$\dot{\rho}(\chi, t) = \left[\mathcal{L}_0 + e^{+\mathrm{i}\chi}\mathcal{L}^+ + e^{-\mathrm{i}\chi}\mathcal{L}^-\right]\rho(\chi, t) = \mathcal{L}(\chi)\rho(\chi, t) \,, \tag{3.15}$$

but at the cost of introducing the parameter χ – called **counting field** further-on.

Exercise 28 (Counting Field Master Equation) *(1 points)*
How would Eqns. (3.12) and (3.15) change when particles could only tunnel in pairs?

The advantage of this form however is that – since χ is a parameter – we can readily write down the solution

$$\rho(\chi, t) = e^{\mathcal{L}(\chi)t}\rho(\chi, 0) = e^{\mathcal{L}(\chi)t}\rho_0 \,, \tag{3.16}$$

where we have used the convention that $\rho^{(n)}(0) = \delta_{n,0}\rho_0$. We stress here again that we have written everything in superoperator notation, i.e., the density matrix elements are arranged in a vector (conventionally, one puts the populations first), such that the Liouvillian acts as a matrix from the left. Stating that the populations evolve independently from the coherences corresponds to a block form of the Liouvillian in this picture. Having solved the master equation for $\rho(t)$, we

can then rearrange the solution vector into matrix form and calculate traces with operators etc. However, noticing that we can of course also represent ordinary operators acting in the Hilbert space of the system as superoperators, it is important to realize that we can conveniently perform all operations in superoperator notation. Since the trace just involves summing over the diagonal elements of the result, this transfers to a product with a transposed vector of the form (we take an $N \times N$ density matrix)

$$\mathrm{Tr}\left\{A\rho\right\} \hat{=} \mathrm{Tr}\left\{\mathcal{A}\rho\right\} = \left(\underbrace{1,\ldots,1}_{N},0,\ldots,0\right)(\mathcal{A})\begin{pmatrix}\rho_{11}\\ \vdots\\ \rho_{NN}\\ \rho_{12}\\ \vdots\\ \rho_{N,N-1}\end{pmatrix}. \tag{3.17}$$

Exercise 29 (Superoperators) *How would the Pauli matrix σ^x act on the density matrix if it was arranged as a superoperator, i.e., determine Σ^x and $\bar{\Sigma}^x$ in*

$$\begin{aligned}\begin{pmatrix}0&1\\1&0\end{pmatrix}\begin{pmatrix}\rho_{00}&\rho_{01}\\\rho_{10}&\rho_{11}\end{pmatrix} &\hat{=} \Sigma^x\begin{pmatrix}\rho_{00}\\\rho_{11}\\\rho_{01}\\\rho_{10}\end{pmatrix},\\ \begin{pmatrix}\rho_{00}&\rho_{01}\\\rho_{10}&\rho_{11}\end{pmatrix}\begin{pmatrix}0&1\\1&0\end{pmatrix} &\hat{=} \bar{\Sigma}^x\begin{pmatrix}\rho_{00}\\\rho_{11}\\\rho_{01}\\\rho_{10}\end{pmatrix}.\end{aligned} \tag{3.18}$$

As an example, we phenomenologically convert the SET master equation (3.11) into an n-resolved version. Since we have a simple rate equation, we have neglected the block describing the evolution of coherences. We choose the right reservoir as the one to monitor and denote the number of particles that have tunneled into the right reservoir by n, where negative n would simply imply a current from right to left. Then, the conditional density matrix obeys

$$\begin{aligned}\dot{\rho}^{(n)} &= \begin{pmatrix}-\Gamma_L f_L-\Gamma_R f_R & +\Gamma_L(1-f_L)\\ +\Gamma_L f_L & -\Gamma_L(1-f_L)-\Gamma_R(1-f_R)\end{pmatrix}\rho^{(n)}\\ &\quad+\begin{pmatrix}0&\Gamma_R(1-f_R)\\0&0\end{pmatrix}\rho^{(n-1)}+\begin{pmatrix}0&0\\+\Gamma_R f_R&0\end{pmatrix}\rho^{(n+1)}.\end{aligned} \tag{3.19}$$

Performing the Fourier transformation (thereby exploiting the shift invariance) reduces the dimension at the price of introducing the counting field

$$\dot{\rho}(\chi,t) = \begin{pmatrix}-\Gamma_L f_L-\Gamma_R f_R & +\Gamma_L(1-f_L)+\Gamma_R(1-f_R)e^{+\mathrm{i}\chi}\\ +\Gamma_L f_L+\Gamma_R f_R e^{-\mathrm{i}\chi} & -\Gamma_L(1-f_L)-\Gamma_R(1-f_R)\end{pmatrix}\rho(\chi,t). \tag{3.20}$$

Formally, this just corresponds to the replacement $(1-f_R)\to(1-f_R)e^{+\mathrm{i}\chi}$ and $f_R\to f_R e^{-\mathrm{i}\chi}$ in the off-diagonal matrix elements of the Liouvillian (which correspond to particle jumps).

The original density matrix can be recovered by summing over all conditioned density matrices

$$\rho(t) = \sum_n \rho^{(n)}(t)\,, \tag{3.21}$$

which also shows that the conditioned ones need not be normalized. We can obtain the information about the tunneled particles by tracing over the system degrees of freedom

$$P_n(t) = \mathrm{Tr}\left\{\rho^{(n)}(t)\right\}\,. \tag{3.22}$$

Unfortunately, obtaining $\rho^{(n)}(t)$ would require to solve an infinite-dimensional system, such that this is usually not a very practical way.

3.2 Microscopic derivation with virtual detectors

Unfortunately, we do not always have a conserved quantity that may only change when tunneling across the system-reservoir junction takes place. A counter-example may be the tunneling between two reservoirs, that is merely modified by the presence of the quantum system (e.g. quantum point contact monitoring a charge qubit) and is not connected with a particle change in the system. In such cases, we may not identify a change in the system state with a microcanonical change of the reservoir state. However, such problems can still be handled with a quantum master equation by introducing a virtual detector at the level of the interaction Hamiltonian. Suppose that in the interaction Hamiltonian we can identify terms associated with a change of the tracked obervable in the reservoir

$$\mathcal{H}_\mathrm{I} = A_+ \otimes B_+ + A_- \otimes B_- + \sum_{\alpha\neq\{+,-\}} A_\alpha \otimes B_\alpha\,, \tag{3.23}$$

where B_+ increases and B_- decreases the reservoir particle number. We extend the system Hilbert space by adding a virtual detector

$$\begin{aligned}
\mathcal{H}_\mathrm{S} &\rightarrow \mathcal{H}_\mathrm{S}\otimes\mathbf{1}\,, \qquad \mathcal{H}_\mathrm{B}\rightarrow\mathcal{H}_\mathrm{B} \\
\mathcal{H}_\mathrm{I} &\rightarrow + \left[A_+\otimes D^\dagger\right]\otimes B_+ + \left[A_-\otimes D\right]\otimes B_- + \sum_{\alpha\neq\{+,-\}}\left[A_\alpha\otimes\mathbf{1}\right]\otimes B_\alpha\,,
\end{aligned} \tag{3.24}$$

where $D = \sum_n |n\rangle\langle n+1|$ and $D^\dagger = \sum_n |n+1\rangle\langle n|$. Here $|n\rangle$ are the eigenstates of the detector, and we see that $D^\dagger|n\rangle = |n+1\rangle$ and $D|n\rangle = |n-1\rangle$. This obviously also implies that $DD^\dagger = D^\dagger D = \mathbf{1}$. Such a detector is ideal in the sense that it does not influence the system dynamics and it does not have its own energy content (its own Hamiltonian vanishes). Therefore, it will be called **virtual detector** here. The detector operators in the interaction Hamiltonian can also be viewed as bookkeeping operators that simply facilitate the correct identification of terms in the master equation. We can now formally consider the detector as part of the system and derive the master equation. Since there is no direct interaction between the original system and the detector, the eigenbasis of both system and detector is now given by $|a,n\rangle = |a\rangle\otimes|n\rangle$, and we may derive e.g. the coarse-graining master equation in the usual way. When we decompose the system density matrix as

$$\rho(t) = \sum_n \rho^{(n)}(t)\otimes|n\rangle\langle n|\,, \tag{3.25}$$

we see that we can reduce the Lindblad master equation by using that

$$\begin{aligned} \langle n|\, DA_-\rho A_+ D^\dagger\, |n\rangle &= A_-\rho^{(n+1)}A_+\,, \\ \langle n|\, D^\dagger A_+\rho A_- D\, |n\rangle &= A_+\rho^{(n-1)}A_- \end{aligned} \tag{3.26}$$

to a form like in Eq. (3.12). The coarse-graining master equation in Box 9 for example shows that such conditioned master equations can be readily derived.

3.3 Full Counting Statistics

To obtain the probability of having n tunneled particles into a respective reservoir, we have to sum over the different system configurations of the corresponding conditional density matrix

$$P_n(t) = \mathrm{Tr}\left\{\rho^{(n)}(t)\right\}\,. \tag{3.27}$$

In view of the identities

$$\mathrm{Tr}\left\{\rho(\chi,t)\right\} = \mathrm{Tr}\left\{e^{\mathcal{L}(\chi)t}\rho_0\right\} = \sum_n P_n(t)e^{+\mathrm{i}n\chi}\,, \tag{3.28}$$

we see that in order to evaluate moments $\langle n^k\rangle$, we simply have to take derivatives with respect to the counting field

$$\left\langle n^k(t)\right\rangle = \sum_n n^k P_n(t) = (-\mathrm{i}\partial_\chi)^k \sum_n P_n(t)e^{+\mathrm{i}n\chi}\bigg|_{\chi=0}\,. \tag{3.29}$$

Based on a conditional master equation, this enables a very convenient calculation of the stationary current. This is a good motivation to introduce the moment-generating function.

Box 10 (Moment-Generating Function) *The moment-generating function is given by*

$$\mathcal{M}(\chi,t) = \mathrm{Tr}\left\{e^{\mathcal{L}(\chi)t}\rho_0\right\}\,, \tag{3.30}$$

and moments can be computed from derivatives with respect to the counting field

$$\left\langle n^k(t)\right\rangle = (-\mathrm{i}\partial_\chi)^k\mathcal{M}(\chi,t)\big|_{\chi=0}\,. \tag{3.31}$$

Often, the initial condition is set to the steady-state solution $\rho_0 = \bar\rho$ with $\mathcal{L}(0)\bar\rho = 0$.

Taking the stationary density matrix $\mathcal{L}(0)\bar\rho = 0$ as initial condition (the stationary current is independent on the initial occupation of the density matrix), we obtain for the current as the time

derivative of the first moment

$$\begin{aligned} I &= \langle \dot{n}(t) \rangle \\ &= -\mathrm{i}\partial_\chi \frac{d}{dt} \operatorname{Tr}\left\{ e^{\mathcal{L}(\chi)t} \bar{\rho} \right\}\big|_{\chi=0} \\ &= -\mathrm{i}\partial_\chi \operatorname{Tr}\left\{ \mathcal{L}(\chi) e^{\mathcal{L}(\chi)t} \bar{\rho} \right\}\big|_{\chi=0} \\ &= -\mathrm{i}\mathrm{Tr}\Big\{ \mathcal{L}'(0)\bar{\rho} + \left[\mathcal{L}'(0)\mathcal{L}(0) + \mathcal{L}(0)\mathcal{L}'(0)\right] t\bar{\rho} \\ &\quad + \left[\mathcal{L}'(0)\mathcal{L}^2(0) + \mathcal{L}(0)\mathcal{L}'(0)\mathcal{L}(0) + \mathcal{L}^2(0)\mathcal{L}'(0)\right] \frac{t^2}{2}\bar{\rho} + \dots \Big\} \\ &= -\mathrm{i}\mathrm{Tr}\left\{ \mathcal{L}'(0)\bar{\rho} \right\} , \end{aligned} \tag{3.32}$$

where we have used $\mathcal{L}(0)\bar{\rho} = 0$ and also $\operatorname{Tr}\{\mathcal{L}(0)\sigma\} = 0$ for all operators σ (trace conservation). This is consistent with common definitions of a current entering or leaving the system, since e.g. for sequential tunneling we have

$$I = -\mathrm{i}\mathrm{Tr}\left\{ \mathcal{L}'(0)\bar{\rho} \right\} = \operatorname{Tr}\left\{ \left[\mathcal{L}_+ - \mathcal{L}_- \right] \bar{\rho} \right\} . \tag{3.33}$$

Formally, we see that a stationary occupation times a transition rate yields a current. More quantitatively, by our initial definition, $\mathcal{L}_+$ contained the rates responsible for particles leaving the system towards the monitored reservoir whereas $\mathcal{L}_-$ described the inverse process.

Exercise 30 (Stationary SET current) *(1 points)*
Calculate the stationary current through the SET (3.20).

Sometimes a description in terms of cumulants is more convenient.

Box 11 (Cumulant-Generating Function) *The cumulant-generating function is defined as the logarithm of the moment-generating function*

$$\mathcal{C}(\chi, t) = \ln \mathcal{M}(\chi, t) = \ln \operatorname{Tr}\left\{ e^{\mathcal{L}(\chi)t} \rho_0 \right\} , \tag{3.34}$$

and all cumulants may be obtained via simple differentiation

$$\left\langle\left\langle n^k \right\rangle\right\rangle = (-\mathrm{i}\partial_\chi)^k \, \mathcal{C}(\chi, t)|_{\chi=0} . \tag{3.35}$$

Cumulants and Moments are of course related, we just summarize relations for the lowest few cumulants

$$\begin{aligned} \langle\langle n \rangle\rangle &= \langle n \rangle , \\ \left\langle\left\langle n^2 \right\rangle\right\rangle &= \left\langle n^2 \right\rangle - \langle n \rangle^2 , \\ \left\langle\left\langle n^3 \right\rangle\right\rangle &= \left\langle n^3 \right\rangle - 3 \langle n \rangle \left\langle n^2 \right\rangle + 2 \langle n \rangle^3 , \\ \left\langle\left\langle n^4 \right\rangle\right\rangle &= \left\langle n^4 \right\rangle - 4 \langle n \rangle \left\langle n^3 \right\rangle - 3 \left\langle n^2 \right\rangle^2 + 12 \langle n \rangle^2 \left\langle n^2 \right\rangle - 6 \langle n \rangle^4 . \end{aligned} \tag{3.36}$$

Obviously, the first two cumulants are just the **mean** and **width** of the probability distribution. For unimodal distributions, the third cumulant (skewness) and the fourth cumulant (kurtosis) describe the shape of the distribution near its maximum. In contrast to moments, higher cumulants are inert when a trivial transformation such as a simple shift is performed on a probability distribution.

3.4 Cumulant-Generating Function

The clear advantage of the description by cumulants however lies in the fact that the long-term evolution of the cumulant-generating function is usually given by the dominant eigenvalue of the Liouvillian

$$\mathcal{C}(\chi, t) \approx \lambda(\chi) t \,, \tag{3.37}$$

where $\lambda(\chi)$ is the (uniqueness assumed) eigenvalue of the Liouvillian that vanishes at zero counting field $\lambda(0) = 0$. For this reason, the dominant eigenvalue is also interpreted as the cumulant-generating function of the stationary current.

Exercise 31 (current CGF for the SET) *(1 points)*
Calculate the dominant eigenvalue of the SET Liouvillian (3.20) in the infinite bias limit $f_L \to 1$ and $f_R \to 0$. What is the value of the current?

We show this by using the decomposition of the Liouvillian in Jordan Block form

$$\mathcal{L}(\chi) = Q(\chi)\mathcal{L}_J(\chi)Q^{-1}(\chi) \,, \tag{3.38}$$

where $Q(\chi)$ is a (non-unitary) similarity matrix and $\mathcal{L}_J(\chi)$ contains the eigenvalues of the Liouvillian on its diagonal – distributed in blocks with a size corresponding to the eigenvalue multiplicity. We assume that there exists one stationary state $\bar{\rho}$, i.e., one eigenvalue $\lambda(\chi)$ with $\lambda(0) = 0$ and that all other eigenvalues have a larger negative real part near $\chi = 0$. Then, we use this decomposition in the matrix exponential to estimate its long-term evolution

$$\begin{aligned}
\mathcal{M}(\chi, t) &= \mathrm{Tr}\left\{e^{\mathcal{L}(\chi)t}\rho_0\right\} = \mathrm{Tr}\left\{e^{Q(\chi)\mathcal{L}_J(\chi)Q^{-1}(\chi)t}\rho_0\right\} = \mathrm{Tr}\left\{Q(\chi)e^{\mathcal{L}_J(\chi)t}Q^{-1}(\chi)\rho_0\right\} \\
&\to \mathrm{Tr}\left\{Q(\chi)\begin{pmatrix} e^{\lambda(\chi)\cdot t} & & & \\ & 0 & & \\ & & \ddots & \\ & & & 0 \end{pmatrix}Q^{-1}(\chi)\rho_0\right\} \\
&= e^{\lambda(\chi)\cdot t}\mathrm{Tr}\left\{Q(\chi)\begin{pmatrix} 1 & & & \\ & 0 & & \\ & & \ddots & \\ & & & 0 \end{pmatrix}Q^{-1}(\chi)\rho_0\right\} = e^{\lambda(\chi)t}c(\chi)
\end{aligned} \tag{3.39}$$

with some polynomial $c(\chi)$ depending on the matrix $Q(\chi)$. This implies that the cumulant-generating function

$$\mathcal{C}(\chi, t) = \ln \mathcal{M}(\chi, t) = \lambda(\chi)t + \ln c(\chi) \approx \lambda(\chi)t \tag{3.40}$$

becomes linear in $\lambda(\chi)$ for large times.

3.5 Energetic Counting

With a similiar theoretical apparatus, it is also possible to count the energetic exchanges between the system and a monitored reservoir. Most systems that are described by a Markovian master equation will only allow for discrete changes of their internal energy. If there is only a finite number of allowed energetic transitions, we may also count the number of such transitions individually, similiar to the number of particles. For many transitions, this would induce many counting fields, but the total energy could be recovered from $E = \sum_i \omega_i n_i$, such that

$$P(E,t) = \sum_{n_1,\ldots,n_k} P_{n_1,\ldots,n_k}(t)\delta(E - \sum_i \omega_i n_i)\,. \tag{3.41}$$

would yield the probability of energy transfer E at time t. The most evident difference to particle counting statistics is that while most Markovian models only allow for the exchange of single particles at a time (a consequence of the usual weak-coupling assumptions), there may be different energy quanta $\omega > 0$ exchanged with the reservoirs

$$\dot{\rho}^{(E)} = \mathcal{L}_0\rho^{(E)} + \sum_\omega \left[\mathcal{L}_{+\omega}\rho^{(E-\omega)} + \mathcal{L}_{-\omega}\rho^{(E+\omega)}\right]\,. \tag{3.42}$$

Here, $\mathcal{L}_{+\omega}$ describes processes triggered by the monitored reservoir that increase the system energy by $+\omega$ whereas $\mathcal{L}_{-\omega}$ decrease the energy by the same amount. Consequently, the summation over ω involves all allowed transitions within the system. Finally, $\mathcal{L}_0$ contains all remaining terms, such that $\mathcal{L} = \mathcal{L}_0 + \sum_\omega \left[\mathcal{L}_{+\omega} + \mathcal{L}_{-\omega}\right]$ holds. A second difference to particle counting is that – for more than a single transition frequency ω – the total transferred energy may become continuous. We therefore perform a continuous Fourier transform

$$\rho(\xi,t) = \int \rho^{(E)}(t)e^{+\mathrm{i}E\xi}dE\,, \tag{3.43}$$

which transforms the master equation into

$$\dot{\rho}(\xi,t) = \mathcal{L}_0 + \sum_\omega \left[\mathcal{L}_{+\omega}e^{+\mathrm{i}\xi\omega} + \mathcal{L}_{-\omega}e^{-\mathrm{i}\xi\omega}\right]\rho(\xi,t) = \mathcal{L}(\xi)\rho(\xi,t)\,. \tag{3.44}$$

Apart from the fact that the counting field ξ has dimension of inverse energy (the counting field ξ was dimensionless), all techniques from the particle counting statistics may be applied to energy counting statistics as well.

As a simple phenomenologic example, we consider a three-state system with unidirectional transport. The system can be empty $|0\rangle$ without carrying any energy $E_0 = 0$, it can be occupied in its left state $|L\rangle$ with energy ϵ_L and occupied in its right state $|R\rangle$ with energy ϵ_R. The rate matrix is in this basis given by

$$\mathcal{L} = \begin{pmatrix} -\Gamma_L & 0 & +\Gamma_R \\ +\Gamma_L & -T & 0 \\ 0 & +T & -\Gamma_R \end{pmatrix}\,, \tag{3.45}$$

demonstrating that the system can only be loaded from the left ($+\Gamma_L$) and unload to the right ($+\Gamma_R$), such that transport is uni-directional. Introducing counting fields for particle (χ) and energy (ξ) transport into the right reservoir, the counting-field-dependent Liouvillian becomes

$$\mathcal{L}(\chi,\xi) = \begin{pmatrix} -\Gamma_L & 0 & +\Gamma_R e^{+\mathrm{i}\chi+\mathrm{i}\xi\epsilon_R} \\ +\Gamma_L & -T & 0 \\ 0 & +T & -\Gamma_R \end{pmatrix}\,, \tag{3.46}$$

and the normalized steady state solution is given by

$$\bar{\rho} = \frac{1}{\Gamma_L\Gamma_R + (\Gamma_L + \Gamma_R)T} \begin{pmatrix} \Gamma_R T \\ \Gamma_L\Gamma_R \\ \Gamma_L T \end{pmatrix} . \tag{3.47}$$

Therefore, we obtain for the matter current

$$I_M = (1,1,1) \begin{pmatrix} 0 & 0 & +\Gamma_R \\ 0 & 0 & 0 \\ 0 & 0 & 0 \end{pmatrix} \bar{\rho} = \frac{\Gamma_L\Gamma_R T}{(\Gamma_L + \Gamma_R)T + \Gamma_L\Gamma_R} . \tag{3.48}$$

Similiarly, the energy current becomes

$$I_E = \epsilon_R I_M . \tag{3.49}$$

Naturally, we observe that these currents vanish when either Γ_L, Γ_R, or T vanish.

Exercise 32 (Counting Terminal) *(1 points)*
Introduce counting fields for energy and matter for the rate equation (3.45) when the left reservoir is monitored and compute both currents.

3.6 Entropy Balance

We now turn our focus to the central quantity in thermodynamics, the entropy. We assume that the dynamics of our system is described by a time-independent quantum master equation of Lindblad form. We can even allow for the possibility that the Lindblad generator $\mathcal{L}(t)$ is explicitly time-dependent due to an external driving (the approximations during the derivation in the previous chapters imply that then this driving must be very slow). Furthermore, we assume that it can be additively decomposed in the number of reservoirs ν to which the system is coupled (this often arises in weak-coupling scenarios, but note that counter-examples exist)

$$\dot{\rho} = \mathcal{L}(t)\rho(t) = \mathcal{L}^{(0)}(t)\rho(t) + \sum_\nu \mathcal{L}^{(\nu)}(t)\rho(t) . \tag{3.50}$$

Here, $\mathcal{L}^{(0)}(t)\rho(t) \hat{=} -\mathrm{i}\,[\mathcal{H}_{\mathrm{S}}(t), \rho(t)]$ describes the action of a possibly driven system Hamiltonian only. We assume that the time-dependent dissipator $\mathcal{L}^{(\nu)}(t)$ (which may e.g. also include the effects of Lamb-shift) obeys some detailed balance relations leading to

$$\mathcal{L}^{(\nu)}(t)\rho^{(\nu)}_{\mathrm{eq}}(t) = 0 , \tag{3.51}$$

where we have introduced the time-dependent grand-canonical equilibrium state

$$\rho^{(\nu)}_{\mathrm{eq}}(t) = \frac{e^{-\beta_\nu[\mathcal{H}_{\mathrm{S}}(t) - \mu_\nu \mathcal{N}_{\mathrm{S}}]}}{Z_\nu(t)} \tag{3.52}$$

with inverse temperature β^ν, chemical potential μ_ν, system Hamiltonian $\mathcal{H}_{\mathrm{S}}(t)$ and system particle number operator $\mathcal{N}_{\mathrm{S}}$. Apart from the time-dependence, these conditions are fulfilled by the quantum-optical Lindblad master equation.

3.6.1 Definitions

When we consider the change of the system energy under Lindblad dynamics, we see that it can be decomposed as

$$\begin{aligned}\dot{E} &= \frac{d}{dt}\mathrm{Tr}\left\{\mathcal{H}_{\mathrm{S}}(t)\rho(t)\right\} \\ &= \mathrm{Tr}\left\{\dot{\mathcal{H}}_{\mathrm{S}}\rho\right\} + \sum_{\nu}\mu_{\nu}\mathrm{Tr}\left\{\mathcal{N}_{\mathrm{S}}\mathcal{L}^{(\nu)}\rho\right\} + \sum_{\nu}\mathrm{Tr}\left\{(\mathcal{H}_{\mathrm{S}}(t)-\mu_{\nu}\mathcal{N}_{\mathrm{S}})\mathcal{L}^{(\nu)}\rho\right\} \\ &= \dot{W}_{\mathrm{drv}} + \dot{W}_{\mathrm{chem}} + \sum_{\nu}\dot{Q}^{(\nu)}\,, \end{aligned} \tag{3.53}$$

where

$$\dot{W}_{\mathrm{drv}} = \mathrm{Tr}\left\{\dot{\mathcal{H}}_{\mathrm{S}}\rho\right\} \tag{3.54}$$

is the **mechanical work** performed on the system due to the external driving,

$$\dot{W}_{\mathrm{chem}} = \sum_{\nu}\mu_{\nu}\mathrm{Tr}\left\{\mathcal{N}_{\mathrm{S}}\mathcal{L}^{(\nu)}\rho\right\} \tag{3.55}$$

is the **chemical work** performed on the system due to the flux of particles from reservoirs ν, and finally

$$\dot{Q}^{(\nu)} = \mathrm{Tr}\left\{(\mathcal{H}_{\mathrm{S}}(t)-\mu_{\nu}\mathcal{N}_{\mathrm{S}})\mathcal{L}^{(\nu)}\rho\right\}\,, \tag{3.56}$$

is the **heat** entering the system from reservoir ν. We note that at steady state and without driving we obtain the usual decomposition into energy and matter currents

$$\dot{Q}^{(\nu)} = \mathrm{Tr}\left\{(\mathcal{H}_{\mathrm{S}}-\mu_{\nu}\mathcal{N}_{\mathrm{S}})\mathcal{L}^{(\nu)}\bar{\rho}\right\} = I_E^{(\nu)} - \mu_{\nu}I_M^{(\nu)}\,. \tag{3.57}$$

Opposed to our previous convention (counting currents entering the reservoir ν positively), here a current counts positive when it enters the system. That is, we have simply changed the pespective, which is unproblematic for currents. We can convince ourselves that e.g. for our the SET model without coherences we have for the energy current entering the system from the left

$$\begin{aligned} I_E^{(L)} &= (1,1)\begin{pmatrix}0 & 0\\ 0 & \epsilon\end{pmatrix}\begin{pmatrix}-\Gamma_L f_L & +\Gamma_L(1-f_L)\\ +\Gamma_L f_L & -\Gamma_L(1-f_L)\end{pmatrix}\begin{pmatrix}1-\bar{f}\\ \bar{f}\end{pmatrix} \\ &= (1,1)\begin{pmatrix}0 & 0\\ +\epsilon\Gamma_L f_L & -\epsilon\Gamma_L(1-f_L)\end{pmatrix}\begin{pmatrix}1-\bar{f}\\ \bar{f}\end{pmatrix} \\ &= (1,1)\begin{pmatrix}+\epsilon\Gamma_L f_L(1-\bar{f})\\ -\epsilon\Gamma_L(1-f_L)\bar{f}\end{pmatrix} = \epsilon\Gamma_L(f_L-\bar{f}) \\ &= \frac{\epsilon\Gamma_L\Gamma_R(f_L-f_R)}{\Gamma_L+\Gamma_R}\,, \end{aligned} \tag{3.58}$$

which is precisely what we had before for the energy current leaving towards the right terminal, i.e., at steady state the currents are conserved, and the first law of thermodynamics is obeyed. The calculation for the matter current is similar $I_E^{(L)} = \epsilon I_M^{(L)}$ and it is of course also conserved.

These energy and matter currents will affect the dynamics of the entropy of the system, which can be quantified by the von-Neumann entropy.

Box 12 (von-Neumann entropy) *The von-Neumann entropy of a quantum system described by the density matrix ρ is given by*

$$S[\rho] = -\mathrm{Tr}\left\{\rho \ln \rho\right\} , \tag{3.59}$$

where $\rho \ln \rho$ is defined by the power series expansion.

The von-Neumann entropy can alternatively be obtained from the eigenvalues P_i of the density matrix

$$S[\rho] = -\mathrm{Tr}\left\{(U\rho_D U^\dagger)\ln(U\rho_D U^\dagger)\right\} = -\mathrm{Tr}\left\{U(\rho_D \ln \rho_D)U^\dagger\right\} = -\mathrm{Tr}\left\{\rho_D \ln \rho_D\right\} = -\sum_i P_i \ln P_i \tag{3.60}$$

It vanishes for a pure state $S[|\Psi\rangle\langle\Psi|] = 0$ and is upper bounded by the dimension of the system Hilbert space N

$$S[\rho] \leq \ln N . \tag{3.61}$$

This upper bound is directly found in the diagonal representation. Since the probabilities P_i have to obey the normalization condition $\sum_{i=1}^N P_i = 1$ we use the method of Lagrange multipliers and maximize $\tilde{S}[\rho] = S[\rho] + \lambda(1 - \sum_i P_i)$ instead. This yields

$$\partial_{p_i}\tilde{S} = -\ln P_i - 1 - \lambda , \qquad \partial_\lambda \tilde{S} = 1 - \sum_i P_i . \tag{3.62}$$

Solving the first equation yields that all probabilities have to be equal to maximize the entropy, and we can directly use the normalization condition to conclude that $P_i = 1/N$ for maximum entropy. Direct insertion then yields

$$S_{\max} = -\sum_i \frac{1}{N}\ln\frac{1}{N} = -\ln\frac{1}{N} = \ln N . \tag{3.63}$$

Exercise 33 (Lagrange Multipliers) *(1 points)*
What is the maximum value of the von-Neumann entropy when – beyond the normalization – we fix a further expectation value

$$\alpha = \langle A\rangle = \mathrm{Tr}\left\{A\sum_i P_i |\Psi_i\rangle\langle\Psi_i|\right\} = \sum_i a_i P_i , \qquad a_i = \langle\Psi_i| A |\Psi_i\rangle \tag{3.64}$$

for an arbitrary operator A?

Alternatively, often the Shannon entropy is used, which involves only the diagonal elements. For a density matrix ρ_{ij} it is given by

$$S_{\mathrm{Sh}} = -\sum_i \rho_{ii}\ln\rho_{ii} . \tag{3.65}$$

We note that the diagonal matrix elements need not coincide with the eigenvalues of ρ when the density matrix is not diagonal. The Shannon entropy depends on the chosen basis, whereas the von-Neumann entropy is invariant

$$S[U\rho U^\dagger] = -\mathrm{Tr}\left\{U\rho U^\dagger \ln U\rho U^\dagger\right\} = -\mathrm{Tr}\left\{U(\rho\ln\rho)U^\dagger\right\} = -\mathrm{Tr}\left\{\rho\ln\rho\right\} = S[\rho]\,, \tag{3.66}$$

and we will therefore favor the von-Neumann entropy. Note however, that for diagonal density matrices, both entropies will coincide.

The time derivative of the von-Neumann entropy can now formally be written as the sum of the entropy flow entering the system in form of heat from its reservoirs and an intrinsic entropy production term.

Box 13 (Entropy Production) *The entropy production is defined as the difference between the change of the von-Neumann entropy and the entropy flows that have left the system*

$$\dot{S}_\mathrm{i} = \dot{S} - \sum_\nu \beta_\nu \dot{Q}^{(\nu)}\,. \tag{3.67}$$

Up to now, these decompositions of energy into work and heat and entropy change into production and flow terms are somewhat arbitrary. The only guiding principle in writing them down was that in well-established cases (e.g. no heat flow but external driving or no driving but steady-state heat flow) they fall back to the usual thermodynamic definitions. Below, we will show that these definitions are sensible by showing that for Lindblad dynamics obeying the assumptions previously discussed one can show that the entropy production is positive.

3.6.2 Positivity of the entropy production

We first consider the time evolution of the von-Neumann entropy

$$\dot{S} = -\frac{d}{dt}\mathrm{Tr}\left\{\rho\ln\rho\right\} = -\mathrm{Tr}\left\{\dot\rho\ln\rho\right\}\,, \tag{3.68}$$

where we have used that $\mathrm{Tr}\left\{\rho\frac{d}{dt}\ln\rho\right\} = 0$, such that the derivative only acts on the first term. This can be shown by exploiting $\rho(t) = U_t\rho_D(t)U_t^\dagger$ with a time-dependent unitary transformation $U_tU_t^\dagger = \mathbf{1}$

$$\begin{aligned}
\mathrm{Tr}\left\{\rho\frac{d}{dt}\ln\rho\right\} &= \mathrm{Tr}\left\{U\rho_DU^\dagger\frac{d}{dt}\ln U\rho_DU^\dagger\right\} = \mathrm{Tr}\left\{U\rho_DU^\dagger\frac{d}{dt}U(\ln\rho_D)U^\dagger\right\}\\
&= \mathrm{Tr}\left\{U\rho_DU^\dagger\dot U(\ln\rho_D)U^\dagger + U\rho_DU^\dagger U\left(\frac{d}{dt}\ln\rho_D\right)U^\dagger + U\rho_DU^\dagger U(\ln\rho_D)\dot U^\dagger\right\}\\
&= \mathrm{Tr}\left\{\rho_DU^\dagger\dot U(\ln\rho_D) + \rho_D\left(\frac{d}{dt}\ln\rho_D\right) + \rho_D(\ln\rho_D)\dot U^\dagger U\right\}\\
&= \mathrm{Tr}\left\{\rho_D(\ln\rho_D)\left[U^\dagger\dot U + \dot U^\dagger U\right]\right\} + \sum_i P_i\frac{d}{dt}\ln P_i\\
&= \sum_i\frac{P_i}{P_i}\dot P_i = 0\,.
\end{aligned} \tag{3.69}$$

Further inserting the Lindblad generator in Eq. (3.68) one can see directly that the Hamiltonian driving does not directly contribute to the change of entropy

$$\mathrm{Tr}\left\{\left[\mathcal{L}^{(0)}\rho\right]\ln\rho\right\} = -\mathrm{iTr}\left\{\left[\mathcal{H}_\mathrm{S}(t)\rho - \rho\mathcal{H}_\mathrm{S}(t)\right]\ln\rho\right\} = 0\,. \tag{3.70}$$

This is somewhat expected, as – even when $\mathcal{H}_\mathrm{S}$ is time-dependent – the system Hamiltonian only generates unitary dynamics, which is known to preserve the von-Neumann entropy. Therefore, the change of the von-Neumann entropy is only determined by the dissipative part

$$\dot{S} = -\sum_\nu \mathrm{Tr}\left\{\left[\mathcal{L}^{(\nu)}\rho\right]\ln\rho\right\}\,. \tag{3.71}$$

Second, we rewrite the second (entropy flow) term in the entropy production (3.67) as

$$\begin{aligned} -\sum_\nu \beta_\nu \dot{Q}^{(\nu)} &= -\sum_\nu \beta_\nu \mathrm{Tr}\left\{(\mathcal{H}_\mathrm{S}(t) - \mu_\nu \mathcal{N}_\mathrm{S})\mathcal{L}^{(\nu)}\rho\right\} \\ &= \sum_\nu \mathrm{Tr}\left\{\left[\ln\rho_\mathrm{eq}^{(\nu)}\right]\left[\mathcal{L}^{(\nu)}\rho\right]\right\} \end{aligned} \tag{3.72}$$

with (3.52) defining the reservoir-specific steady state. Here, we need not care about the normalization factor, since its contribution vanishes due to $\mathrm{Tr}\left\{\mathcal{L}^{(\nu)}\rho\right\} = 0$ (every dissipator obeys trace conservation).

Third, combining these manipulations, we can at all times additively decompose the entropy production rate into reservoir-specific contributions

$$\dot{S}_\mathrm{i} = -\sum_\nu \mathrm{Tr}\left\{\left[\mathcal{L}^{(\nu)}\rho\right]\left[\ln\rho - \ln\rho_\mathrm{eq}^{(\nu)}\right]\right\}\,. \tag{3.73}$$

Finally, we will show that the contribution arising from each individual ν term is positive. To do this, we need to introduce the quantum relative entropy.

Box 14 (Quantum relative entropy) *The quantum relative entropy between two density matrices ρ and σ is given by*

$$D(\rho,\sigma) = \mathrm{Tr}\left\{\rho\ln\rho\right\} - \mathrm{Tr}\left\{\rho\ln\sigma\right\} = \mathrm{Tr}\left\{\rho\left(\ln\rho - \ln\sigma\right)\right\}\,. \tag{3.74}$$

It is non-negative $D(\rho,\sigma) \geq 0$ and vanishes if and only if $\rho = \sigma$.

Although it is not symmetric $D(\rho,\sigma) \neq D(\sigma,\rho)$, it may serve as a distance measure in the space of density matrices.

We now use that completely positive and trace-preserving maps – in particular the evolution V generated by Lindblad generators – are **contractive**, i.e., they decrease the distance between any two states

$$D(VA, VB) \leq D(A,B)\,. \tag{3.75}$$

This also holds for more general distances as the (unsymmetric) quantum relative entropy. Choosing $A = \rho(t)$, $B = \rho_\mathrm{eq}^{(\nu)}(t)$, and $V^{(\nu)}(t+\Delta t, t)$ as the propagator associated to a single-reservoir

evolution $\dot{\rho} = \mathcal{L}^{(\nu)}(t)\rho$ from time t to $t + \Delta t$, it follows that $V(t + \Delta t, t)\rho(t) = \rho(t + \Delta t)$ by construction and

$$V(t + \Delta t, t)\rho_{\rm eq}^{(\nu)}(t) = V(t, t)\rho_{\rm eq}^{(\nu)}(t) + \mathcal{L}^{(\nu)}(t)\rho_{\rm eq}^{(\nu)}(t) + \mathcal{O}\{\Delta t^2\} = \rho_{\rm eq}^{(\nu)}(t) + \mathcal{O}\{\Delta t^2\}\,, \tag{3.76}$$

since by definition of $\rho_{\rm eq}^{(\nu)}(t)$ the first order term vanishes. Consequently, we have

$$\begin{aligned}
0 \quad &\geq \quad D(VA, VB) - D(A, B) \\
&= \quad \frac{1}{\Delta t}\left[D(V(t + \Delta t, t)\rho(t), V(t + \Delta t, t)\rho_{\rm eq}^{(\nu)}(t)) - D(\rho(t), \rho_{\rm eq}^{(\nu)}(t))\right] \\
&= \quad \frac{1}{\Delta t}\left[D(\rho(t + \Delta t), \rho_{\rm eq}^{(\nu)}(t) + \mathcal{O}\{\Delta t^2\}) - D(\rho(t), \rho_{\rm eq}^{(\nu)}(t))\right] \\
&= \quad \frac{1}{\Delta t}\Big[{\rm Tr}\left\{\rho(t + \Delta t)\ln\rho(t + \Delta t)\right\} - {\rm Tr}\left\{\rho(t + \Delta t)\ln\rho_{\rm eq}^{(\nu)}(t)\right\} \\
&\quad\quad -{\rm Tr}\left\{\rho(t)\ln\rho(t)\right\} + {\rm Tr}\left\{\rho(t)\ln\rho_{\rm eq}^{(\nu)}(t)\right\}\Big] + \mathcal{O}\{\Delta t\} \\
\overset{\Delta t\to 0}{\longrightarrow} \quad &\frac{d}{dt}{\rm Tr}\left\{\rho\ln\rho\right\} - {\rm Tr}\left\{\dot{\rho}\ln\rho_{\rm eq}^{(\nu)}\right\} = {\rm Tr}\left\{\dot{\rho}\left[\ln\rho - \ln\rho_{\rm eq}^{(\nu)}\right]\right\} \\
= \quad &{\rm Tr}\left\{\left[\mathcal{L}^{(\nu)}\rho\right]\left[\ln\rho - \ln\rho_{\rm eq}^{(\nu)}\right]\right\} \leq 0
\end{aligned} \tag{3.77}$$

where we again used the same arguments as below Eq. (3.59). Comparing with Eq. (3.73), we finally obtain the second law for finite times, in presence of driving and multiple reservoirs

$$\dot{S}_{\rm i} \geq 0\,, \tag{3.78}$$

justifying the definitions made. This is a second law of thermodynamics in a composite non-equilibrium setup, also valid far from equilibrium. More general formulations of the second law (going beyond Lindblad master equations) do not predict a positive production rate, but just an increase of the entropy production with respect to the initial time.

3.6.3 Steady-State Dynamics

We will discuss the simpler case of steady-state dynamics here. Given a finite-dimensional Hilbert space and ergodic dynamics, the von-Neumann entropy of the system will saturate at some point $\dot{S} \to 0$ and the entropy production rate is given by the heat flows

$$\dot{S}_{\rm i} \to -\sum_\nu \beta_\nu \dot{Q}^{(\nu)} = -\sum_\nu \beta_\nu \left[I_E^{(\nu)} - \mu_\nu I_M^{(\nu)}\right] \geq 0\,, \tag{3.79}$$

where $I_E^{(\nu)}$ and $I_M^{(\nu)}$ are the energy and matter currents entering the system from reservoir ν, respectively. Whereas energy and matter conservation imply equalities among the currents at steady state

$$\sum_\nu I_M^{(\nu)} = 0\,, \qquad \sum_\nu I_E^{(\nu)} = 0\,, \tag{3.80}$$

the positivity of entropy production imposes a further constraint among the currents, e.g. for a two-terminal system

$$\begin{aligned}
\dot{S}_{\rm i} \quad &= \quad -\beta_L(I_E^{(L)} - \mu_L I_M^{(L)}) - \beta_R(I_E^{(R)} - \mu_R I_M^{(R)}) \\
&= \quad (\beta_R - \beta_L)I_E + (\mu_L\beta_L - \mu_R\beta_R)I_M \geq 0\,,
\end{aligned} \tag{3.81}$$

where we have introduced the currents from left to right $I_E = +I_E^{(L)} = -I_E^{(R)}$ and $I_M = +I_M^{(L)} = -I_M^{(R)}$.

We first discuss the case of equal temperatures $\beta = \beta_L = \beta_R$. The second law implies that

$$(\mu_L - \mu_R) I_M \geq 0\,, \tag{3.82}$$

which is nothing but the trivial statement that the current is directed from a lead with large chemical potential towards the lead with smaller chemical potential.

Next, we consider equal chemical potentials $\mu_L = \mu_R = \mu$ but different temperatures. Then, our setup has to obey

$$(\beta_R - \beta_L)(I_E - \mu I_M) \geq 0\,, \tag{3.83}$$

where $I_E - \mu I_M$ can now be interpreted as the heat transferred from left to right. When $\beta_R > \beta_L$ (i.e. the left lead is hotter than the right one $T_L > T_R$), the second law just implies that $I_E - \mu I_M \geq 0$, i.e., heat flows from hot to cold.

Finally, when there is both a thermal and a potential gradient present, it is possible to use temperature differences to drive a current against a potential bias, i.e. to perform work. This is the limit of a **thermoelectric generator**. Conversely, one may apply a thermal gradient to a system and use it to let the heat flow against the usual direction, e.g. to cool a cold reservoir (**refrigerator**) or to heat a hot reservoir (**heat pump**).

3.7 The double quantum dot

We consider a double quantum dot with internal tunnel coupling T and Coulomb interaction U that is weakly coupled to two fermionic contacts via the rates Γ_L and Γ_R, see Fig. 3.2. The

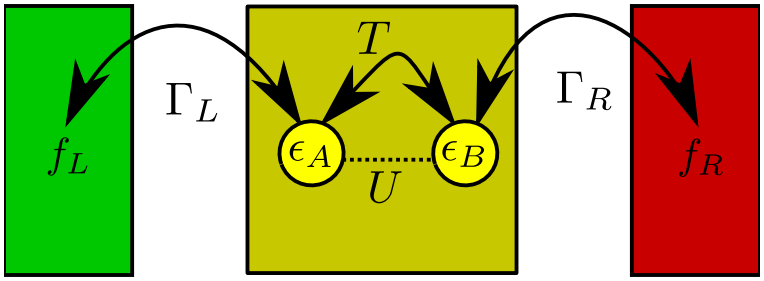

Figure 3.2: A double quantum dot (system) with on-site energies $\epsilon_{A/B}$ and internal tunneling amplitude T and Coulomb interaction U may host at most two electrons. It is weakly tunnel-coupled to two fermionic contacts via the rates $\Gamma_{L/R}$ at different thermal equilibria described by the Fermi distributions $f_{L/R}(\omega)$.

corresponding Hamiltonian reads

$$\begin{aligned}
\mathcal{H}_{\rm S} &= \epsilon_A d_A^\dagger d_A + \epsilon_B d_B^\dagger d_B + T\left(d_A d_B^\dagger + d_B d_A^\dagger\right) + U d_A^\dagger d_A d_B^\dagger d_B\,,\\
\mathcal{H}_{\rm B} &= \sum_k \epsilon_{kL} c_{kL}^\dagger c_{kL} + \sum_k \epsilon_{kR} c_{kR}^\dagger c_{kR}\,,\\
\mathcal{H}_{\rm I} &= \sum_k \left(t_{kL} d_A c_{kL}^\dagger + t_{kL}^* c_{kL} d_A^\dagger\right) + \sum_k \left(t_{kR} d_B c_{kR}^\dagger + t_{kR}^* c_{kR} d_B^\dagger\right)\,.
\end{aligned} \tag{3.84}$$

In contrast to our previously treated simple rate equation, the internal tunneling T is not a transition rate but an amplitude, since it occurs at the level of the Hamiltonian. Furthermore, we note that strictly speaking we do not have a tensor product decomposition in the interaction Hamiltonian, as the coupling operators anti-commute, e.g.,

$$\{d, c_{kR}\} = 0\,. \tag{3.85}$$

We may however use the Jordan Wigner transform, which decomposes the Fermionic operators in terms of Pauli matrices acting on different spins

$$\begin{aligned} d_A &= \sigma^- \otimes \mathbf{1} \otimes \mathbf{1} \otimes \ldots \otimes \mathbf{1}\,, \qquad d_B = \sigma^z \otimes \sigma^- \otimes \mathbf{1} \otimes \ldots \otimes \mathbf{1}\,, \\ c_{kL} &= \sigma^z \otimes \sigma^z \otimes \underbrace{\sigma^z \otimes \ldots \otimes \sigma^z}_{k-1} \otimes \sigma^- \otimes \mathbf{1} \otimes \ldots \otimes \mathbf{1}\,, \\ c_{kR} &= \sigma^z \otimes \sigma^z \otimes \underbrace{\sigma^z \otimes \ldots \otimes \sigma^z}_{K_L} \otimes \underbrace{\sigma^z \otimes \ldots \otimes \sigma^z}_{k-1} \otimes \sigma^- \otimes \mathbf{1} \otimes \ldots \otimes \mathbf{1} \end{aligned} \tag{3.86}$$

to map to a tensor-product decomposition of the interaction Hamiltonian, where $\sigma^{\pm} = \frac{1}{2}\left[\sigma^x \pm \mathrm{i}\sigma^y\right]$. The remaining operators follow from $(\sigma^+)^\dagger = \sigma^-$ and vice versa. This decomposition automatically obeys the fermionic anti-commutation relations such as e.g. $\left\{c_k, d^\dagger\right\} = 0$ and may therefore also be used to create a fermionic operator basis with computer algebra programs (e.g. use `KroneckerProduct` in Mathematica).

Exercise 34 (Jordan-Wigner transform) *(1 points)*
Show that for fermions distributed on N sites, the decomposition

$$c_i = \underbrace{\sigma^z \otimes \ldots \otimes \sigma^z}_{i-1} \otimes \sigma^- \otimes \underbrace{\mathbf{1} \otimes \ldots \otimes \mathbf{1}}_{N-i}$$

preserves the fermionic anti-commutation relations

$$\{c_i, c_j\} = \mathbf{0} = \left\{c_i^\dagger, c_j^\dagger\right\}\,, \qquad \left\{c_i, c_j^\dagger\right\} = \delta_{ij}\mathbf{1}\,.$$

Show also that the fermionic Fock space basis $c_i^\dagger c_i \left|n_1, \ldots, n_N\right\rangle = n_i \left|n_1, \ldots, n_N\right\rangle$ obeys $\sigma_i^z \left|n_1, \ldots, n_N\right\rangle = (-1)^{n_i+1} \left|n_1, \ldots, n_N\right\rangle$.

Inserting the decomposition (3.86) in the Hamiltonian, we may simply use the relations

$$\begin{aligned} (\sigma^x)^2 &= (\sigma^y)^2 = (\sigma^z)^2 = \mathbf{1}\,, \qquad \sigma^+\sigma^- = \frac{1}{2}\left[\mathbf{1} + \sigma^z\right]\,, \qquad \sigma^-\sigma^+ = \frac{1}{2}\left[\mathbf{1} - \sigma^z\right]\,, \\ \sigma^z\sigma^- &= -\sigma^-\,, \qquad \sigma^-\sigma^z = +\sigma^-\,, \qquad \sigma^z\sigma^+ = +\sigma^+\,, \qquad \sigma^+\sigma^z = -\sigma^+ \end{aligned} \tag{3.87}$$

to obtain a system of interacting spins

$$\begin{aligned}
\mathcal{H}_{\rm S} &= \epsilon_A \frac{1}{2}\left[\mathbf{1}+\sigma_A^z\right] + \epsilon_B \frac{1}{2}\left[\mathbf{1}+\sigma_B^z\right] + T\left[\sigma_A^-\sigma_B^+ + \sigma_A^+\sigma_B^-\right] + U\frac{1}{2}\left[\mathbf{1}+\sigma_A^z\right]\frac{1}{2}\left[\mathbf{1}+\sigma_B^z\right] \\
\mathcal{H}_{\rm B} &= \sum_k \epsilon_{kL}\frac{1}{2}\left[\mathbf{1}+\sigma_{kL}^z\right] + \sum_k \epsilon_{kR}\frac{1}{2}\left[\mathbf{1}+\sigma_{kR}^z\right] \\
\mathcal{H}_{\rm I} &= \sigma_A^-\sigma_B^z \otimes \sum_k t_{kL}\left[\prod_{k'<k}\sigma_{k'L}^z\right]\sigma_{kL}^+ + \sigma_A^+\sigma_B^z \otimes \sum_k t_{kL}^*\left[\prod_{k'<k}\sigma_{k'L}^z\right]\sigma_{kL}^- \\
&\quad + \sigma_B^- \otimes \sum_k t_{kR}\left[\prod_{k'}\sigma_{k'L}^z\right]\left[\prod_{k''<k}\sigma_{k''R}^z\right]\sigma_{kR}^+ + \sigma_B^+ \otimes \sum_k t_{kR}^*\left[\prod_{k'}\sigma_{k'L}^z\right]\left[\prod_{k''<k}\sigma_{k''R}^z\right]\sigma_{kR}^- \\
&\quad .
\end{aligned} \tag{3.88}$$

With this, we could proceed by simply viewing the Hamiltonian as a complicated total system of non-locally interacting spins. However, the order of operators in the nonlocal Jordan-Wigner transformation may be chosen as convenient without destroying the fermionic anticommutation relations. We may therefore also define new fermionic operators on the subspace of the system (first two sites, with reversed order) and the baths (all remaining sites with original order), respectively

$$\begin{aligned}
\tilde{d}_A &= \sigma^- \otimes \sigma^z\,, \qquad \tilde{d}_B = \mathbf{1}\otimes\sigma^-\,, \\
\tilde{c}_{kL} &= \underbrace{\sigma^z\otimes\ldots\otimes\sigma^z}_{k-1}\otimes\sigma^-\otimes\mathbf{1}\otimes\ldots\otimes\mathbf{1}\,, \\
\tilde{c}_{kR} &= \underbrace{\sigma^z\otimes\ldots\otimes\sigma^z}_{K_L}\otimes\underbrace{\sigma^z\otimes\ldots\otimes\sigma^z}_{k-1}\otimes\sigma^-\otimes\mathbf{1}\otimes\ldots\otimes\mathbf{1}\,.
\end{aligned} \tag{3.89}$$

These new operators obey fermionic anti-commutation relations in system and bath separately (e.g. $\{\tilde{d}_A,\tilde{d}_B\}=\mathbf{0}$ and $\{\tilde{c}_{kL},\tilde{c}_{k'L}\}=\mathbf{0}$), but act on different Hilbert spaces, such that system and bath operators do commute by construction (e.g. $[\tilde{d}_A,\tilde{c}_{kL}]=0$). In the new operator basis, the Hamiltonian appears as

$$\begin{aligned}
\mathcal{H}_{\rm S} &= \left[\epsilon_A\tilde{d}_A^\dagger\tilde{d}_A + \epsilon_B\tilde{d}_B^\dagger\tilde{d}_B + T\left(\tilde{d}_A\tilde{d}_B^\dagger + \tilde{d}_B\tilde{d}_A^\dagger\right) + U\tilde{d}_A^\dagger\tilde{d}_A\tilde{d}_B^\dagger\tilde{d}_B\right]\otimes\mathbf{1}\,, \\
\mathcal{H}_{\rm B} &= \mathbf{1}\otimes\left[\sum_k \epsilon_{kL}\tilde{c}_{kL}^\dagger\tilde{c}_{kL} + \sum_k \epsilon_{kR}\tilde{c}_{kR}^\dagger\tilde{c}_{kR}\right]\,, \\
\mathcal{H}_{\rm I} &= \tilde{d}_A\otimes\sum_k t_{kL}\tilde{c}_{kL}^\dagger + \tilde{d}_A^\dagger\otimes\sum_k t_{kL}^*\tilde{c}_{kL} + \tilde{d}_B\otimes\sum_k t_{kR}\tilde{c}_{kR}^\dagger + \tilde{d}_B^\dagger\otimes\sum_k t_{kR}^*\tilde{c}_{kR}\,,
\end{aligned} \tag{3.90}$$

which is the same (for this and some more special cases) as if we had ignored the fermionic nature of the annihilation operators from the beginning. We do now proceed by calculating the Fourier transforms of the bath correlation functions

$$\begin{aligned}
\gamma_{12}(\omega) &= \Gamma_L(-\omega)f_L(-\omega)\,, \qquad \gamma_{21}(\omega) = \Gamma_L(+\omega)[1-f_L(+\omega)]\,, \\
\gamma_{34}(\omega) &= \Gamma_R(-\omega)f_R(-\omega)\,, \qquad \gamma_{43}(\omega) = \Gamma_R(+\omega)[1-f_R(+\omega)]
\end{aligned} \tag{3.91}$$

with the continuum tunneling rates $\Gamma_\alpha(\omega)=2\pi\sum_k|t_{k\alpha}|^2\delta(\omega-\epsilon_{k\alpha})$ and Fermi functions $f_\alpha(\epsilon_{k\alpha})=\left\langle c_{k\alpha}^\dagger c_{k\alpha}\right\rangle = \left[e^{\beta_\alpha(\epsilon_{k\alpha}-\mu_\alpha)}+1\right]^{-1}$.

Exercise 35 (DQD bath correlation functions) *(1 points)*
Calculate the Fourier transforms (3.91) of the bath correlation functions for the double quantum dot, assuming that the reservoirs are in a thermal equilibrium state with inverse temperatures β_α and chemical potential μ_α.

Next, we diagonalize the system Hamiltonian (in the Fock space basis)

$$\begin{aligned}
E_0 &= 0\,, \qquad |v_0\rangle = |00\rangle\,, \\
E_- &= \epsilon - \sqrt{\Delta^2+T^2}\,, \qquad |v_-\rangle \propto \left[\left(\Delta+\sqrt{\Delta^2+T^2}\right)|10\rangle + T\,|01\rangle\right]\,, \\
E_+ &= \epsilon + \sqrt{\Delta^2+T^2}\,, \qquad |v_+\rangle \propto \left[\left(\Delta-\sqrt{\Delta^2+T^2}\right)|10\rangle + T\,|01\rangle\right]\,, \\
E_2 &= 2\epsilon + U\,, \qquad |v_2\rangle = |11\rangle\,,
\end{aligned} \tag{3.92}$$

where $\Delta = (\epsilon_B - \epsilon_A)/2$ and $\epsilon = (\epsilon_A + \epsilon_B)/2$ and $|01\rangle = -\tilde{d}_B^\dagger|00\rangle$, $|10\rangle = \tilde{d}_A^\dagger|00\rangle$, and $|11\rangle = \tilde{d}_B^\dagger\tilde{d}_A^\dagger|00\rangle$. We have not symmetrized the coupling operators but to obtain the BMS limit, we may alternatively use Eqns. (2.58) and (2.59) when $\tau\to\infty$. Specifically, when we have no degeneracies in the system Hamiltonian ($\Delta^2+T^2>0$), the master equation in the energy eigenbasis (where $a,b\in\{0,-,+,2\}$) becomes a rate equation (2.43), where for non-hermitian coupling operators the transition rates from b to a are given by

$$\gamma_{ab,ab} = \sum_{\alpha\beta}\gamma_{\alpha\beta}(E_b-E_a)\,\langle a|\,A_\beta\,|b\rangle\,\langle a|\,A_\alpha^\dagger\,|b\rangle^*\,. \tag{3.93}$$

We may calculate the Liouvillians for the interaction with the left and right contact separately

$$\gamma_{ab,ab} = \gamma^L_{ab,ab} + \gamma^R_{ab,ab}\,, \tag{3.94}$$

since we are constrained to second order perturbation theory in the tunneling amplitudes. Since we have $\tilde{d}_A = A_2^\dagger = A_1 = \tilde{d}_A$ and $\tilde{d}_B = A_4^\dagger = A_2 = \tilde{d}_B$, we obtain for the left-associated dampening coefficients

$$\begin{aligned}
\gamma^L_{ab,ab} &= \gamma_{12}(E_b-E_a)|\langle a|\,A_2\,|b\rangle|^2 + \gamma_{21}(E_b-E_a)|\langle a|\,A_1\,|b\rangle|^2\,, \\
\gamma^R_{ab,ab} &= \gamma_{34}(E_b-E_a)|\langle a|\,A_4\,|b\rangle|^2 + \gamma_{43}(E_b-E_a)|\langle a|\,A_3\,|b\rangle|^2\,.
\end{aligned} \tag{3.95}$$

In the wideband (flatband) limit $\Gamma_{L/R}(\omega)=\Gamma_{L/R}$, we obtain for the nonvanishing transition rates in the energy eigenbasis

$$\begin{aligned}
\gamma^L_{0-,0-} &= \Gamma_L\gamma_+[1-f_L(\epsilon-\sqrt{\Delta^2+T^2})]\,, \qquad \gamma^R_{0-,0-} = \Gamma_R\gamma_-[1-f_R(\epsilon-\sqrt{\Delta^2+T^2})]\,, \\
\gamma^L_{0+,0+} &= \Gamma_L\gamma_-[1-f_L(\epsilon+\sqrt{\Delta^2+T^2})]\,, \qquad \gamma^R_{0+,0+} = \Gamma_R\gamma_+[1-f_R(\epsilon+\sqrt{\Delta^2+T^2})]\,, \\
\gamma^L_{-2,-2} &= \Gamma_L\gamma_-[1-f_L(\epsilon+U+\sqrt{\Delta^2+T^2})]\,, \qquad \gamma^R_{-2,-2} = \Gamma_R\gamma_+[1-f_R(\epsilon+U+\sqrt{\Delta^2+T^2})]\,, \\
\gamma^L_{+2,+2} &= \Gamma_L\gamma_+[1-f_L(\epsilon+U-\sqrt{\Delta^2+T^2})]\,, \qquad \gamma^R_{+2,+2} = \Gamma_R\gamma_-[1-f_R(\epsilon+U-\sqrt{\Delta^2+T^2})]\,, \\
\gamma^L_{-0,-0} &= \Gamma_L\gamma_+ f_L(\epsilon-\sqrt{\Delta^2+T^2})\,, \qquad \gamma^R_{-0,-0} = \Gamma_R\gamma_- f_R(\epsilon-\sqrt{\Delta^2+T^2})\,, \\
\gamma^L_{+0,+0} &= \Gamma_L\gamma_- f_L(\epsilon+\sqrt{\Delta^2+T^2})\,, \qquad \gamma^R_{+0,+0} = \Gamma_R\gamma_+ f_R(\epsilon+\sqrt{\Delta^2+T^2})\,, \\
\gamma^L_{2-,2-} &= \Gamma_L\gamma_- f_L(\epsilon+U+\sqrt{\Delta^2+T^2})\,, \qquad \gamma^R_{2-,2-} = \Gamma_R\gamma_+ f_R(\epsilon+U+\sqrt{\Delta^2+T^2})\,, \\
\gamma^L_{2+,2+} &= \Gamma_L\gamma_+ f_L(\epsilon+U-\sqrt{\Delta^2+T^2})\,, \qquad \gamma^R_{2+,2+} = \Gamma_R\gamma_- f_R(\epsilon+U-\sqrt{\Delta^2+T^2})\,,
\end{aligned} \tag{3.96}$$

with the dimensionless coefficients

$$\gamma_\pm = \frac{1}{2}\left[1 \pm \frac{\Delta}{\sqrt{\Delta^2 + T^2}}\right] \tag{3.97}$$

arising from the matrix elements of the system coupling operators. This rate equation can also be visualized with a network, see Fig. 3.3. We note that although both reservoirs drive all transitions,

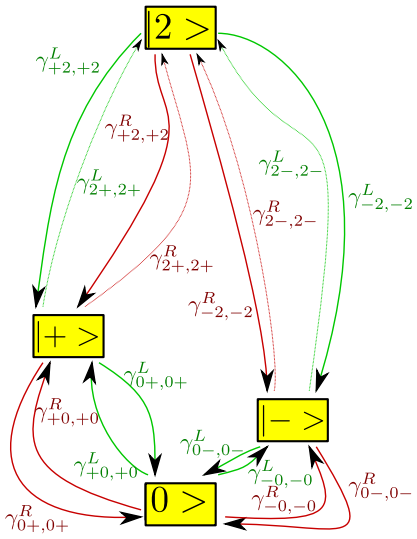

Figure 3.3: Configuration space of a serial double quantum dot coupled to two leads. Due to the hybridization of the two levels, electrons may jump directly from the left contact to right-localized modes and vice versa, such that in principle all transitios are driven by both contacts. However, the relative strength of the couplings is different, such that the two Liouillians have a different structure. In the Coulomb-blockade limit, transitions to the doubly occupied state are forbidden (dotted lines), such that the system dimension can be reduced.

their relative strength is different, and we do not have a simple situation as discussed previously in Eq. (3.6). Consequently, the stationary state of the rate equation cannot be written as some grand-canonical equilibrium state, which is most conveniently shown by disproving the relations $\bar{\rho}_{--}/\bar{\rho}_{00} = e^{-\beta(E_- - E_0 - \mu)}$, $\bar{\rho}_{++}/\bar{\rho}_{00} = e^{-\beta(E_+ - E_0 - \mu)}$ and $\bar{\rho}_{++}/\bar{\rho}_{--} = e^{-\beta(E_+ - E_-)}$.

As the simplest example of the resulting rate equation, we study the high-bias and Coulomb-blockade limit $f_{L/R}(\epsilon + U \pm \sqrt{\Delta^2 + T^2}) \to 0$ and $f_L(\epsilon \pm \sqrt{\Delta^2 + T^2}) \to 1$ and $f_R(\epsilon \pm \sqrt{\Delta^2 + T^2}) \to 0$ when $\Delta \to 0$ (such that $\gamma_\pm \to 1/2$). This removes any dependence on the internal tunneling amplitude T. Consequently, derived quantities such as e.g. the current will not depend on T either and we would obtain a current even when $T \to 0$ (where we have a disconnected structure). However, precisely in this limit (i.e. $\Delta \to 0$ and $T \to 0$), the two levels E_- and E_+ become energetically degenerate, and a simple rate equation description is not applicable. The take-home message of this failure is that one should not use plug and play formulas without learning about their limits. Therefore, keeping in mind that $T \neq 0$, the resulting Liouvillian reads

$$\mathcal{L} = \frac{1}{2}\begin{pmatrix} -2\Gamma_L & \Gamma_R & \Gamma_R & 0 \\ \Gamma_L & -\Gamma_R & 0 & \Gamma_L + \Gamma_R \\ \Gamma_L & 0 & -\Gamma_R & \Gamma_L + \Gamma_R \\ 0 & 0 & 0 & -2(\Gamma_L + \Gamma_R) \end{pmatrix}, \tag{3.98}$$

where it becomes visible that the doubly occupied state will simply decay and may therefore – since we are interested in the long-term dynamics – be eliminated completely

$$\mathcal{L}_{\text{CBHB}} = \frac{1}{2}\begin{pmatrix} -2\Gamma_L & \Gamma_R & \Gamma_R \\ \Gamma_L & -\Gamma_R & 0 \\ \Gamma_L & 0 & -\Gamma_R \end{pmatrix}. \tag{3.99}$$

Introducing counting fields for matter (χ) and energy (ξ) entering the right junction we obtain

$$\mathcal{L}_{\rm CBHB}(\chi,\xi) \;=\; \frac{1}{2}\begin{pmatrix} -2\Gamma_L & \Gamma_R e^{+i\chi+i\xi E_-} & \Gamma_R e^{+i\chi+i\xi E_+} \\ \Gamma_L & -\Gamma_R & 0 \\ \Gamma_L & 0 & -\Gamma_R \end{pmatrix}. \tag{3.100}$$

Exercise 36 (Stationary DQD currents) *(1 points)*
Calculate the stationary currents entering the right reservoir with the help of Eq.(3.100).

At finite bias voltages, it becomes of course harder to calculate steady states and stationary currents. However, for low temperatures, the Fermi functions will behave similiar to step functions, and the transport window becomes sharp. Then, by enlarging the bias voltage, the transport window is opened, and the currents will exhibit steps when a new transport channel is inside the transport window, see Fig. 3.4. A further obvious observation is that at zero bias voltage, we have

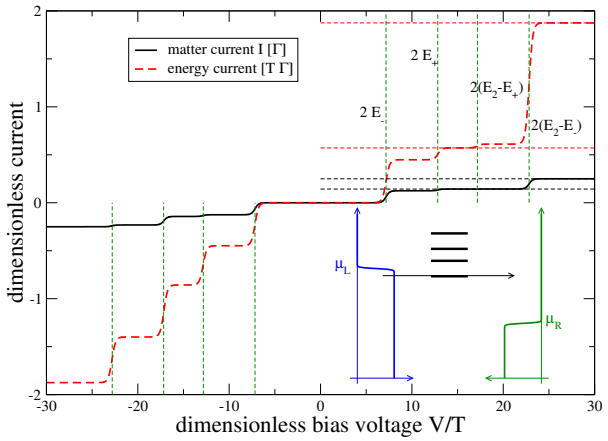

Figure 3.4: Plot of matter (solid black) and energy (dashed red) currents. At sufficiently low temperatures, the steps in the currents occur for positive bias voltage at $\mu_L = V/2 \in \{E_- - E_0, E_+ - E_0, E_2 - E_+, E_2 - E_-\}$. The inset displays the configuration of these transition energies relative to left (blue) and right (green) Fermi functions taken at $V = 10T$. Then, only the lowest transition energy (arrow) is inside the transport window, such that transport is dominated by transitions between $|-\rangle$ and $|0\rangle$. Other parameters have been chosen as $\mu_L = -\mu_R = V/2$, $\Gamma_L = \Gamma_R = \Gamma$, $\epsilon_A = 4T$, $\epsilon_B = 6T$,$U = 5T$, and $\beta T = 10$.

vanishing currents. This must happen only at equal temperatures. The entropy production in this case is fully determined by the matter current $\dot{S}_{\rm i} = \beta(\mu_L - \mu_R)I_M$, where I_M denotes the current from left to right. Identifying $P = (\mu_L - \mu_R)I_M$ with the power dissipated by the device, the entropy production just becomes $\dot{S}_{\rm i} = \beta P$.

3.8 Phonon-Assisted Tunneling

We consider here a three-terminal system, comprised as before of two quantum dots. The left dot is tunnel-coupled to the left lead, the right dot to the right, but in addition, tunneling between the dots is now triggered by a third (bosonic) reservoir that does not change the particle content. That is, without the bosonic reservoir (e.g. phonons or photons) the model would not support a steady state matter current – which is in contrast to the previous model

The system is described by the Hamiltonian

$$\mathcal{H}_{\rm S} = \epsilon_A d_A^\dagger d_A + \epsilon_B d_B^\dagger d_B + U d_A^\dagger d_A d_B^\dagger d_B \tag{3.101}$$

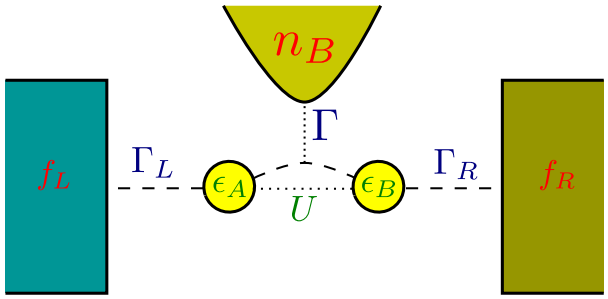

Figure 3.5: Sketch of two quantum dots that are separately tunnel-coupled to their adjacent reservoir in the conventional way by rates Γ_L and Γ_R. The mere Coulomb interaction U only allows for the exchange of energy between the dots, but with phonons present (rounded terminals), tunneling between A and B becomes possible (dotted and dashed). The device may act as a thermoelectric generator converting thermal gradients into power.

with on-site energies $\epsilon_A < \epsilon_B$ and Coulomb interaction U. Since there is no internal tunneling, its energy eigenstates coincide with the localized basis $|n_A, n_B\rangle$ with the dot occupations $n_A, n_B \in \{0, 1\}$. This structure makes it particularly simple to derive a master equation in rate equation representation. The jumps between states are triggered by the electronic tunneling Hamiltonians and the electron-phonon interaction

$$\begin{aligned}\mathcal{H}_{\mathrm{I}} &= \sum_k \left(t_{kL} d_A c_{kL}^\dagger + t_{kL}^* c_{kL} d_A^\dagger \right) + \sum_k \left(t_{kR} d_B c_{kR}^\dagger + t_{kR}^* c_{kR} d_B^\dagger \right) \\ &\quad + \left(d_A d_B^\dagger + d_B d_A^\dagger \right) \otimes \sum_q \left(h_q a_q + h_q^* a_q^\dagger \right) , \end{aligned} \tag{3.102}$$

where $c_{k\alpha}$ are fermionic and a_q bosonic annihilation operators. The three reservoirs

$$\mathcal{H}_{\mathrm{B}} = \sum_k \epsilon_{kL} c_{kL}^\dagger c_{kL} + \sum_k \epsilon_{kR} c_{kR}^\dagger c_{kR} + \sum_q \omega_q a_q^\dagger q_q \tag{3.103}$$

are assumed to remain in separate thermal equilibrium states, such that the reservoir density matrix is assumed to be a product of the single density matrices. This automatically implies that the expectation value of linear combinations of the coupling operators vanishes. In the weak-coupling limit, the rate matrix will be additively decomposed into contributions resulting from the electronic (L, R) and bosonic (B) reservoirs $\mathcal{L} = \mathcal{L}_L + \mathcal{L}_R + \mathcal{L}_B$ From our results with the single-electron transistor, we may readily reproduce the rates for the electronic jumps. Ordering the basis as $\rho_{00,00}$, $\rho_{10,10}$, $\rho_{01,01}$, and $\rho_{11,11}$ and using for simplicity the wide-band limit $\Gamma_\alpha(\omega) \approx \Gamma_\alpha$ these read

$$\begin{aligned}\mathcal{L}_L &= \Gamma_L \begin{pmatrix} -f_L(\epsilon_A) & 1 - f_L(\epsilon_A) & 0 & 0 \\ +f_L(\epsilon_A) & -[1 - f_L(\epsilon_A)] & 0 & 0 \\ 0 & 0 & -f_L(\epsilon_A + U) & 1 - f_L(\epsilon_A + U) \\ 0 & 0 & +f_L(\epsilon_A + U) & -[1 - f_L(\epsilon_A + U)] \end{pmatrix} \\ \mathcal{L}_R &= \Gamma_R \begin{pmatrix} -f_R(\epsilon_B) & 0 & 1 - f_R(\epsilon_B) & 0 \\ 0 & -f_R(\epsilon_B + U) & 0 & 1 - f_R(\epsilon_B + U) \\ +f_R(\epsilon_B) & 0 & -[1 - f_R(\epsilon_B)] & 0 \\ 0 & +f_R(\epsilon_B + U) & 0 & -[1 - f_R(\epsilon_B + U)] \end{pmatrix} , \end{aligned} \tag{3.104}$$

where the electronic tunneling rates are as usual obtained via (in the wide-band limit) $\Gamma_\alpha \approx \Gamma_\alpha(\omega) = 2\pi \sum_k |t_{k\alpha}|^2 \delta(\omega - \epsilon_{k\alpha})$ from the microscopic tunneling amplitudes $t_{k\alpha}$. We note that the

Fermi functions are evaluated at the energy difference of the jump to which they refer. Although energy may be transferred between the left and right junctions without the presence of phonons, it is not possible to transfer charges.

For the spin-boson example, we have also already calculated the correlation function for the phonons for a spin-boson model in Sec. 2.2.4. Since the reservoir coupling operator is identical, we may use our result from Eq. (2.73).

$$\gamma(\omega) = \Gamma(+\omega)\Theta(+\omega)[1 + n_B(+\omega)] + \Gamma(-\omega)\Theta(-\omega)n_B(-\omega)\,, \tag{3.105}$$

where $\Gamma(\omega) = 2\pi \sum_k |h_k|^2 \delta(\omega - \omega_k)$ was the bosonic emission or absorption rate and $n_B(\omega)$ denoted the Bose-Einstein distribution function. For consistency, we just note that the KMS condition is obeyed. With this, we may readily evaluate the rates due to the phonon reservoirs, i.e., we have with $\Gamma = \Gamma(\epsilon_B - \epsilon_A)$

$$\mathcal{L}_B = \Gamma \begin{pmatrix} 0 & 0 & 0 & 0 \\ 0 & -n_B(\epsilon_B - \epsilon_A) & 1 + n_B(\epsilon_B - \epsilon_A) & 0 \\ 0 & +n_B(\epsilon_B - \epsilon_A) & -[1 + n_B(\epsilon_B - \epsilon_A)] & 0 \\ 0 & 0 & 0 & 0 \end{pmatrix}. \tag{3.106}$$

The rate matrices in Eqs. (3.104) and (3.106) can be used to extract the full electron-phonon counting statistics after all jumps have been identified. We have a three terminal system, where the phonon terminal only allows for the exchange of energy, i.e., in total we can calculate five non-vanishing currents. With the conservation laws on matter and energy currents, we can at steady state eliminate two of these, and the entropy production becomes

$$\begin{aligned} \dot{S}_\mathrm{i} &= -\beta_\mathrm{ph} I_E^B - \beta_L (I_E^L - \mu_L I_M^L) - \beta_R (I_E^R - \mu_R I_M^R) \\ &= -\beta_\mathrm{ph} I_E^B - \beta_L (I_E^L - \mu_L I_M^L) + \beta_R (I_E^L + I_E^B - \mu_R I_M^L) \\ &= (\beta_R - \beta_\mathrm{ph}) I_E^B + (\beta_R - \beta_L) I_E^L + (\beta_L \mu_L - \beta_R \mu_R) I_M^L\,, \end{aligned} \tag{3.107}$$

which has the characteristic affinity-flux form. In usual electronic setups, the electronic temperatures will be the same $\beta_\mathrm{el} = \beta_L = \beta_R$, such that the entropy production further reduces to

$$\dot{S}_\mathrm{i} = (\beta_\mathrm{el} - \beta_\mathrm{ph}) I_E^B + \beta_\mathrm{el}(\mu_L - \mu_R) I_M^L \geq 0\,, \tag{3.108}$$

where we can identify the term $(\mu_L - \mu_R) I_M^L$ as a power consumed or produced by the device. Furthermore, we note that the device obeys the tight-coupling property: Every electron traversing the system from left to right must absorb energy $\epsilon_B - \epsilon_A$ from the phonon reservoir $I_E^B = (\epsilon_B - \epsilon_A) I_M^L$. Therefore, the entropy production can also be written as

$$\dot{S}_\mathrm{i} = \left[(\beta_\mathrm{el} - \beta_\mathrm{ph})(\epsilon_B - \epsilon_A) + \beta_\mathrm{el}(\mu_L - \mu_R)\right] I_M^L \geq 0\,. \tag{3.109}$$

We note that the prefactor of the matter current vanishes at

$$V^* = \mu_L^* - \mu_R^* = \left(\frac{T_\mathrm{el}}{T_\mathrm{ph}} - 1\right)(\epsilon_B - \epsilon_A)\,. \tag{3.110}$$

Since the prefactor switches sign at this voltage, the matter current must vanish at this voltage, too – otherwise the entropy production would not be positive. Without calculation, we have therefore found that at bias voltage V^* the current must vanish.

For simplicity, we decide to count matter at the left junction (χ) and energy transfers at the bosonic junction (ξ). To keep a compact description, we introduce the abbreviations

$$\begin{aligned} n_B &= n_B(\epsilon_B - \epsilon_A)\,, \qquad f_L = f_L(\epsilon_A)\,, \qquad f_R = f_R(\epsilon_B)\,, \\ \bar{f}_L &= f_L(\epsilon_A + U)\,, \qquad \bar{f}_R = f_R(\epsilon_B + U)\,, \qquad \Gamma = \Gamma(\epsilon_B - \epsilon_A)\,. \end{aligned} \tag{3.111}$$

With the counting fields, the complete system then becomes

$$\begin{aligned} \mathcal{L} &= \Gamma_L \begin{pmatrix} -f_L & (1-f_L)e^{-\mathrm{i}\chi} & 0 & 0 \\ +f_L e^{+\mathrm{i}\chi} & -[1-f_L] & 0 & 0 \\ 0 & 0 & -\bar{f}_L & (1-\bar{f}_L)e^{-\mathrm{i}\chi} \\ 0 & 0 & +\bar{f}_L e^{+\mathrm{i}\chi} & -(1-\bar{f}_L) \end{pmatrix} \\ &\quad +\Gamma \begin{pmatrix} 0 & 0 & 0 & 0 \\ 0 & -n_B & (1+n_B)e^{-\mathrm{i}(\epsilon_B-\epsilon_A)\xi} & 0 \\ 0 & +n_B e^{+\mathrm{i}(\epsilon_B-\epsilon_A)\xi} & -(1+n_B) & 0 \\ 0 & 0 & 0 & 0 \end{pmatrix} \\ &\quad +\Gamma_R \begin{pmatrix} -f_R & 0 & 1-f_R & 0 \\ 0 & -\bar{f}_R & 0 & 1-\bar{f}_R \\ +f_R & 0 & -(1-f_R) & 0 \\ 0 & +\bar{f}_R & 0 & -(1-\bar{f}_R) \end{pmatrix}. \end{aligned} \tag{3.112}$$

Noting that the total entropy production is positive does not imply that all contributions are separately positive. Fig. 3.6 displays the current as a function of the bias voltage for different electronic and phonon temperature configurations. It is visible that at zero bias, the matter current does not vanish when electron and phonon temperatures are not chosen equal.

3.8.1 Thermoelectric performance

We concentrate on the simple case discussed before and use $\beta_L = \beta_R = \beta_{\mathrm{el}}$ and $\beta_{\mathrm{ph}} = \beta_B$. In regions where the current runs against the bias, the power

$$P = -(\mu_L - \mu_R) I_M^L \tag{3.113}$$

becomes positive, and we can define an efficiency via

$$\eta = \frac{-(\mu_L - \mu_R) I_M^L}{\dot{Q}_{\mathrm{in}}} \Theta(P)\,, \tag{3.114}$$

where $\dot{Q}_{\mathrm{in}}$ is the heat entering the system from the hot reservoir. The purpose of the Heaviside function is just to avoid misinterpretations of the efficiency.

Consequently, when the phonon temperature is larger than the electron temperature $T_{\mathrm{ph}} > T_{\mathrm{el}}$, the input heat is given by the positive energy flow from the hot phonon bath into the system, such that – due to the tight-coupling property – the efficiency becomes trivially dependent on the bias voltage

$$\eta_{T_{\mathrm{ph}}>T_{\mathrm{el}}} = \frac{P}{I_E^B} \Theta(P) = -\frac{V}{\epsilon_B - \epsilon_A} \Theta(P)\,. \tag{3.115}$$

At first sight, one might think that this efficiency could become larger than one. It should be kept in mind however that it is only valid in regimes where the power (3.113) is positive, which limits

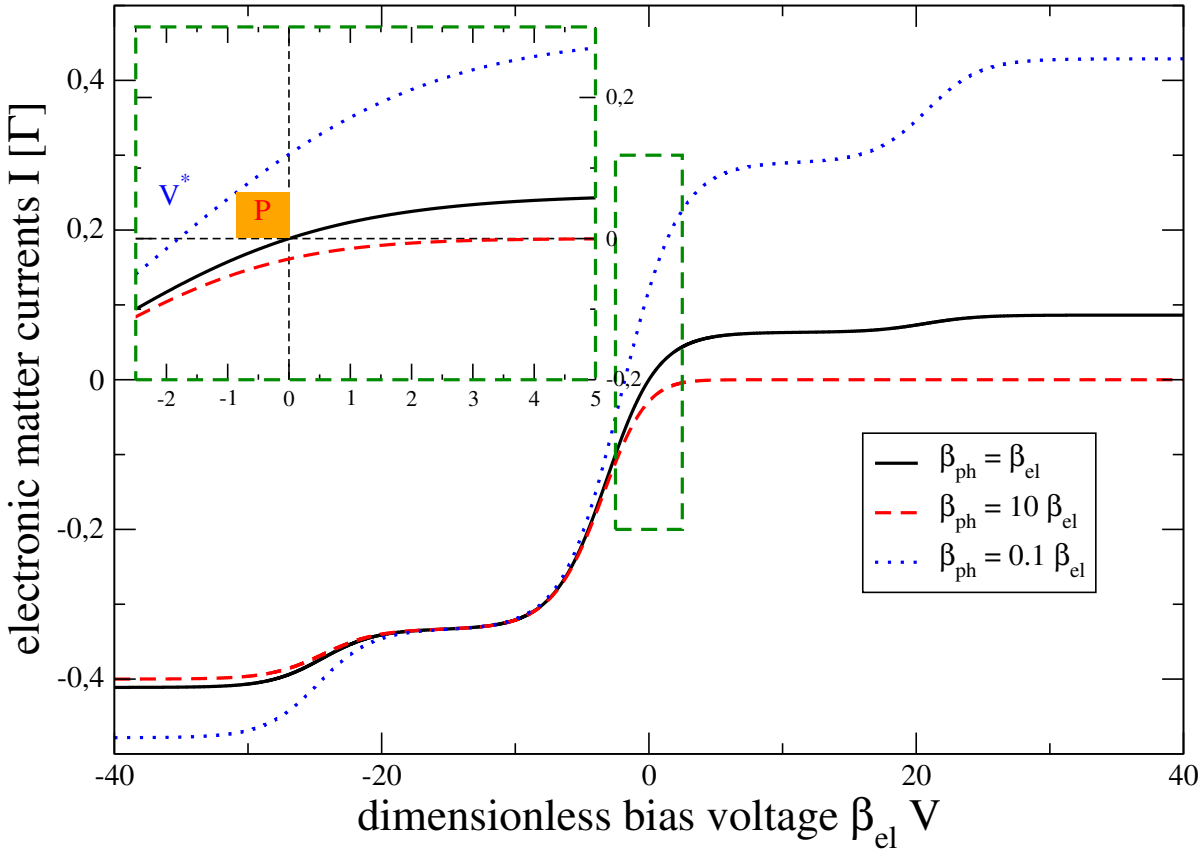

Figure 3.6: Electronic matter current in units of $\Gamma_L = \Gamma_R = \Gamma$ versus dimensionless bias voltage $\beta_{\rm el}V$. For low phonon temperatures $\beta_{\rm ph}(\epsilon_B - \epsilon_A) \gg 1$, the current cannot flow from left to right, such that the system acts as a rectifier (dashed red). For large phonon temperatures $\beta_{\rm ph}(\epsilon_B - \epsilon_A) \ll 1$, the energy driving the current against the bias (see zoomed inset) is supplied by the phonon bath. Other parameters: $\beta_{\rm el}\epsilon_B = 2$, $\beta_{\rm el}\epsilon_A = 0$, $\beta_{\rm el}U = 10$, $J_B = \Gamma$, $\beta_L = \beta_R = \beta_{\rm el}$, and $\mu_L = +V/2 = -\mu_R$.

the applicability of these efficiencies to voltages within $V = 0$ and $V = V^*$ from Eq. (3.110). The maximum efficiency is reached at $V = V^*$ and reads

$$\eta_{T_{\rm ph}>T_{\rm el}} < 1 - \frac{T_{\rm el}}{T_{\rm ph}} = \eta_{\rm Ca}\,, \tag{3.116}$$

and is thus upper-bounded by Carnot efficiency

$$\eta_{\rm Ca} = 1 - \frac{T_{\rm cold}}{T_{\rm hot}}\,. \tag{3.117}$$

In the opposite case, where $T_{\rm ph} < T_{\rm el}$, the input heat is given by the sum of the energy currents entering from the hot electronic leads $\dot{Q}_{\rm in} = \dot{Q}^L + \dot{Q}^R = I_E^L + I_E^R + P = -I_E^B + P$, such that the efficiency becomes

$$\eta_{T_{\rm ph}<T_{\rm el}} = \frac{P}{-I_E^B + P} = \frac{(\mu_L - \mu_R)}{(\epsilon_B - \epsilon_A) + (\mu_L - \mu_R)} = \frac{1}{1 + \frac{\epsilon_B - \epsilon_A}{\mu_L - \mu_R}}\,, \tag{3.118}$$

which also trivially depends on the bias voltage. Inserting the maximum bias voltage with positive power in Eq. (3.110) we obtain the maximum efficiency

$$\eta_{T_{\rm ph}<T_{\rm el}} < \frac{1}{1 + \frac{1}{\frac{T_{\rm el}}{T_{\rm ph}} - 1}} = 1 - \frac{T_{\rm ph}}{T_{\rm el}}\,, \tag{3.119}$$

which is also just the Carnot efficiency.

Unfortunately, Carnot efficiencies are reached at vanishing current, i.e., at zero power. At these parameters, a thermoelectric device is useless. It is therefore more practical to consider the efficiency at maximum power. However, since the currents depend in a highly nonlinear fashion on all parameters (coupling constants, temperatures, chemical potentials, and system parameters), this becomes a numerical optimization problem – unless one restricts the analysis to the linear response regime.

3.9 Fluctuation Theorems

The probability distribution $P_n(t)$ is given by the inverse Fourier transform of the moment-generating function

$$P_n(t) = \frac{1}{2\pi}\int_{-\pi}^{+\pi} \mathcal{M}(\chi, t) e^{-{\rm i}n\chi} d\chi = \frac{1}{2\pi}\int_{-\pi}^{+\pi} e^{\mathcal{C}(\chi,t) - {\rm i}n\chi} d\chi\,. \tag{3.120}$$

Accordingly, a symmetry in the cumulant-generating function (or moment-generating function) of the form

$$\mathcal{C}(-\chi, t) = \mathcal{C}(+\chi + {\rm i}\alpha, t) \tag{3.121}$$

leads to a symmetry of the probabilities

$$\begin{aligned}\frac{P_{+n}(t)}{P_{-n}(t)} &= \frac{\frac{1}{2\pi}\int_{-\pi}^{+\pi} e^{\mathcal{C}(\chi,t)-\mathrm{i}n\chi}d\chi}{\frac{1}{2\pi}\int_{-\pi}^{+\pi} e^{\mathcal{C}(\chi,t)+\mathrm{i}n\chi}d\chi} = \frac{\int_{-\pi}^{+\pi} e^{\mathcal{C}(\chi,t)-\mathrm{i}n\chi}d\chi}{\int_{-\pi}^{+\pi} e^{\mathcal{C}(-\chi,t)-\mathrm{i}n\chi}d\chi} \\ &= \frac{\int_{-\pi}^{+\pi} e^{\mathcal{C}(\chi,t)-\mathrm{i}n\chi}d\chi}{\int_{-\pi}^{+\pi} e^{\mathcal{C}(\chi+\mathrm{i}\alpha,t)-\mathrm{i}n\chi}d\chi} = \frac{\int_{-\pi}^{+\pi} e^{\mathcal{C}(\chi,t)-\mathrm{i}n\chi}d\chi}{\int_{-\pi+\mathrm{i}\alpha}^{+\pi+\mathrm{i}\alpha} e^{\mathcal{C}(\chi,t)-\mathrm{i}n[\chi-\mathrm{i}\alpha]}d\chi} \\ &= \frac{\int_{-\pi}^{+\pi} e^{\mathcal{C}(\chi,t)-\mathrm{i}n\chi}d\chi}{e^{-n\alpha}\int_{-\pi}^{+\pi} e^{\mathcal{C}(\chi,t)-\mathrm{i}n\chi}d\chi} \\ &= e^{+n\alpha}\,, \end{aligned} \tag{3.122}$$

where we have used in the last step that the counting field always enters as a function of $e^{\pm\mathrm{i}\chi}$. This automatically implies that $\mathcal{C}(-\pi+\mathrm{i}\sigma,t) = \mathcal{C}(+\pi+\mathrm{i}\sigma,t)$ for all real numbers σ, such that we can add two further integration paths from $-\pi$ to $-\pi+\mathrm{i}\alpha$ and from $+\pi+\mathrm{i}\alpha$ to $+\pi$ to the integral in the denominator. The value of the cumulant-generating function along these paths is the same, such that due to the different integral orientation there is no net change. Finally, using analyticity of the integrand, we deform the integration contour in the denominator, leaving two identical integrals in numerator and denominator. Note that the system may be very far from thermodynamic equilibrium but still obey a symmetry of the form (3.121), which leads to a fluctuation theorem of the form (3.122) being valid far from equilibrium.

As example, we consider the SET (which is always in thermal equilibrium). The characteristic polynomial $\mathcal{D}(\chi) = |\mathcal{L}(\chi) - \lambda\mathbf{1}|$ of the Liouvillian (3.20) and therefore also all eigenvalues obeys the symmetry

$$\mathcal{D}(-\chi) = \mathcal{D}\left(+\chi + \mathrm{i}\ln\left[\frac{f_L(1-f_R)}{(1-f_L)f_R}\right]\right) = \mathcal{D}\left(\chi + \mathrm{i}\left[(\beta_R-\beta_L)\,\epsilon + \beta_L\mu_L - \beta_R\mu_R\right]\right)\,. \tag{3.123}$$

Exercise 37 (Eigenvalue Symmetry) *(1 points)*
Compute the characteristic polynomial of the Liouvillian (3.20) and confirm the symmetry (3.123).

which leads to the fluctuation theorem

$$\lim_{t\to\infty}\frac{P_{+n}(t)}{P_{-n}(t)} = e^{n[(\beta_R-\beta_L)\epsilon+\beta_L\mu_L-\beta_R\mu_R]}\,. \tag{3.124}$$

We note that the exponent does not depend on the microscopic details of the model (ϵ, Γ_α) but only on the thermodynamic quantities. We would obtain the same result for a DQD coupled to two terminals. For equal temperatures, this becomes

$$\lim_{t\to\infty}\frac{P_{+n}(t)}{P_{-n}(t)} = e^{n\beta V}\,, \tag{3.125}$$

which directly demonstrates that the average current

$$I = \frac{d}{dt}\langle n(t)\rangle = \frac{d}{dt}\sum_{n=-\infty}^{+\infty} nP_n(t) = \sum_{n=1}^{\infty} n\left[P_{+n}(t) - P_{-n}(t)\right] = \sum_{n=1}^{\infty} nP_n(t)\left[1 - e^{-n\beta V}\right] \tag{3.126}$$

always follows the voltage. We can interpret the exponent in Eq. (3.124) in terms of the entropy that has been produced: The quantity $n\epsilon$ describes the energy that has traversed the SET for large times, and consequently, the term in the exponent approximates the entropy production, which is for large times simply proportional to the number of particles that have travelled from left to right

$$\Delta S_{\mathrm{i}} \approx (\beta_R - \beta_L)\, n\epsilon + (\beta_L \mu_L - \beta_R \mu_R)\, n\,. \tag{3.127}$$

Therefore, we can interpret the fluctuation theorem also as a stochastic manifestation of the second law

$$\frac{P(+\Delta S_{\mathrm{i}})}{P(-\Delta S_{\mathrm{i}})} = e^{+\Delta S_{\mathrm{i}}}\,. \tag{3.128}$$

Here, trajectories with a negative entropy production ΔS_{i} are not forbidden. They are just less likely to occur than their positive-production counterparts, such that – on average – the second law is always obeyed.

The SET has the property of **tight coupling** between enery and matter currents: Every electron carries the same energy. For more general systems, where this property is not present, one still obtains a fluctuation theorem for the entropy production. Then, the combined counting statistics of energy and matter currents is necessary to obtain it. Furthermore, one will for an n-terminal system need $2n$ counting fields to quantify the entropy production. In the long-term limit, one can use conservation laws, such that the maximum number of counting fields is given by $2n-2$, which can be further reduced when one has further symmetries (like tight-coupling).

Exercise 38 (Fluctuation Theorem) *(1 points)*
Calculate the long-term fluctuation theorem for Eq. (3.112) in the Coulomb-blockade regime $\bar{f}_\alpha \to 0$, when only matter transfer from left to right is counted. To do so, first reduce the dimension of the system (Coulomb blockade). Then, introduce a matter counting field at the junction of your choice and try to find a symmetry of the characteristic polynomial.

Chapter 4

Direct bath coupling : Non-Equilibrium Case II

Another nonequilibrium situation may be generated by a multi-component bath with components interacting directly (i.e., even without the presence of the system) via a small interface. However, the interaction may be modified by the presence of the quantum system and may also back-act on the quantum system itself. A prototypical example for such a bath is a quantum point contact: It consists of two leads that are connected by a tiny contact. The two leads are held at different potentials and through the tiny contact charges may tunnel from one lead to the other. The tunneling process is however highly sensitive to the presence of nearby charges, in the Hamiltonian this is modeled by a capacitive change of the tunneling amplitudes. When already the baseline tunneling amplitudes (in a low transparency QPC) are small, we may apply the master equation formalism without great efforts, as will be demonstrated at two examples.

4.1 Monitored SET

High-precision tests of counting statistics have been performed with a quantum point contact that is capacitively coupled to a single-electron transistor. The Hamiltonian of the system depicted in Fig. 4.1 reads

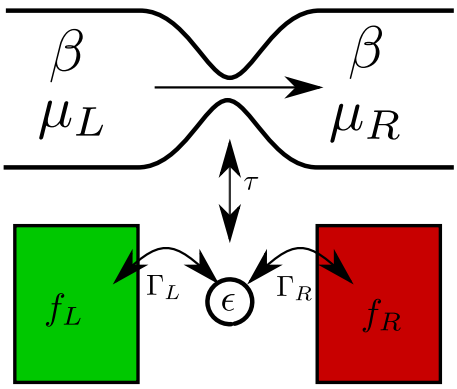

Figure 4.1: Sketch of a quantum point contact (in fact, a two component bath with the components held at different chemical potential) monitoring a single electron transistor. The tunneling through the quantum point contact is modified when the SET is occupied.

$$\begin{aligned}
\mathcal{H}_{\rm S} &= \epsilon d^\dagger d\,, \\
\mathcal{H}_{\rm B} &= \sum_k \epsilon_{kL} c_{kL}^\dagger c_{kL} + \sum_k \epsilon_{kL} c_{kR}^\dagger c_{kR} + \sum_k \varepsilon_{kL} \gamma_{kL}^\dagger \gamma_{kL} + \sum_k \varepsilon_{kL} \gamma_{kR}^\dagger \gamma_{kR}\,, \\
\mathcal{H}_{\rm I} &= \left[\sum_k t_{kL} d c_{kL}^\dagger + \sum_k t_{kR} d c_{kR}^\dagger + \text{h.c.}\right] + \left[\sum_{kk'} \left(t_{kk'} + d^\dagger d \tau_{kk'}\right) \gamma_{kL} \gamma_{k'R}^\dagger + \text{h.c.}\right], \quad (4.1)
\end{aligned}$$

where ϵ denotes the dot level, $c_{k\alpha}$ annihilate electrons on SET lead α and $\gamma_{k\alpha}$ are the annihilation operators for the QPC lead α. The QPC baseline tunneling amplitude is given by $t_{kk'}$ and describes the scattering of and electron from mode k in the left lead to mode k' in the right QPC contact. When the nearby SET is occupied it is modified to $t_{kk'} + \tau_{kk'}$, where $\tau_{kk'}$ represents the change of the tunneling amplitude.

We will derive a master equation for the dynamics of the SET due to the interaction with the QPC and the two SET contacts. In addition, we are interested not only in the charge counting statistics of the SET but also the QPC. The Liouvillian for the SET-contact interaction is well known and has been stated previously (we insert counting fields at the right lead to count charges traversing the SET from left to right)

$$\mathcal{L}_{\rm SET}(\chi) = \begin{pmatrix} -\Gamma_L f_L - \Gamma_R f_R & +\Gamma_L(1-f_L) + \Gamma_R(1-f_R) e^{+{\rm i}\chi} \\ +\Gamma_L f_L + \Gamma_R f_R e^{-{\rm i}\chi} & -\Gamma_L(1-f_L) - \Gamma_R(1-f_R) \end{pmatrix}. \quad (4.2)$$

We will therefore derive the dissipator for the SET-QPC interaction separately. To keep track of the tunneled QPC electrons, we insert a virtual detector operator in the respective tunneling Hamiltonian

$$\begin{aligned}
\mathcal{H}_{\rm I}^{\rm QPC} &= \sum_{kk'} \left(t_{kk'}\mathbf{1} + d^\dagger d \tau_{kk'}\right) B^\dagger \gamma_{kL} \gamma_{k'R}^\dagger + \sum_{kk'} \left(t_{kk'}^*\mathbf{1} + d^\dagger d \tau_{kk'}^*\right) B \gamma_{k'R} \gamma_{kL}^\dagger \\
&= \mathbf{1} \otimes B^\dagger \otimes \sum_{kk'} t_{kk'} \gamma_{kL} \gamma_{k'R}^\dagger + \mathbf{1} \otimes B \otimes \sum_{kk'} t_{kk'}^* \gamma_{k'R} \gamma_{kL}^\dagger \\
&\quad + d^\dagger d \otimes B^\dagger \otimes \sum_{kk'} \tau_{kk'} \gamma_{kL} \gamma_{k'R}^\dagger + d^\dagger d \otimes B \otimes \sum_{kk'} \tau_{kk'}^* \gamma_{k'R} \gamma_{kL}^\dagger\,. \quad (4.3)
\end{aligned}$$

Note that we have implicitly performed the mapping to a tensor product representation of the fermionic operators, which is unproblematic here as between SET and QPC no particle exchange takes place and the electrons in the QPC and the SET may be treated as different particle types. To simplify the system, we assume that the change of tunneling amplitudes affects all modes in the same manner, i.e., $\tau_{kk'} = \tilde{\tau} t_{kk'}$, which enables us to combine some coupling operators

$$\mathcal{H}_{\rm I}^{\rm QPC} = \left[\mathbf{1} + \tilde{\tau} d^\dagger d\right] \otimes B^\dagger \otimes \sum_{kk'} t_{kk'} \gamma_{kL} \gamma_{k'R}^\dagger + \left[\mathbf{1} + \tilde{\tau}^* d^\dagger d\right] \otimes B \otimes \sum_{kk'} t_{kk'}^* \gamma_{k'R} \gamma_{kL}^\dagger\,. \quad (4.4)$$

The evident advantage of this approximation is that only two correlation functions have to be computed. We can now straightforwardly (since the baseline tunneling term is not included in the bath Hamiltonian) map to the interaction picture

$$B_1(\tau) = \sum_{kk'} t_{kk'} \gamma_{kL} \gamma_{k'R}^\dagger e^{-{\rm i}(\varepsilon_{kL} - \varepsilon_{k'R})\tau}\,, \qquad B_2(\tau) = \sum_{kk'} t_{kk'}^* \gamma_{k'R} \gamma_{kL}^\dagger e^{+{\rm i}(\varepsilon_{kL} - \varepsilon_{k'R})\tau}\,. \quad (4.5)$$

For the first bath correlation function we obtain

$$\begin{aligned} C_{12}(\tau) &= \sum_{kk'}\sum_{\ell\ell'} t_{kk'}t^*_{\ell\ell'}e^{-\mathrm{i}(\varepsilon_{kL}-\varepsilon_{k'R})\tau}\left\langle \gamma_{kL}\gamma^\dagger_{k'R}\gamma_{\ell' R}\gamma^\dagger_{\ell L}\right\rangle \\ &= \sum_{kk'}|t_{kk'}|^2 e^{-\mathrm{i}(\varepsilon_{kL}-\varepsilon_{k'R})\tau}\left[1-f_L(\varepsilon_{kL})\right]f_R(\varepsilon_{k'R}) \\ &= \frac{1}{2\pi}\int\int T(\omega,\omega')\left[1-f_L(\omega)\right]f_R(\omega')e^{-\mathrm{i}(\omega-\omega')\tau}d\omega d\omega' , \end{aligned} \tag{4.6}$$

where we have introduced $T(\omega,\omega') = 2\pi\sum_{kk'}|t_{kk'}|^2\delta(\omega-\varepsilon_{kL})\delta(\omega-\varepsilon_{k'R})$. Note that in contrast to previous tunneling rates, this quantity is dimensionless. The integral factorizes when $T(\omega,\omega')$ factorizes (or when it is flat $T(\omega,\omega')=t$). In this case, the correlation function $C_{12}(\tau)$ is expressed as a product in the time domain, such that its Fourier transform will be given by a convolution integral

$$\begin{aligned} \gamma_{12}(\Omega) &= \int C_{12}(\tau)e^{+\mathrm{i}\Omega\tau}d\tau \\ &= t\int d\omega d\omega'\left[1-f_L(\omega)\right]f_R(\omega')\delta(\omega-\omega'-\Omega) \\ &= t\int\left[1-f_L(\omega)\right]f_R(\omega-\Omega)d\omega . \end{aligned} \tag{4.7}$$

For the other correlation function, we have

$$\gamma_{21}(\Omega) = t\int f_L(\omega)\left[1-f_R(\omega+\Omega)\right]d\omega . \tag{4.8}$$

Exercise 39 (Correlation functions for the QPC) *(1 points)*
Show the validity of Eqns. (4.8).

The structure of the Fermi functions demonstrates that the shift Ω can be included in the chemical potentials. Therefore, we consider integrals of the type

$$I = \int f_1(\omega)\left[1-f_2(\omega)\right]d\omega . \tag{4.9}$$

At zero temperature, these should behave as $I \approx (\mu_1-\mu_2)\Theta(\mu_1-\mu_2)$, where $\Theta(x)$ denotes the Heaviside-Θ function, which follows from the structure of the integrand, see Fig. 4.2. For finite temperatures, the value of the integral can also be calculated, for simplicity we constrain ourselves to the (experimentally relevant) case of equal temperatures ($\beta_1=\beta_2=\beta$), for which we obtain

$$\begin{aligned} I &= \int\frac{1}{\left(e^{\beta(\mu_2-\omega)}+1\right)\left(e^{-\beta(\mu_1-\omega)}+1\right)}d\omega \\ &= \lim_{\delta\to\infty}\int\frac{1}{\left(e^{\beta(\mu_2-\omega)}+1\right)\left(e^{-\beta(\mu_1-\omega)}+1\right)}\frac{\delta^2}{\delta^2+\omega^2}d\omega , \end{aligned} \tag{4.10}$$

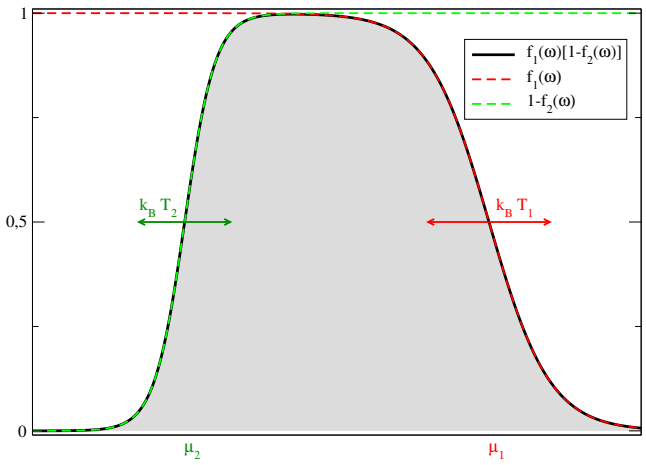

Figure 4.2: Integrand in Eq. (4.9). At zero temperature at both contacts, we obtain a product of two step functions and the area under the curve is given by the difference $\mu_1 - \mu_2$ as soon as $\mu_1 > \mu_2$ (and zero otherwise).

where we have introduced the Lorentzian-shaped regulator to enforce convergence. By identifying the poles of the integrand

$$\begin{aligned} \omega^*_{\pm} &= \pm \mathrm{i}\delta\,, \\ \omega^*_{1,n} &= \mu_1 + \frac{\pi}{\beta}(2n+1) \\ \omega^*_{2,n} &= \mu_2 + \frac{\pi}{\beta}(2n+1) \end{aligned} \tag{4.11}$$

where $n \in \{0, \pm 1, \pm 2, \pm 3, \ldots$ we can solve the integral by using the residue theorem, see also Fig. 4.3 for the integration contour. Finally, we obtain for the integral

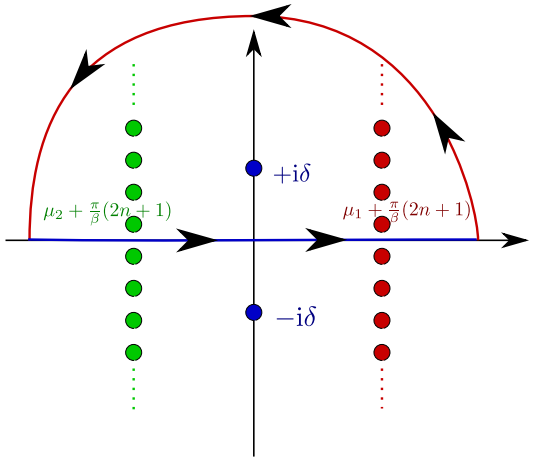

Figure 4.3: Poles and integration contour for Eq. (4.9) in the complex plane. The integral along the real axis (blue line) closed by an arc (red curve) in the upper complex plane, along which (due to the regulator) the integrand vanishes sufficiently fast.

$$\begin{aligned} I &= 2\pi \mathrm{i} \lim_{\delta\to\infty} \Big\{ \mathrm{Res}\, f_1(\omega)\,[1-f_2(\omega)]\, \frac{\delta^2}{\delta^2+\omega^2}\Big|_{\omega=+\mathrm{i}\delta} + \sum_{n=0}^{\infty} \mathrm{Res}\, f_1(\omega)\,[1-f_2(\omega)]\, \frac{\delta^2}{\delta^2+\omega^2}\Big|_{\omega=\mu_1+\frac{\pi}{\beta}(2n+1)} \\ &\quad + \sum_{n=0}^{\infty} \mathrm{Res}\, f_1(\omega)\,[1-f_2(\omega)]\, \frac{\delta^2}{\delta^2+\omega^2}\Big|_{\omega=\mu_2+\frac{\pi}{\beta}(2n+1)} \Big\} \\ &= \frac{\mu_1-\mu_2}{1-e^{-\beta(\mu_1-\mu_2)}}\,, \end{aligned} \tag{4.12}$$

which automatically obeys the simple zero-temperature ($\beta \to \infty$) limit. With the replacements

$\mu_1 \to \mu_R + \Omega$ and $\mu_2 \to \mu_L$, we obtain for the first bath correlation function

$$\gamma_{12}(\Omega) = t\frac{\Omega - V}{1 - e^{-\beta(\Omega - V)}}\,, \tag{4.13}$$

where $V = \mu_L - \mu_R$ is the QPC bias voltage. Likewise, with the replacements $\mu_1 \to \mu_L$ and $\mu_2 \to \mu_R - \Omega$, the second bath correlation function becomes

$$\gamma_{21}(\Omega) = t\frac{\Omega + V}{1 - e^{-\beta(\Omega + V)}}\,. \tag{4.14}$$

Now we can calculate the transition rates in our system (containing the virtual detector and the quantum dot) for a non-degenerate system spectrum. However, now the detector is part of our system. Therefore, the system state is not only characterized by the number of charges on the SET dot $a \in \{0, 1\}$ but also by the number of charges n that have tunneled through the QPC and have thereby changed the detector state

$$\dot{\rho}_{(a,n)(a,n)} = \sum_{b,m} \gamma_{(a,n)(b,m),(a,n)(b,m)} \rho_{(b,m)(b,m)} - \left[\sum_{b,m} \gamma_{(b,m)(a,n),(b,m)(a,n)}\right] \rho_{(a,n)(a,n)}\,. \tag{4.15}$$

Shortening the notation by omitting the double-indices we may also write

$$\dot{\rho}^{(n)}_{aa} = \sum_{b,m} \gamma_{(a,n),(b,m)} \rho^{(m)}_{bb} - \left[\sum_{b,m} \gamma_{(b,m),(a,n)}\right] \rho^{(n)}_{aa}\,, \tag{4.16}$$

where $\rho^{(n)}_{aa} = \rho_{(a,n),(a,n)}$ and $\gamma_{(a,n),(b,m)} = \gamma_{(a,n)(a,n),(b,m)(b,m)}$. It is evident that the coupling operators $A_1 = (\mathbf{1} + \tilde{\tau} d^\dagger d) \otimes B^\dagger$ and $A_2 = (\mathbf{1} + \tilde{\tau}^* d^\dagger d) \otimes B$ only allow for sequential tunneling through the QPC at lowest order (i.e., $m = n \pm 1$) and do not induce transitions between different dot states (i.e., $a = b$), such that the only non-vanishing contributions may arise for

$$\begin{aligned}
\gamma_{(0,n)(0,n+1)} &= \gamma_{12}(0) \langle 0, n| A_2 |0, n+1\rangle \langle 0, n| A_1^\dagger |0, n+1\rangle^* = \gamma_{12}(0)\,,\\
\gamma_{(0,n)(0,n-1)} &= \gamma_{21}(0) \langle 0, n| A_1 |0, n-1\rangle \langle 0, n| A_2^\dagger |0, n-1\rangle^* = \gamma_{21}(0)\,,\\
\gamma_{(1,n)(1,n+1)} &= \gamma_{12}(0) \langle 1, n| A_2 |1, n+1\rangle \langle 1, n| A_1^\dagger |1, n+1\rangle^* = \gamma_{12}(0)|1 + \tilde{\tau}|^2\,,\\
\gamma_{(1,n)(1,n-1)} &= \gamma_{21}(0) \langle 1, n| A_1 |1, n-1\rangle \langle 1, n| A_2^\dagger |1, n-1\rangle^* = \gamma_{21}(0)|1 + \tilde{\tau}|^2\,.
\end{aligned} \tag{4.17}$$

The remaining terms just account for the normalization.

Exercise 40 (Normalization terms) *(1 points)*
Compute the remaining rates

$$\sum_m \gamma_{(0,m)(0,m),(0,n)(0,n)}\,, \qquad \text{and} \qquad \sum_m \gamma_{(1,m)(1,m),(1,n)(1,n)}$$

explicitly.

Adopting the notation of conditional master equations, this leads to the connected system

$$\begin{aligned}\dot{\rho}_{00}^{(n)} &= \gamma_{12}(0)\rho_{00}^{(n+1)} + \gamma_{21}(0)\rho_{00}^{(n-1)} - [\gamma_{12}(0)+\gamma_{21}(0)]\,\rho_{00}^{(n)} \\ \dot{\rho}_{11}^{(n)} &= |1+\tilde{\tau}|^2\gamma_{12}(0)\rho_{11}^{(n+1)} + |1+\tilde{\tau}|^2\gamma_{21}(0)\rho_{11}^{(n-1)} - |1+\tilde{\tau}|^2\,[\gamma_{12}(0)+\gamma_{21}(0)]\,\rho_{11}^{(n)}\,, \end{aligned} \quad (4.18)$$

such that after Fourier transformation with the counting field ξ for the QPC, we obtain the following dissipator

$$\mathcal{L}_{\rm QPC}(\xi) = \begin{pmatrix} \left[\gamma_{21}\left(e^{+{\rm i}\xi}-1\right)+\gamma_{12}\left(e^{-{\rm i}\xi}-1\right)\right] & 0 \\ 0 & |1+\tilde{\tau}|^2\left[\gamma_{21}\left(e^{+{\rm i}\xi}-1\right)+\gamma_{12}\left(e^{-{\rm i}\xi}-1\right)\right] \end{pmatrix}, \quad (4.19)$$

which could not have been deduced directly from a Liouvillian for the SET alone. More closely analyzing the Fourier transforms of the bath correlation functions

$$\begin{aligned}\gamma_{21} &= \gamma_{21}(0) = t\frac{V}{1-e^{-\beta V}}\,, \\ \gamma_{12} &= \gamma_{12}(0) = t\frac{V}{e^{+\beta V}-1} \end{aligned} \quad (4.20)$$

we see that for sufficiently large QPC bias voltages $V\to\infty$, transport becomes unidirectional: One contribution becomes linear in the voltage $\gamma_{21}\to tV$ and the other one is exponentially suppressed $\gamma_{12}\to 0$. Despite the unusual form of the tunneling rates we see that they obey the usual detailed balance relations

$$\frac{\gamma_{21}}{\gamma_{12}} = e^{+\beta V}\,. \quad (4.21)$$

The sum of both Liouvillians (4.2) and (4.19) constitutes the total dissipator

$$\mathcal{L}(\chi,\xi) = \mathcal{L}_{\rm SET}(\chi) + \mathcal{L}_{\rm QPC}(\xi)\,, \quad (4.22)$$

which can be used to calculate the probability distributions for tunneling through both transport channels (QPC and SET).

Exercise 41 (QPC current) *(1 points)*
Show that the stationary state of the SET is unaffected by the additional QPC dissipator and calculate the stationary current through the QPC for Liouvillian (4.22).

When we consider the case $\{\Gamma_L,\Gamma_R\}\ll\{tV,|1+\tilde{\tau}|tV\}$, we approach a bistable system, where for a nearly stationary SET the QPC transmits many charges. Then, the QPC current measured at finite times will be large when the SET dot is empty and reduced otherwise. In this case, the counting statistics approaches the case of telegraph noise. When the dot is empty or filled throughout respectively, the current can easily be determined as

$$I_0 = [\gamma_{21}(0)-\gamma_{12}(0)]\,, \qquad I_1 = |1+\tilde{\tau}|^2\,[\gamma_{21}(0)-\gamma_{12}(0)]\,. \quad (4.23)$$

For finite time intervals Δt, the number of electrons tunneling through the QPC Δn is determined by the probability distribution

$$P_{\Delta n}(\Delta t) = \frac{1}{2\pi}\int_{-\pi}^{+\pi} \mathrm{Tr}\left\{e^{\mathcal{L}(0,\xi)\Delta t - \mathrm{i}\Delta n\xi}\rho(t)\right\} d\xi\,, \tag{4.24}$$

where $\rho(t)$ represents the initial density matrix. This quantity can e.g. be evaluated numerically. When Δt is not too large (such that the stationary state is not really reached) and not too small (such that there are sufficiently many particles tunneling through the QPC to meaningfully define a current), a continuous measurement of the QPC current maps to a fixed-point iteration as follows: Measuring a certain particle number corresponds to a projection, i.e., the system-detector density matrix is projected to a certain measurement outcome which occurs with the probability $P_{\Delta n}(\Delta t)$

$$\rho = \sum_n \rho^{(n)} \otimes |n\rangle\langle n| \xrightarrow{m} \frac{\rho^{(m)}}{\mathrm{Tr}\left\{\rho^{(m)}\right\}}\,. \tag{4.25}$$

It is now essential to use the density matrix after the measurement as the initial state for the next iteration. This ensures that e.g. after measuring a large current it is in the next step more likely to measure a large current than a low current. Consequently, the ratio of measured particles divided by measurement time gives a current estimate $I(t) \approx \frac{\Delta n}{\Delta t}$ for the time interval. Such current trajectories are used to track the full counting statistics through quantum point contacts, see Fig. 4.4 In this way, the QPC acts as a detector for the counting statistics of the SET circuit. Finally, we note that for an SET, a QPC only acts as a reliable detector when the SET transport is unidirectional (large bias).

4.2 Monitored charge qubit

A quantum point contact may also be used to monitor a nearby charge qubit, see Fig. 4.5. The QPC performs a measurement of the electronic position, since its current is highly sensitive on it. This corresponds to a σ^x measurement performed on the qubit. However, the presence of a detector does of course also lead to a back-action on the probed system. Here, we will derive a master equation for the system to quantify this back-action.

The Hamiltonian of the charge qubit is given by

$$H_{\mathrm{CQB}} = \epsilon_A d_A^\dagger d_A + \epsilon_B d_B^\dagger d_B + T\left(d_A d_B^\dagger + d_B d_A^\dagger\right)\,, \tag{4.26}$$

where we can safely neglect Coulomb interaction, since to form a charge qubit, the number of electrons on this double quantum dot is fixed to one. The matrix representation is therefore just two-dimensional in the $|n_A, n_B\rangle \in \{|10\rangle, |01\rangle\}$ basis and can be expressed by Pauli matrices

$$H_{\mathrm{CQB}} = \begin{pmatrix} \epsilon_A & T \\ T & \epsilon_B \end{pmatrix} = \frac{\epsilon_A+\epsilon_B}{2}\mathbf{1} + \frac{\epsilon_A-\epsilon_B}{2}\sigma^z + T\sigma^x \equiv \epsilon\mathbf{1} + \Delta\sigma^z + T\sigma^x\,, \tag{4.27}$$

i.e., we may identify $d_A^\dagger d_A = \frac{1}{2}(\mathbf{1}+\sigma^z)$ and $d_B^\dagger d_B = \frac{1}{2}(\mathbf{1}-\sigma^z)$. The tunneling part of the QPC Hamiltonian reads

$$\mathcal{H}_{\mathrm{I}} \;=\; d_A^\dagger d_A \otimes \sum_{kk'} t^A_{kk'}\gamma_{kL}\gamma^\dagger_{k'R} + d_B^\dagger d_B \otimes \sum_{kk'} t^B_{kk'}\gamma_{kL}\gamma^\dagger_{k'R} + \mathrm{h.c.}\,, \tag{4.28}$$

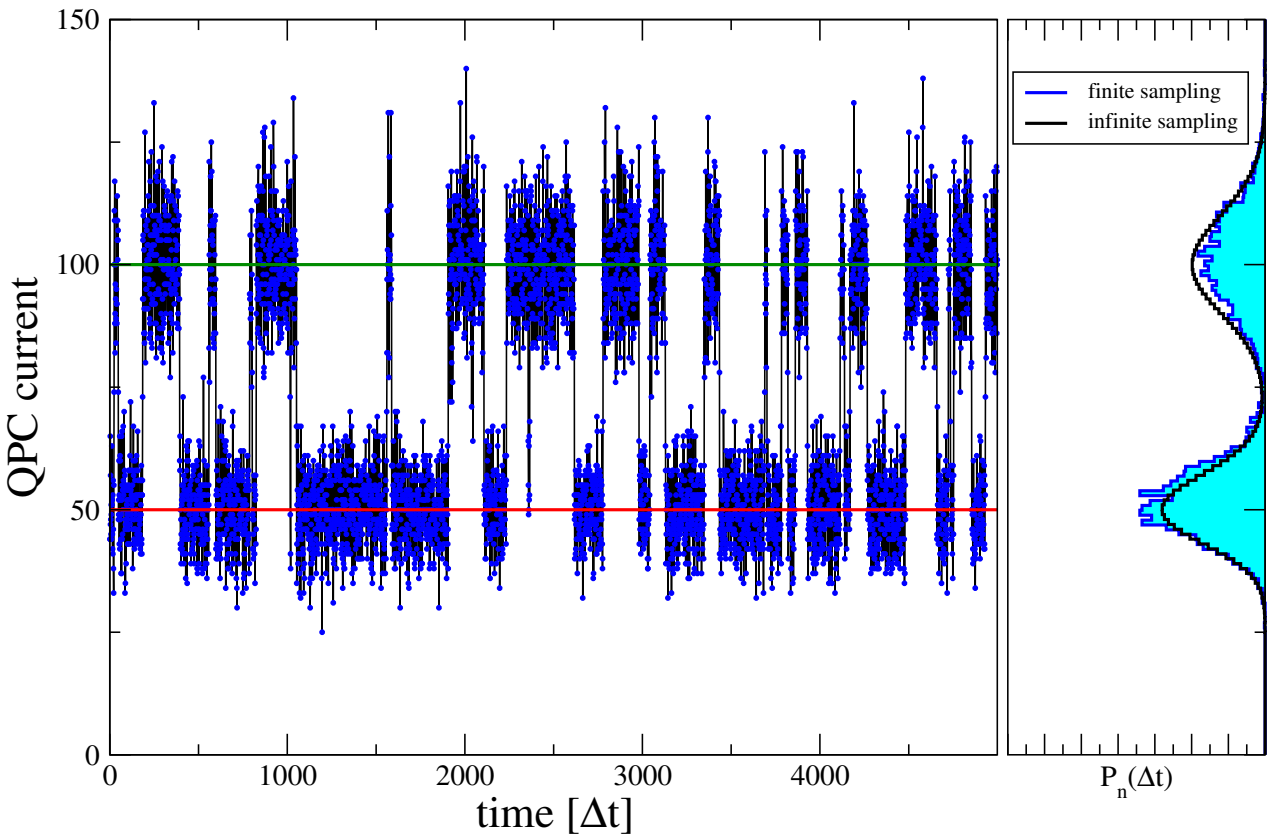

Figure 4.4: Numerical simulation of the time-resolved QPC current for a fluctuating dot occupation. At infinite SET bias, the QPC current allows to reconstruct the full counting statistics of the SET, since each current blip from low (red line) to high (green line) current corresponds to an electron leaving the SET to its right junction. Parameters: $\Gamma_L \Delta t = \Gamma_R \Delta t = 0.01$, $\gamma_{12}(0) = |1+\tilde{\tau}|^2 \gamma_{12}(0) = 0$, $\gamma_{21}(0) = 100.0$, $|1+\tilde{\tau}|^2 \gamma_{21}(0) = 50.0$, $f_L = 1.0$, $f_R = 0.0$. The right panel shows the corresponding probability distribution $P_n(\Delta t)$ versus $n = I\Delta t$, where the blue curve is sampled from the left panel and the black curve is the theoretical limit for infinitely long times.

where $t^{A/B}_{kk'}$ represents the tunneling amplitudes when the electron is localized on dots A and B, respectively. After representing the charge qubit in terms of Pauli matrices, the full Hamiltonian reads

$$\begin{aligned} H &= \epsilon \mathbf{1} + \Delta \sigma^z + T\sigma^x \\ &\quad + \frac{1}{2}\left[\mathbf{1} + \sigma^z\right] \otimes \left[\sum_{kk'} t^A_{kk'} \gamma_{kL} \gamma^\dagger_{k'R} + \sum_{kk'} t^{A*}_{kk'} \gamma_{k'R} \gamma^\dagger_{kL}\right] \\ &\quad + \frac{1}{2}\left[\mathbf{1} - \sigma^z\right] \otimes \left[\sum_{kk'} t^B_{kk'} \gamma_{kL} \gamma^\dagger_{k'R} + \sum_{kk'} t^{B*}_{kk'} \gamma_{k'R} \gamma^\dagger_{kL}\right] \\ &\quad + \sum_k \varepsilon_{kL} \gamma^\dagger_{kL} \gamma_{kL} + \sum_k \varepsilon_{kR} \gamma^\dagger_{kR} \gamma_{kR} \,. \end{aligned} \tag{4.29}$$

To reduce the number of correlation functions we again assume that all tunneling amplitudes are modified equally $t^A_{kk'} = \tilde{\tau}_A t_{kk'}$ and $t^B_{kk'} = \tilde{\tau}_B t_{kk'}$ with baseline tunneling amplitudes $t_{kk'}$ and real

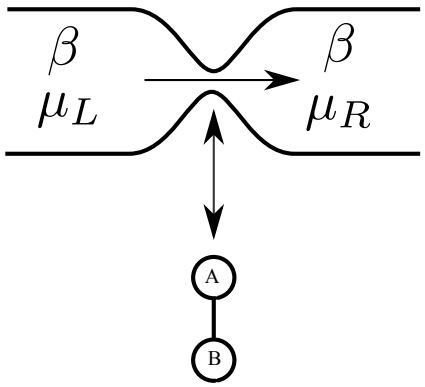

Figure 4.5: Sketch of a quantum point contact monitoring a double quantum dot with a single electron loaded (charge qubit). The current through the quantum point contact is modified by the position of the charge qubit electron, i.e., a measurement in the σ^z basis is performed.

constants τ_A and τ_B. Then, only a single correlation function needs to be calculated

$$\mathcal{H}_{\rm I} = \left[\frac{\tilde{\tau}_A}{2}\left(\mathbf{1}+\sigma^z\right)+\frac{\tilde{\tau}_B}{2}\left(\mathbf{1}-\sigma^z\right)\right]\otimes\left[\sum_{kk'} t_{kk'}\gamma_{kL}\gamma^\dagger_{k'R}+\sum_{kk'} t^*_{kk'}\gamma_{k'R}\gamma^\dagger_{kL}\right], \tag{4.30}$$

which becomes explicitly

$$\begin{aligned} C(\tau) &= \left\langle \sum_{kk'\ell\ell'}\left[t_{kk'}\gamma_{kL}\gamma^\dagger_{k'R}e^{-{\rm i}(\varepsilon_{kL}-\varepsilon_{k'R})\tau}+t^*_{kk'}\gamma_{k'R}\gamma^\dagger_{kL}e^{+{\rm i}(\varepsilon_{kL}-\varepsilon_{k'R})\tau}\right]\left[t_{\ell\ell'}\gamma_{\ell L}\gamma^\dagger_{\ell'R}+t^*_{\ell\ell'}\gamma_{\ell'R}\gamma^\dagger_{\ell L}\right]\right\rangle \\ &= \sum_{kk'}|t_{kk'}|^2\left[e^{-{\rm i}(\varepsilon_{kL}-\varepsilon_{k'R})\tau}\left\langle\gamma_{kL}\gamma^\dagger_{k'R}\gamma_{k'R}\gamma^\dagger_{kL}\right\rangle+e^{+{\rm i}(\varepsilon_{kL}-\varepsilon_{k'R})\tau}\left\langle\gamma_{k'R}\gamma^\dagger_{kL}\gamma_{kL}\gamma^\dagger_{k'R}\right\rangle\right] \\ &= \frac{1}{2\pi}\int d\omega d\omega' T(\omega,\omega')\left[e^{-{\rm i}(\omega-\omega')\tau}[1-f_L(\omega)]f_R(\omega')+e^{+{\rm i}(\omega-\omega')\tau}f_L(\omega)[1-f_R(\omega')]\right] \end{aligned} \tag{4.31}$$

where we have in the last step replaced the summation by a continuous integration with $T(\omega,\omega') = 2\pi\sum_{kk'}|t_{kk'}|^2\delta(\omega-\varepsilon_{kL})\delta(\omega'-\varepsilon_{k'R})$. We directly conclude for the Fourier transform of the bath correlation function

$$\begin{aligned} \gamma(\Omega) &= \int d\omega d\omega' T(\omega,\omega')\left[\delta(\Omega-\omega+\omega')[1-f_L(\omega)]f_R(\omega')+\delta(\Omega+\omega-\omega')f_L(\omega)[1-f_R(\omega')]\right] \\ &= \int d\omega\left[T(\omega,\omega-\Omega)[1-f_L(\omega)]f_R(\omega-\Omega)+T(\omega,\omega+\Omega)f_L(\omega)[1-f_R(\omega+\Omega)]\right]. \end{aligned} \tag{4.32}$$

In what follows, we will consider the wideband limit $T(\omega,\omega')=1$ (the weak-coupling limit enters the $\tilde{\tau}_{A/B}$ parameters), such that we may directly use the result – compare Eqn. (4.12) – from the previous section

$$\gamma(\Omega) = \frac{\Omega+V}{1-e^{-\beta(\Omega+V)}}+\frac{\Omega-V}{1-e^{-\beta(\Omega-V)}}, \tag{4.33}$$

where $V=\mu_L-\mu_R$ denotes the bias voltage of the QPC. Since we are not interested in its counting statistics here, we need not introduce any virtual detectors. The derivation of the master equation

in the system energy eigenbasis requires diagonalization of the system Hamiltonian first – compare Eq. (2.69)

$$\begin{aligned} E_- &= \epsilon - \sqrt{\Delta^2+T^2}\,, \qquad |-\rangle = \frac{\Delta - \sqrt{\Delta^2+T^2}\,|0\rangle + T\,|1\rangle}{\sqrt{T^2+\left(\Delta-\sqrt{\Delta^2+T^2}\right)^2}} \\ E_+ &= \epsilon + \sqrt{\Delta^2+T^2}\,, \qquad |+\rangle = \frac{\Delta + \sqrt{\Delta^2+T^2}\,|0\rangle + T\,|1\rangle}{\sqrt{T^2+\left(\Delta+\sqrt{\Delta^2+T^2}\right)^2}}\,. \end{aligned} \tag{4.34}$$

Following the Born-, Markov-, and secular approximations – compare definition 8 – we obtain a Lindblad Master equation for the qubit

$$\dot\rho = -\mathrm{i}\left[\mathcal{H}_\mathrm{S} + H_\mathrm{LS}, \rho\right] + \sum_{abcd}\gamma_{ab,cd}\left[|a\rangle\langle b|\,\rho\,(|c\rangle\langle d|)^\dagger - \frac{1}{2}\left\{(|c\rangle\langle d|)^\dagger|a\rangle\langle b|\,,\rho\right\}\right], \tag{4.35}$$

where the summation only goes over the two energy eigenstates and H_LS denotes the frequency renormalization. Since the two eigenvalues of our system are non-degenerate, the Lamb-shift Hamiltonian is diagonal in the system energy eigenbasis and does not affect the dynamics of the populations. In particular, we have for the populations the rate equation

$$\begin{pmatrix}\dot\rho_{--}\\ \dot\rho_{++}\end{pmatrix} = \begin{pmatrix}-\gamma_{+-,+-} & +\gamma_{-+,-+}\\ +\gamma_{+-,+-} & -\gamma_{-+,-+}\end{pmatrix}\begin{pmatrix}\rho_{--}\\ \rho_{++}\end{pmatrix}. \tag{4.36}$$

The required dampening coefficients read

$$\begin{aligned} \gamma_{-+,-+} &= \gamma(E_+-E_-)|\langle-|\,A\,|+\rangle|^2 = \gamma(+2\sqrt{\Delta^2+T^2})\frac{T^2}{4(\Delta^2+T^2)}\left(\tilde\tau_A-\tilde\tau_B\right)^2, \\ \gamma_{+-,+-} &= \gamma(E_--E_+)|\langle+|\,A\,|-\rangle|^2 = \gamma(-2\sqrt{\Delta^2+T^2})\frac{T^2}{4(\Delta^2+T^2)}\left(\tilde\tau_A-\tilde\tau_B\right)^2. \end{aligned} \tag{4.37}$$

Exercise 42 (Qubit Dissipation) *(1 points)*
Show the validity of Eqns. (4.37).

This shows that when the QPC current is not dependent on the qubit state $\tilde\tau_A = \tilde\tau_B$, the dissipation on the qubit vanishes completely, which is consistent with our initial interaction Hamiltonian. In addition, in the pure dephasing limit $T \to 0$, we do not have any dissipative back-action of the measurement device on the qubit. Equation (4.36) obviously also preserves the trace of the density matrix. The stationary density matrix is therefore defined by

$$\frac{\bar\rho_{++}}{\bar\rho_{--}} = \frac{\gamma_{+-,+-}}{\gamma_{-+,-+}} = \frac{\gamma(-2\sqrt{\Delta^2+T^2})}{\gamma(+2\sqrt{\Delta^2+T^2})}. \tag{4.38}$$

When the QPC bias voltage vanishes (at equilibrium), we have

$$\frac{\gamma(-2\sqrt{\Delta^2+T^2})}{\gamma(+2\sqrt{\Delta^2+T^2})} \to e^{-\beta 2\sqrt{\Delta^2+T^2}} = e^{-\beta(E_+-E_-)}, \tag{4.39}$$

i.e., the qubit thermalizes with the temperature of the QPC. When the QPC bias voltage is large, the qubit is driven away from this thermal state.

The evolution of coherences decouples from the diagonal elements of the density matrix. The hermiticity of the density matrix allows to consider only one coherence

$$\begin{aligned}\dot{\rho}_{-+} &= -\mathrm{i}\left(E_- + \Delta E_- - E_+ - \Delta E_+\right)\rho_{-+} \\ &\quad + \left[\gamma_{--,++} - \frac{1}{2}\left(\gamma_{--,--} + \gamma_{++,++} + \gamma_{-+,-+} + \gamma_{+-,+-}\right)\right]\rho_{-+}\,, \end{aligned} \tag{4.40}$$

where $\Delta E_\pm$ corresponds to the energy renormalization due to the Lamb-shift, which induces a frequency renormalization of the qubit. The real part of the above equation is responsible for the dampening of the coherence, its calculation requires the evaluation of all remaining nonvanishing dampening coefficients

$$\begin{aligned}\gamma_{-+,-+} + \gamma_{+-,+-} &= \left[\gamma(+2\sqrt{\Delta^2+T^2}) + \gamma(-2\sqrt{\Delta^2+T^2})\right]\frac{T^2}{4(T^2+\Delta^2)}\left(\tilde{\tau}_A - \tilde{\tau}_B\right)^2\,, \\ \gamma_{--,--} + \gamma_{++,++} - 2\gamma_{--,++} &= \gamma(0)\frac{\Delta^2}{T^2+\Delta^2}\left(\tilde{\tau}_A - \tilde{\tau}_B\right)^2\,. \end{aligned} \tag{4.41}$$

Using the decomposition of the dampening, we may now calculate the decoherence rate σ

$$\begin{aligned}\sigma &= (\gamma_{-+,-+} + \gamma_{+-,+-}) + (\gamma_{--,--} + \gamma_{++,++} - 2\gamma_{--,++}) \\ &= \frac{\left(\tilde{\tau}_A - \tilde{\tau}_B\right)^2}{4}\frac{T^2}{\Delta^2+T^2}\Big\{\left(V + 2\sqrt{\Delta^2+T^2}\right)\coth\left[\frac{\beta}{2}\left(V + 2\sqrt{\Delta^2+T^2}\right)\right] \\ &\quad + \left(V - 2\sqrt{\Delta^2+T^2}\right)\coth\left[\frac{\beta}{2}\left(V - 2\sqrt{\Delta^2+T^2}\right)\right]\Big\} \\ &\quad + \left(\tilde{\tau}_A - \tilde{\tau}_B\right)^2\frac{\Delta^2}{\Delta^2+T^2}V\coth\left[\frac{\beta V}{2}\right]\,, \end{aligned} \tag{4.42}$$

which vanishes as reasonably expected when we set $\tilde{\tau}_A = \tilde{\tau}_B$. Noting that $x\coth(x) \geq 1$ does not only prove its positivity (i.e., the coherences always decay) but also enables one to obtain a rough lower bound

$$\sigma \geq \frac{\left(\tilde{\tau}_A - \tilde{\tau}_B\right)^2}{\beta}\frac{T^2+2\Delta^2}{T^2+\Delta^2} \tag{4.43}$$

on the dephasing rate. This lower bound is valid when the QPC voltage is rather small. For large voltages $|V| \gg \sqrt{\Delta^2+T^2}$, the dephasing rate is given by

$$\sigma \approx \left(\tilde{\tau}_A - \tilde{\tau}_B\right)^2\frac{T^2+2\Delta^2}{T^2+\Delta^2}|V| \tag{4.44}$$

and thus is limited by the voltage rather than the temperature.

Chapter 5

Controlled systems: Non-Equilibrium Case III

Time-dependent equations of the form

$$\dot{\rho} = \mathcal{L}(t)\rho(t) \tag{5.1}$$

are notoriously difficult to solve unless $\mathcal{L}(t)$ fulfills special properties.

- One such special case is e.g. the case of commuting superoperators, where the solution can be obtained from the exponential of an integral

$$[\mathcal{L}(t), \mathcal{L}(t')] = \mathbf{0} \qquad \Longrightarrow \qquad \rho(t) = \exp\left(-\mathrm{i}\int_0^t \mathcal{L}(t')dt'\right)\rho_0\,. \tag{5.2}$$

- Another special case is one with a very slow time-dependence and a unique stationary state $\mathcal{L}(t)\bar{\rho}_t = 0$, where the time-dependent density matrix can be assumed to adiabatically follow the stationary state $\rho(t) \approx \bar{\rho}_t$.

- For fast time-dependencies, there exists the analytically solvable case of a train of δ-kicks

$$\mathcal{L}(t) = \mathcal{L}_0 + \sum_{i=1}^{\infty} \ell_i \delta(t - t_i)\,, \tag{5.3}$$

  where the solution reads $(t_n < t < t_{n+1})$

$$\rho(t) = e^{\mathcal{L}_0(t-t_n)}\left[e^{\ell_n} e^{\mathcal{L}_0(t_n - t_{n-1})}\right] \times \ldots \times \left[e^{\ell_2} e^{\mathcal{L}_0(t_2-t_1)}\right]\left[e^{\ell_1} e^{\mathcal{L}_0(t_1)}\right]\rho_0\,, \tag{5.4}$$

  which can be considerably simplified using e.g. Baker-Campbell-Haussdorff relations when the kicks $\ell_i = \ell$ and the timesteps $t_n - t_{n-1} = \Delta t$ are identical.

- For periodic time-dependencies, Floquet theory may be applicable.

- Finally, a very simple case arises for piecewise-constant time-dependencies. This allows to map the problem to ordinary differential equations with constant coefficients, which are evolved a certain amount of time. After an instantaneous switch of the coefficients, one simply has initial conditions taken from the final state of the last evolution period, which can be evolved further and so on. Since it does not require an extension of the theoretical framework, we will consider this case in the following.

5.1 Electronic pump

We consider a system with the simplest possible internal structure, which has just the two states empty and filled. A representative of such a system is the single-electron transistor. The tunneling of electrons through such a transistor is stochastic and thereby in some sense uncontrolled. This implies that e.g. the current fluctuations through such a device (noise) can not be suppressed completely.

5.1.1 Time-dependent tunneling rates

We consider piecewise-constant time-dependencies of the tunneling rates $\Gamma_L(t)$ and $\Gamma_R(t)$ with an otherwise arbitrary protocol

$$\mathcal{L}(\chi,t)=\begin{pmatrix} -\Gamma_L(t)f_L-\Gamma_R(t)f_R & +\Gamma_L(t)(1-f_L)+\Gamma_R(t)(1-f_R)e^{+\mathrm{i}\chi} \\ +\Gamma_L(t)f_L+\Gamma_R(t)f_Re^{-\mathrm{i}\chi} & -\Gamma_L(t)(1-f_L)-\Gamma_R(t)(1-f_R)\end{pmatrix}. \tag{5.5}$$

The situation is also depicted in Fig. 5.1.

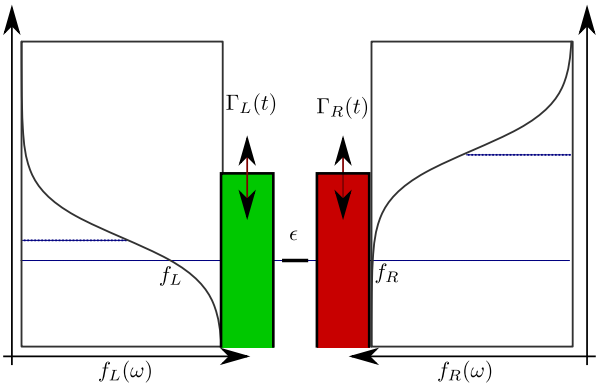

Figure 5.1: Time-dependent tunneling rates which follow a piecewise constant protocol. Dot level and left and right Fermi functions are assumed constant.

Let the tunneling rates during the i-th time interval be denoted by Γ_L^i and Γ_R^i and the corresponding constant Liouvillian during this time interval by $\mathcal{L}_i(\chi)$. The density matrix after the time interval Δt is now given by

$$\rho_{i+1}=e^{\mathcal{L}_i(0)\Delta t}\rho_i\,, \tag{5.6}$$

such that it has no longer the form of a master equation but becomes a fixed-point iteration. In what follows, we will without loss of generality assume $f_L\leq f_R$, such that the source lead is right and the drain lead is left. Utilizing previous results, the stationary state of the Liouvillian $\mathcal{L}_i$ is given by

$$\bar{f}_i=\frac{\Gamma_L^i f_L+\Gamma_R^i f_R}{\Gamma_L^i+\Gamma_R^i} \tag{5.7}$$

and thereby ($\Gamma_{L/R}^i\geq 0$) obeys $f_L\leq\bar{f}_i\leq f_R$. This implies that after a few transient iterations, the density vector will hover around within the transport window

$$f_L\leq n_i=\left\langle d^\dagger d\right\rangle_i\leq f_R\qquad\forall\qquad i\geq i^*\,. \tag{5.8}$$

The occupations will therefore follow the iteration equation

$$\begin{pmatrix}1-n_{i+1}\\ n_{i+1}\end{pmatrix}=e^{\mathcal{L}_i(0)\Delta t}\begin{pmatrix}1-n_i\\ n_i\end{pmatrix}. \tag{5.9}$$

To calculate the number of particles tunneling into the source reservoir, we consider the moment-generating function

$$\mathcal{M}_i(\chi,\Delta t)=\mathrm{Tr}\left\{e^{\mathcal{L}_i(\chi)\Delta t}\begin{pmatrix}1-n_i\\ n_i\end{pmatrix}\right\} \tag{5.10}$$

and calculate the first moment

$$\begin{aligned}\langle n\rangle_i &= (-\mathrm{i})\partial_\chi\,\mathcal{M}_i(\chi,\Delta t)|_{\chi=0}\\ &= \frac{1}{(\Gamma_L^i+\Gamma_R^i)^2}\Big[-(\Gamma_R^i)^2(f_R-n_i)\left(1-e^{-(\Gamma_L^i+\Gamma_R^i)\Delta t}\right)\\ &\quad+\Gamma_L^i\Gamma_R^i\left((n_i-f_L)\left(1-e^{-(\Gamma_L^i+\Gamma_R^i)\Delta t}\right)-(f_R-f_L)(\Gamma_L^i+\Gamma_R^i)\Delta t\right)\Big]\le 0\,. \end{aligned}\tag{5.11}$$

Exercise 43 (Pumping Failure) *(1 points)*
Show that under the assumption $f_L\le n_i\le f_R$ – and of course $(\Gamma_L^i+\Gamma_R^i)\Delta t>0$ – the average number of electrons travelling from left to right in Eq. (5.11) is always negative.

It follows that the average current always points from source to drain (in our case, since $f_R>f_L$, from right to left), regardless of the actual protocol $\Gamma_{L/R}^\alpha$ chosen. Since any general time-dependence $\Gamma_\alpha(t)$ can be approximated by piecewise-constant ones, we conclude that with simply modifying the tunneling rates, it is not possible to revert the direction of the current. From a thermodynamic perspective, this is reasonable, since by changing the rates $\Gamma_\alpha(t)$ we do not inject energy into the system, and thus should not expect to get anything out of it. Note for later reference however that this implies that the driving does not depend on whether the dot is occupied or not, i.e., the rates are modified unconditionally (open-loop control).

5.1.2 With performing work

To revert the direction of transport, one could modify the Fermi functions e.g. by changing the chemical potentials or temperatures in the contacts. However, this first possibility may for fast driving destroy the thermal equilibrium in the contacts, such that the whole approach might not be applicable. Second, this approach would simply exchange the roles of source and drain, and a pump that manages to pump water from a well into a bucket by lifting the complete lake faces poor economic perspectives.

Consequently, we consider changing the dot level $\epsilon(t)$ to change the value of the Fermi functions. Intuitively, it is quite straightforward to arrive at a protocol $\epsilon(t)$ and $\Gamma_\alpha(t)$ that should lift electrons from left to right and thereby pumps electrons from low to high chemical potentials, see Fig. 5.2. The Liouvillians for the first and second half cycles read

$$\begin{aligned}\mathcal{L}_1(\chi) &= \begin{pmatrix}-\Gamma_L^{\max}f_L(\epsilon^{\min})-\Gamma_R^{\min}f_R(\epsilon^{\min}) & +\Gamma_L^{\max}[1-f_L(\epsilon^{\min})]+\Gamma_R^{\min}[1-f_R(\epsilon^{\min})]e^{+\mathrm{i}\chi}\\ +\Gamma_L^{\max}f_L(\epsilon^{\min})+\Gamma_R^{\min}f_R(\epsilon^{\min})e^{-\mathrm{i}\chi} & -\Gamma_L^{\max}[1-f_L(\epsilon^{\min})]-\Gamma_R^{\min}[1-f_R(\epsilon^{\min})]\end{pmatrix},\\ \mathcal{L}_2(\chi) &= \begin{pmatrix}-\Gamma_L^{\min}f_L(\epsilon^{\max})-\Gamma_R^{\max}f_R(\epsilon^{\max}) & +\Gamma_L^{\min}[1-f_L(\epsilon^{\max})]+\Gamma_R^{\max}[1-f_R(\epsilon^{\max})]e^{+\mathrm{i}\chi}\\ +\Gamma_L^{\min}f_L(\epsilon^{\max})+\Gamma_R^{\max}f_R(\epsilon^{\max})e^{-\mathrm{i}\chi} & -\Gamma_L^{\min}[1-f_L(\epsilon^{\max})]-\Gamma_R^{\max}[1-f_R(\epsilon^{\max})]\end{pmatrix},\end{aligned}\tag{5.12}$$

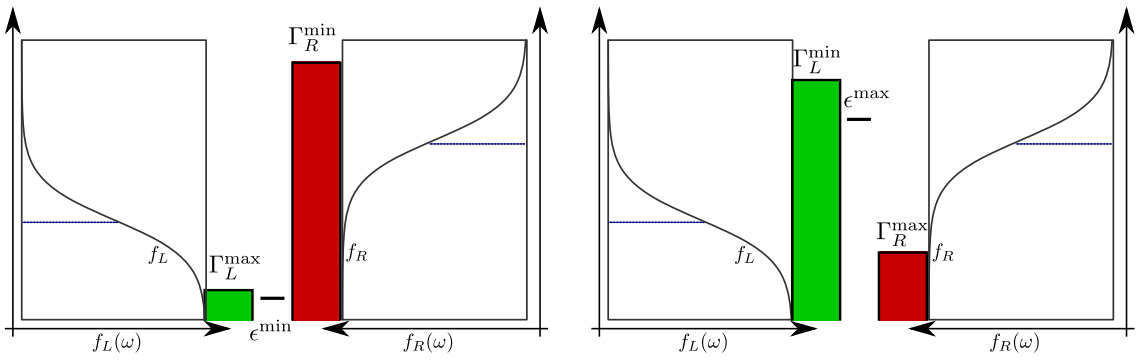

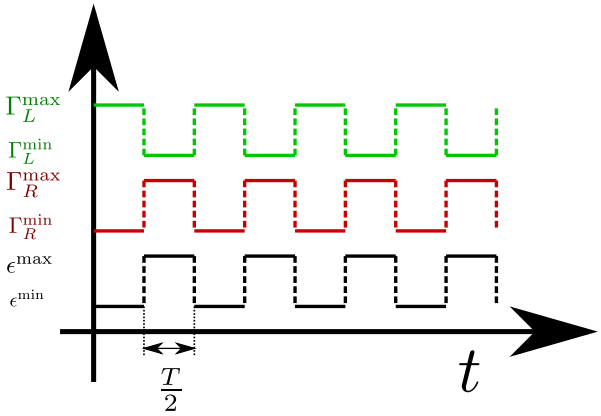

Figure 5.2: Here, tunneling rates and the dot level also follow a piecewise constant protocol, which admits only two possible values (top left and right) and is periodic (see left panel). The state of the contacts is assumed as stationary. For small pumping cycle times T, the protocol is expected to pump electrons from the left towards the right contact and thereby lifts electrons to a higher chemical potential.

respectively. The evolution of the density vector now follows the fixed point iteration scheme

$$\rho(t+T) = \mathcal{P}_2\mathcal{P}_1\rho(t) = e^{\mathcal{L}_2(0)T/2}e^{\mathcal{L}_1(0)T/2}\rho(t)\,. \tag{5.13}$$

After a period of transient evolution, the density vector at the end of the pump cycle will approach a value where $\rho(t+T) \approx \rho(t) = \bar{\rho}$. This value is the stationary density matrix in a stroboscopic sense and is defined by the eigenvalue equation

$$e^{\mathcal{L}_2(0)T/2}e^{\mathcal{L}_1(0)T/2}\bar{\rho} = \bar{\rho} \tag{5.14}$$

with $\mathrm{Tr}\,\{\bar{\rho}\} = 1$. Once this stationary state has been determined, we can easily define the moment-generating functions for the pumping period in the (stroboscopically) stationary regime

$$\mathcal{M}_1(\chi, T/2) = \mathrm{Tr}\left\{e^{\mathcal{L}_1(\chi)T/2}\bar{\rho}\right\}\,, \qquad \mathcal{M}_2(\chi, T/2) = \mathrm{Tr}\left\{e^{\mathcal{L}_2(\chi)T/2}e^{\mathcal{L}_1(0)T/2}\bar{\rho}\right\}\,, \tag{5.15}$$

where $\mathcal{M}_1$ describes the statistics in the first half cycle and $\mathcal{M}_2$ in the second half cycle and the moments can be extracted in the usual way. The distribution for the total number of particles tunneling during the complete pumping cycle $n = n_1 + n_2$ is given by

$$P_n(T) = \sum_{n_1,n_2\,:\,n_1+n_2=n} P_{n_1}(T/2)P_{n_2}(T/2) = \sum_{n_1,n_2} \delta_{n,n_1+n_2}P_{n_1}(T/2)P_{n_2}(T/2)\,. \tag{5.16}$$

Then, the first moment may be calculated by simply adding the first moments of the particles tunneling through both half-cycles

$$\begin{aligned}\langle n\rangle &= \sum_n nP_n = \sum_n n\sum_{n_1,n_2}\delta_{n,n_1+n_2}P_{n_1}(T/2)P_{n_2}(T/2) = \sum_{n_1,n_2}(n_1+n_2)P_{n_1}(T/2)P_{n_2}(T/2)\\ &= \langle n_1\rangle + \langle n_2\rangle\,.\end{aligned} \tag{5.17}$$

In the following, we will constrain ourselves for simplicity to symmetric tunneling rates $\Gamma_L^{\min} = \Gamma_R^{\min} = \Gamma^{\min}$ and $\Gamma_L^{\max} = \Gamma_R^{\max} = \Gamma^{\max}$. In this case, we obtain the simple expression for the average number of particles during one pumping cycle

$$\begin{aligned}\langle n\rangle &= \frac{\Gamma^{\max}\Gamma^{\min}}{\Gamma^{\max}+\Gamma^{\min}}\frac{T}{2}\left[f_L(\epsilon^{\max}) - f_R(\epsilon^{\max}) + f_L(\epsilon^{\min}) - f_R(\epsilon^{\min})\right] \\ &+\frac{\Gamma^{\max}-\Gamma^{\min}}{\left(\Gamma^{\max}+\Gamma^{\min}\right)^2}\left[\Gamma^{\max}\left(f_L(\epsilon^{\min}) - f_R(\epsilon^{\max})\right) + \Gamma^{\min}\left(f_R(\epsilon^{\min}) - f_L(\epsilon^{\max})\right)\right] \times \\ &\times \tanh\left[\frac{T}{4}\left(\Gamma^{\min}+\Gamma^{\max}\right)\right] . \end{aligned} \tag{5.18}$$

The first term (which dominates for slow pumping, i.e., large T) is negative when $f_L(\omega) < f_R(\omega)$. It is simply given by the average of the two SET currents one would obtain for the two half cycles. The second term however is present when $\Gamma^{\max} > \Gamma^{\min}$ and may be positive when the dot level is changed strongly enough souch that $f_L(\epsilon^{\min}) > f_R(\epsilon^{\max})$ and $f_R(\epsilon^{\min}) > f_L(\epsilon^{\max})$. For large differences in the tunneling rates and small pumping times T it may even dominate the first term, such that the net particle number may be positive even though the bias would favor the opposite current direction, see Fig. 5.3. The second cumulant can be similarly calculated

$$\left\langle n^2\right\rangle - \langle n\rangle^2 = \left\langle n_1^2\right\rangle - \langle n_1\rangle^2 + \left\langle n_2^2\right\rangle - \langle n_2\rangle^2 . \tag{5.19}$$

Exercise 44 (Second Cumulant for joint distributions) *(1 points)*
Show the validity of the above equation.

When the dot level is shifted to very low and very large values (large pumping power), the bias is negligible (alternatively, we may also consider an unbiased situation from the beginning). In this case, we can assume $f_L(\epsilon^{\min}) = f_R(\epsilon^{\min}) = f(\epsilon^{\min})$ and $f_L(\epsilon^{\max}) = f_R(\epsilon^{\max}) = f(\epsilon^{\max})$. Then, the second term dominates always and the particle number simplifies to

$$\langle n\rangle = \left[f(\epsilon^{\min}) - f(\epsilon^{\max})\right]\frac{\Gamma^{\max}-\Gamma^{\min}}{\Gamma^{\max}+\Gamma^{\min}}\tanh\left[\frac{T}{4}\left(\Gamma^{\min}+\Gamma^{\max}\right)\right] . \tag{5.20}$$

This becomes maximal for large pumping time and large power consumption ($f(\epsilon^{\min}) - f(\epsilon^{\max}) = 1$). In this idealized limit, we easily obtain for the Fano factor for large cycle times T

$$F_T = \frac{\langle n^2\rangle - \langle n\rangle^2}{|\langle n\rangle|} \overset{T\to\infty}{\to} \frac{2\Gamma^{\max}\Gamma^{\min}}{\left(\Gamma^{\max}+\Gamma^{\min}\right)^2} , \tag{5.21}$$

which demonstrates that the pump works efficient and noiseless when $\Gamma^{\max} \gg \Gamma^{\min}$.

At infinite bias $f_L(\omega) =$ and $f_R(\omega) = 0$, the pump does not transport electrons against any potential or thermal gradient but can still be used to control the statistics of the tunneled electrons. For example, it is possible to reduce the noise to zero also in this limit when $\Gamma^{\min} \to 0$.

5.2 Piecewise-Constant feedback control

Closed-loop (or feedback) control means that the system is monitored (either continuously or at certain times) and that the result of these measurements is fed back by changing some parameter of

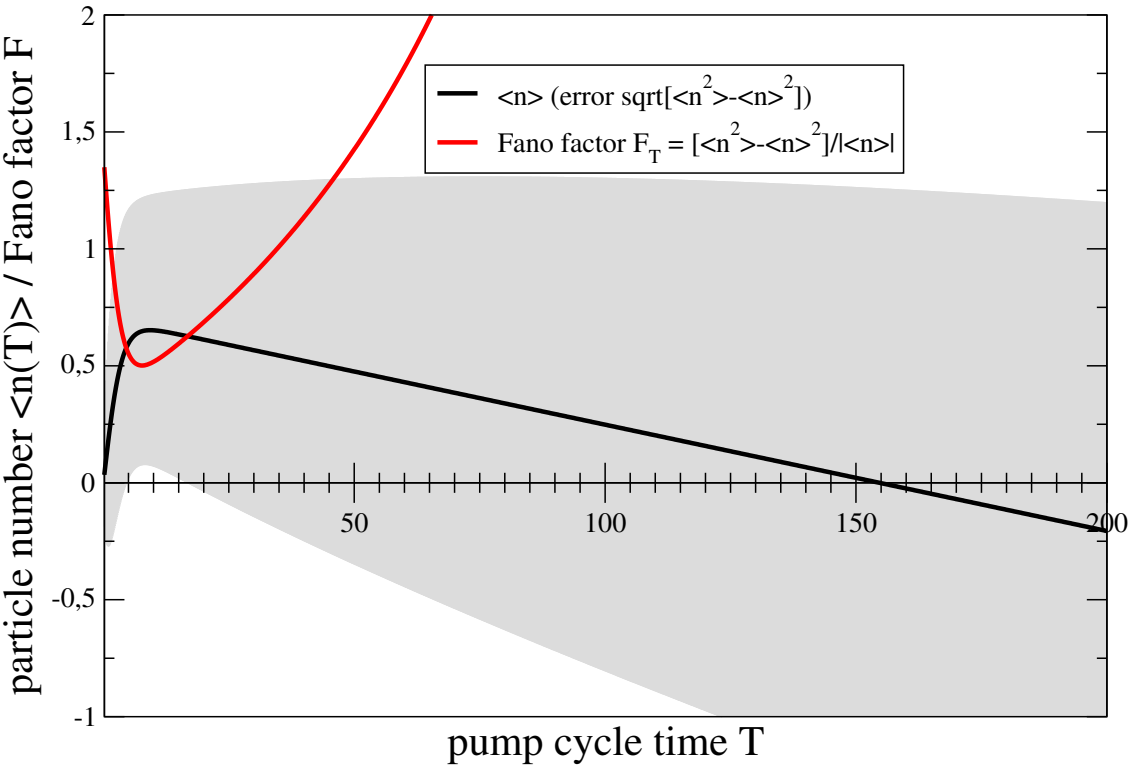

Figure 5.3: Average number of tunneled particles during one pump cycle. Parameters have been chosen as $\Gamma^{\max} = 1$, $\Gamma^{\min} = 0.1$, $f_L(\epsilon^{\min}) = 0.9$, $f_R(\epsilon^{\min}) = 0.95$, $f_L(\epsilon^{\max}) = 0$, $f_R(\epsilon^{\max}) = 0.05$, such that for slow pumping (large T), the current $I = \langle n \rangle / T$ must become negative. The shaded region characterizes the width of the distribution, and the Fano factor demonstrates that around the maximum pump current, the signal-to-noise ratio is most favorable.

the system. Under measurement with outcome m (an index characterizing the possible outcomes), the density matrix transforms as

$$\rho \xrightarrow{m} \frac{M_m \rho M_m^\dagger}{\mathrm{Tr}\left\{M_m^\dagger M_m \rho\right\}}\,, \tag{5.22}$$

and the probability at which this outcome occurs is given by $\mathrm{Tr}\left\{M_m^\dagger M_m \rho\right\} = \mathrm{Tr}\left\{M_m \rho M_m^\dagger\right\}$. This can also be written in superoperator notation ($\mathcal{M}_m \rho \hat{=} M_m \rho M_m^\dagger$)

$$\rho \xrightarrow{m} \frac{\mathcal{M}_m \rho}{\mathrm{Tr}\left\{\mathcal{M}_m \rho\right\}}\,. \tag{5.23}$$

Let us assume that conditioned on the measurement result m at time t, we apply a propagator for the time interval Δt. Then, a measurement result m at time t provided, the density matrix at time $t + \Delta t$ will be given by

$$\rho^{(m)}(t + \Delta t) = e^{\mathcal{L}^{(m)} \Delta t} \frac{\mathcal{M}_m \rho}{\mathrm{Tr}\left\{\mathcal{M}_m \rho\right\}}\,. \tag{5.24}$$

However, to obtain an effective description of the density matrix evolution, we have to average over all measurement outcomes – where we have to weight each outcome by the corresponding

probability

$$\rho(t+\Delta t) = \sum_m \mathrm{Tr}\left\{\mathcal{M}_m\rho(t)\right\} e^{\mathcal{L}^{(m)}\Delta t}\frac{\mathcal{M}_m\rho}{\mathrm{Tr}\left\{\mathcal{M}_m\rho\right\}} = \sum_m e^{\mathcal{M}^{(m)}\Delta t}\mathcal{M}_m\rho(t)\,. \tag{5.25}$$

Note that this is an iteration scheme and not a conventional master equation. More generally – not constraining the conditioned dynamics to Lindblad evolutions – one could also write

$$\rho(t+\Delta t) = \sum_m \mathcal{K}^{(m)}(\Delta t)\mathcal{M}_m\rho(t)\,, \tag{5.26}$$

where $\mathcal{K}^{(m)}(\Delta t)\rho \hat{=} \sum_\alpha K_\alpha^{(m)}(\Delta t)\rho K_\alpha^{(m)\dagger}(\Delta t)$ with $\sum_\alpha K_\alpha^{(m)\dagger}K_\alpha^{(m)} = \mathbf{1}$ is a conditioned Kraus map. Furthermore, the conditioned Liouvillian $\mathcal{L}^{(m)}$ or the Kraus map $\mathcal{K}^{(m)}$ may well depend on the time t (at which the measurement is performed) as long as it is constant during the interval $[t, t+\Delta t]$.

Expanding now the exponential of the Liouvillian in the limit of a continuous feedback control scheme $\Delta t \to 0$, we may under the condition that

$$\sum_m \mathcal{M}_m = \mathbf{1} \tag{5.27}$$

obtain an effective Liouvillian under feedback control

$$\mathcal{L}_{\mathrm{fb}}\rho = \lim_{\Delta t\to 0}\frac{\rho(t+\Delta t)-\rho(t)}{\Delta t} \qquad \to \mathcal{L}_{\mathrm{fb}} = \sum_m \mathcal{L}_m\mathcal{M}_m\,. \tag{5.28}$$

We note that the above condition $\sum_m \mathcal{M}_m = \mathbf{1}$ will only hold in specific cases and only for particular subspaces. When it does not hold, an effective Liouvillian under feedback control does not exist, and the evolution is described rather by an iteration of the form (5.25) or (5.26).

5.3 Maxwell's demon

Maxwell invented his famous demon as a thought experiment to demonstrate that thermodynamics is a macroscopic effective theory: An intelligent being (the demon) living in a box is measuring the speed of molecules of some gas in the box. An initial thermal distribution of molecules implies that the molecules have different velocities. The demon measures the velocities and inserts an impermeable wall whenever the the molecule is too fast or lets it pass into another part of the box when it is slow. As time progresses, this would lead to a sorting of hot and cold molecules, and the temperature difference could be exploited to perform work.

This is nothing but a feedback (closed-loop) control scheme: The demon performs a measurement (is the molecule slow or fast) and then uses the information to perform an appropriate control action on the system (inserting a wall or not). Classically, the insertion of a wall requires in the idealized case no work, such that only information is used to create a temperature gradient. However, the Landauer principle states that with each bit of information erased, heat of at least $k_B T\ln(2)$ is dissipated into the environment. To remain functionable, the demon must at some point start to delete the information, which leads to the dissipation of heat. The dissipated heat will exceed the energy obtainable from the thermal gradient.

An analog of a Maxwell demon may be implemented in an electronic context: There, an experimentalist takes the role of the demon. The box is replaced by the SET (including the

contacts), on which by a nearby QPC a measurement of the dot state (simply empty or filled) is performed. Depending on the measurement outcome, the tunneling rates are modified in time in a piecewise constant manner: When there is no electron on the dot, the left tunneling rate Γ_L is increased (low barrier) and the right tunneling rate Γ_R is decreased (high barrier). The opposite is done when there is an electron on the dot, see Fig. 5.4. Thus, the only difference in comparison

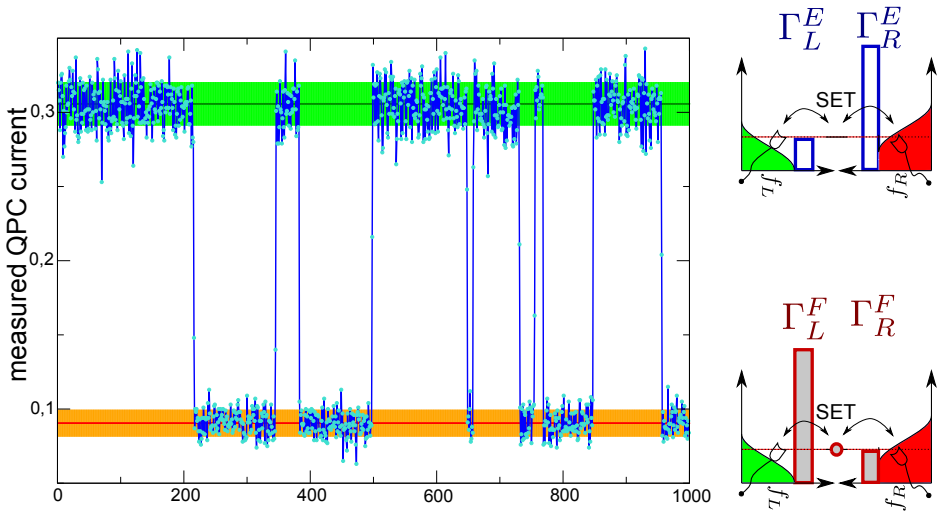

Figure 5.4: Sketch of the feedback scheme: For a filled dot (low QPC current), the left tunneling rate is minimal and the right tunneling rate is maximal and vice-versa for an empty dot. The dot level itself is not changed.

to Sec. 5.1.1 is that now **information of the system state is used to modify the tunneling rates**. Very simple considerations already demonstrate that with this scheme, it will be possible to transport electrons against an existing bias only with time-dependent tunneling rates. When one junction is completely decoupled $\Gamma_{L/R}^{\min} \to 0$, this will completely rectify the transport from left to right also against the bias (if the bias is finite). In the following, we will address the statistics of this device.

The first step is to identify an effective evolution equation for the density matrix accounting for measurement and control. A measurement of a low QPC current will imply – compare Eq. (4.25) – that the system is most likely filled, whereas a large QPC current indicates an empty SET dot. In the idealized limit of no measurement errors, this simply corresponds to a projection

$$M_E = |0\rangle\langle 0| \ , \qquad M_F = |1\rangle\langle 1| \tag{5.29}$$

onto the empty and filled SET dot states, respectively. In the full space (ordering the density matrix as $(\rho_{00}, \rho_{11}, \rho_{01}, \rho_{10})^T$ these have superoperator representations (defining $\mathcal{M}_\sigma \rho \hat{=} M_\sigma \rho M_\sigma^\dagger$) as

$$\mathcal{M}_E = \begin{pmatrix} 1 & 0 & 0 & 0 \\ 0 & 0 & 0 & 0 \\ 0 & 0 & 0 & 0 \\ 0 & 0 & 0 & 0 \end{pmatrix} , \qquad \mathcal{M}_F = \begin{pmatrix} 0 & 0 & 0 & 0 \\ 0 & 1 & 0 & 0 \\ 0 & 0 & 0 & 0 \\ 0 & 0 & 0 & 0 \end{pmatrix} , \tag{5.30}$$

and we see that $\mathcal{M}_E + \mathcal{M}_F \neq \mathbf{1}$. However, since due to the common block structure of the individual dissipators and the measurement superoperators we can reduce the dynamics to the

populations only, where with

$$\bar{\mathcal{M}}_E = \begin{pmatrix} 1 & 0 \\ 0 & 0 \end{pmatrix}, \qquad \bar{\mathcal{M}}_F = \begin{pmatrix} 0 & 0 \\ 0 & 1 \end{pmatrix} \tag{5.31}$$

we indeed have $\bar{\mathcal{M}}_E + \bar{\mathcal{M}}_F = \mathbf{1}$. Therefore, for a continuous measurement and feedback control loop, the effective population Liouvillian under feedback control becomes with Eq. (5.28)

$$\mathcal{L}_{\text{eff}} = \mathcal{L}^{(E)}\bar{\mathcal{M}}_E + \mathcal{L}^{(F)}\bar{\mathcal{M}}_F \tag{5.32}$$

Note that this can be performed with and without counting fields. Taking into account the diagonal structure of the projection superoperators, this simply implies that the effective Liouvillian under feedback has the first column from the Liouvillian conditioned on an empty dot and the second column from the Liouvillian conditioned on the filled dot

$$\mathcal{L}_{\text{eff}}(\chi_L, \chi_R) = \begin{pmatrix} -\Gamma_L^E f_L - \Gamma_R^E f_R & +\Gamma_L^F(1-f_L)e^{+\mathrm{i}\chi_L} + \Gamma_R^F(1-f_R)e^{+\mathrm{i}\chi_R} \\ +\Gamma_L^E f_L e^{-\mathrm{i}\chi_L} + \Gamma_R^E f_R e^{-\mathrm{i}\chi_R} & -\Gamma_L^F(1-f_L) - \Gamma_R^F(1-f_R) \end{pmatrix}. \tag{5.33}$$

Evidently, it still obeys trace conservation but now the tunneling rates in the two columns are different ones.

Exercise 45 (Current at zero bias) *(1 points)*
Calculate the feedback-current at zero bias $f_L = f_R = f$ in dependence on f. What happens at zero temperatures, where $f \to \{0, 1\}$?

The effective Liouvillian describes the average evolution of trajectories under continuous monitoring and feedback. The validity of the effective description can be easily checked by calculating Monte-Carlo solutions as follows:

Starting e.g. with a filled dot, the probability to jump out e.g. to the right lead during the small time interval Δt reads $P^{(F)}_{\text{out,R}} = \Gamma^F_R(1-f_R)\Delta t$. Similarly, we can write down the probabilities to jump out to the left lead and also the probabilities to jump onto an empty dot from either the left or right contact

$$\begin{aligned} P^{(F)}_{\text{out,R}} &= \Gamma^F_R(1-f_R)\Delta t\,, \qquad P^{(F)}_{\text{out,L}} = \Gamma^F_L(1-f_L)\Delta t\,, \\ P^{(E)}_{\text{in,R}} &= \Gamma^E_R f_R \Delta t\,, \qquad P^{(E)}_{\text{in,L}} = \Gamma^E_L f_L \Delta t\,. \end{aligned} \tag{5.34}$$

Naturally, these jump probabilities also uniquely determine the change of the particle number on either contact. The remaining probability is simply the one that no jump occurs during Δt. A Monte-Carlo simulation is obtained by drawing a random number and choosing one out of three possible outcomes for empty (jumping in from left contact, from right contact, or remaining empty) and for a filled (jumping out to left contact, to right contact, or remaining filled) dot. Repeating the procedure several times yields a single trajectory for $n(t)$, $n_L(t)$, and $n_R(t)$. The ensemble average of many such trajectories agree perfectly with the solution

$$\begin{aligned} \langle n \rangle_t &= \mathrm{Tr}\left\{ d^\dagger d e^{\mathcal{L}_{\text{eff}}(0,0)t}\rho_0 \right\}, \\ \langle n_L \rangle_t &= (-\mathrm{i}\partial_\chi)\,\mathrm{Tr}\left\{ e^{\mathcal{L}_{\text{eff}}(\chi,0)t}\rho_0 \right\}\big|_{\chi=0}, \\ \langle n_R \rangle_t &= (-\mathrm{i}\partial_\chi)\,\mathrm{Tr}\left\{ e^{\mathcal{L}_{\text{eff}}(0,\chi)t}\rho_0 \right\}\big|_{\chi=0} \end{aligned} \tag{5.35}$$

of the effective feedback master equation, see Fig. 5.5. To compare with the case without feedback, we parametrize the change of tunneling rates by dimensionless constants

$$\Gamma_L^E = e^{\delta_L^E}\Gamma_L\,, \qquad \Gamma_R^E = e^{\delta_R^E}\Gamma_R\,, \qquad \Gamma_L^F = e^{\delta_L^F}\Gamma_L\,, \qquad \Gamma_R^F = e^{\delta_R^F}\Gamma_R\,, \tag{5.36}$$

where $\delta_\alpha^\beta \to 0$ reproduces the case without feedback and $\delta_\alpha^\beta > 0 (< 0)$ increases (decreases) the tunneling rate to contact α conditioned on dot state β. The general current can directly be

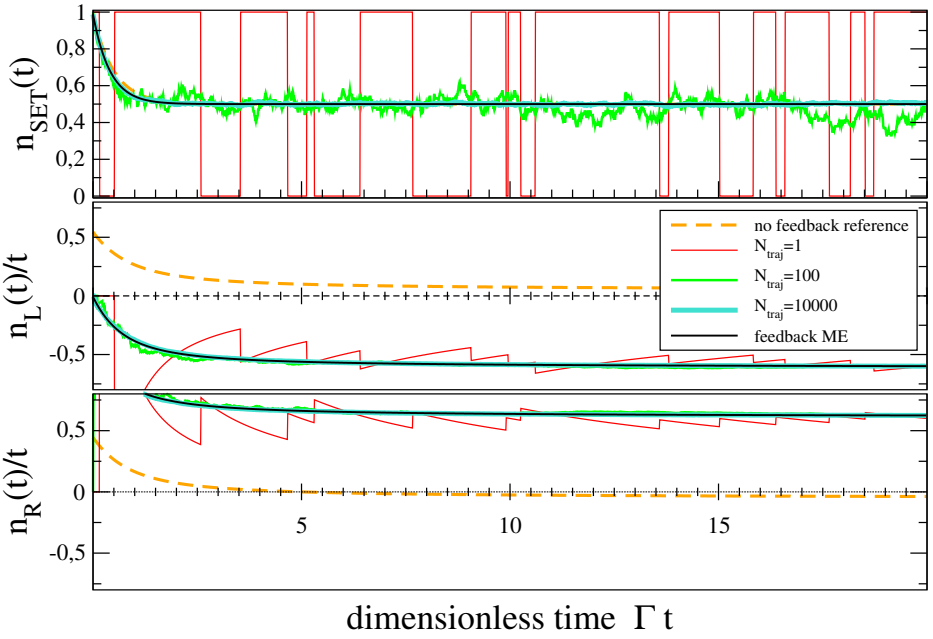

Figure 5.5: Comparison of a single (thin red curve with jumps, same realization in all panels) and the average of 100 (medium thickness, green) and 10000 (bold smooth curve, turquoise) trajectories with the solution from the effective feedback master equation (thin black) for the dot occupation (top), the number of particles on the left (middle), and the number of particles on the right (bottom). The average of the trajectories converges to the effective feedback master equation result. The reference curve without feedback (dashed orange) may be obtained by using vanishing feedback parameters and demonstrates that the direction of the current may actually be reversed via sufficiently strong feedback. Parameters: $\Gamma_L = \Gamma_R \equiv \Gamma$, $f_L = 0.45$, $f_R = 0.55$, $\delta_L^E = \delta_R^F = 1.0$, $\delta_R^E = \delta_L^F = -10.0$, and $\Gamma\Delta t = 0.01$.

calculated as

$$I = \frac{f_L(1-f_R)\Gamma_L^E\Gamma_R^F - (1-f_L)f_R\Gamma_L^F\Gamma_R^E}{\Gamma_L^E f_L + \Gamma_L^F(1-f_L) + \Gamma_R^E f_R + \Gamma_R^F(1-f_R)}\,, \tag{5.37}$$

which reduces to the conventional current without feedback when $\Gamma_\alpha^\beta \to \Gamma_\alpha$. For finite feedback strength however, this will generally induce a non-vanishing current at zero bias, see Fig. 5.6. In our idealized setup, this current is only generated by the information on whether the dot is occupied or empty – hence the interpretation as a Maxwell demon. When the contacts are held at equal temperatures $\beta_L = \beta_R = \beta$, this raises the question for the maximum power

$$P = -IV \tag{5.38}$$

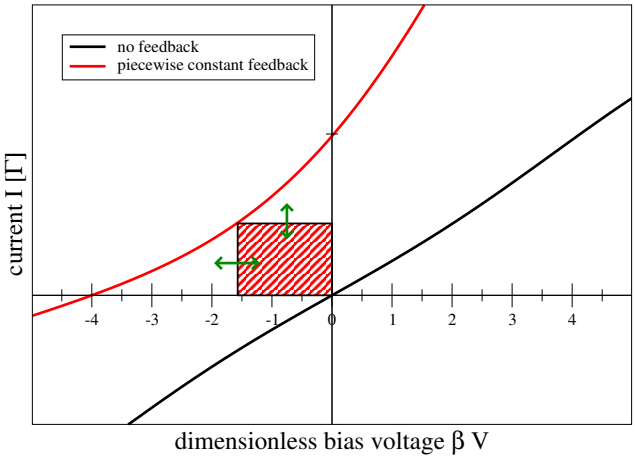

Figure 5.6: Current voltage characteristics for finite feedback strength $\delta = 1$ (red curve) and without feedback $\delta = 0$ (black curve). For finite feedback, the current may point in the other direction than the voltage leading to a positive power $P = -IV$ (shaded region) generated by the device.

generated by the device.

In what follows, we will consider symmetric feedback characterized by a single parameter

$$\delta_L^E = \delta_R^F = -\delta_L^F = -\delta_R^E = +\delta\,, \tag{5.39}$$

where $\delta > 0$ favors transport from left to right and $\delta < 0$ transport from right to left and also symmetric tunneling rates $\Gamma = \Gamma_L = \Gamma_R$. With these assumptions, it is easy to see that for large feedback strengths $\delta \gg 1$, the current simply becomes

$$I \to \Gamma e^{\delta} \frac{f_L(1-f_R)}{f_L + (1-f_R)}\,. \tag{5.40}$$

To determine the maximum power, we would have to maximize with respect to left and right chemical potentials μ_L and μ_R, the lead temperature β and the dot level ϵ. However, as these parameters only enter implicitly in the Fermi functions, it is more favorable to use that for equal temperatures

$$\beta(\mu_L - \mu_R) = \beta V = \ln\left[\frac{f_L(1-f_R)}{(1-f_L)f_R}\right]\,, \tag{5.41}$$

such that we can equally maximize

$$P = -IV = \frac{1}{\beta}(-I\beta V) \to \frac{\Gamma e^{\delta}}{\beta}\left[-\frac{f_L(1-f_R)}{f_L+(1-f_R)}\ln\left(\frac{f_L(1-f_R)}{(1-f_L)f_R}\right)\right]\,. \tag{5.42}$$

The term in square brackets can now be maximized numerically with respect to the parameters f_L and f_R in the range $0 \le f_{L/R} \le 1$, such that one obtains for the maximum power at strong feedback

$$P \le k_{\rm B}T\Gamma e^{\delta} 0.2785 \qquad \text{at} \qquad f_L = 0.2178 \qquad f_R = 0.7822\,. \tag{5.43}$$

The average work performed between two QPC measurement points at t and $t + \Delta t$ is therefore given by

$$W \le k_{\rm B}T\Gamma e^{\delta}\Delta t 0.2785\,. \tag{5.44}$$

However, to perform feedback efficiently, it is required that the QPC sampling rate is fast enough that all state changes of the SET are faithfully detected (no tunneling charges are missed). This requires that $\Gamma e^{\delta}\Delta t < 1$. Therefore, we can refine the upper bound for the average work

$$W \leq k_{\mathrm{B}}T 0.2785\,. \tag{5.45}$$

This has to be contrasted with the Landauer principle, which states that for each deleted bit in the demons brain (each QPC data point enconding high current or low current) heat of

$$Q \geq k_{\mathrm{B}}T\ln(2) \approx k_{\mathrm{B}}T 0.6931 \tag{5.46}$$

is dissipated. These rough estimates indicate that the second law does not appear to be violated.

The conventional fluctuation theorem for the SET at equal temperatures

$$\frac{P_{+n}(t)}{P_{-n}(t)} = e^{n\beta V} \tag{5.47}$$

is modified in presence of feedback. However, since the Liouvillian still contains the counting fields in the conventional way, simply the factor in the exponential, not the dependence on the number of tunneled electrons n is changed. To evaluate the FT, we identify symmetries in the moment-generating function (or alternatively the eigenvalues of the Liouvillian)

$$\begin{aligned}
\lambda(-\chi) &= \lambda\left(+\chi + \mathrm{i}\ln\left[\frac{\Gamma_L^E\Gamma_R^F}{\Gamma_L^F\Gamma_R^E}\frac{f_L(1-f_R)}{(1-f_L)f_R}\right]\right) \\
&= \lambda\left(+\chi + \mathrm{i}\ln\left[e^{+4\delta}\frac{f_L(1-f_R)}{(1-f_L)f_R}\right]\right) = \lambda\left(+\chi + \mathrm{i}\ln\left[e^{+4\delta}e^{\beta V}\right]\right) \\
&= \lambda(+\chi + \mathrm{i}(4\delta+\beta V))\,.
\end{aligned} \tag{5.48}$$

From this symmetry of the cumulant-generating function we obtain for the fluctuation theorem under feedback

$$\lim_{t\to\infty}\frac{P_{+n}(t)}{P_{-n}(t)} = e^{n(\beta V+4\delta)} = e^{n\beta(V-V^*)}\,, \tag{5.49}$$

where $V^* = -4\delta/\beta$ denotes the voltage at which the current (under feedback) vanishes.

In the exponential, we do no longer have the conventional entropy production that is in the long-term limit essentially given by the heat transfer. Instead, the modification indicates that the second law must be modified by the information that is used to implement the control loop.

Exercise 46 (Vanishing feedback current) *(1 points)*
Show for equal temperatures that the feedback current vanishes when $V = V^* = -4\delta/\beta$.

The fact that the estimates concerning the second law are rather vague result from the missing physical implementation of the control loop. In our model, it could be anything, even represented by a human being pressing a button whenever the QPC current changes. The entropy produced by such a humanoid implementation of the control loop would by far exceed the local entropy reduction manifested by a current running against the bias. Below, we discuss an all-inclusive implementation of the control loop, where we can answer these things quantitatively.

5.4 An all-inclusive description of Maxwell's demon

Consider a single-electron transistor as before now capacitively interacting with another quantum dot, which is coupled to its own reservoir as depicted in Fig. 5.7. The system Hamiltonian of this

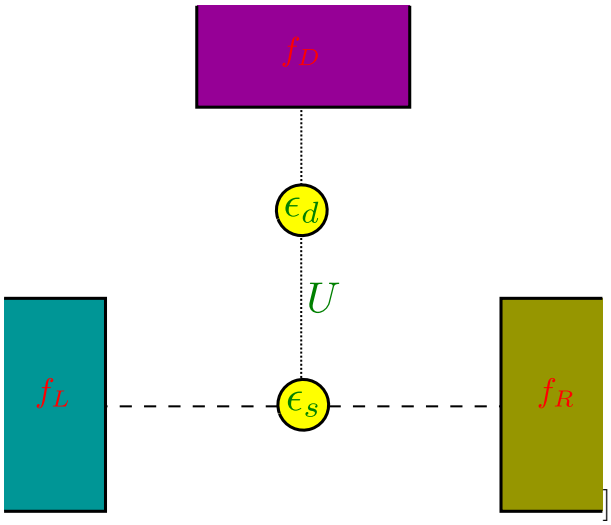

Figure 5.7: Sketch of an SET (bottom circuit) that is capacitively coupled via the Coulomb interaction U to another quantum dot. The additional quantum dot is tunnel-coupled to its own reservoir with Fermi function f_D. Since the associated stationary matter current vanishes, only energy can be transferred across this junction (dotted line).

three-terminal system reads

$$\mathcal{H}_{\mathrm{S}} = \epsilon_d c_d^\dagger c_d + \epsilon_s c_s^\dagger c_s + U c_d^\dagger c_d c_s^\dagger c_s \,, \tag{5.50}$$

where ϵ_s and ϵ_d denote the on-site energies of the SET dot and the demon dot, respectively, whereas U denotes the Coulomb interaction between the two dots. The system dot is tunnel-coupled to left and right leads, whereas the demon dot is tunnel-coupled to its junction only

$$\mathcal{H}_{\mathrm{I}} = \sum_k \left(t_{kL} c_s c_{kL}^\dagger + t_{kL}^* c_{kL} c_s^\dagger \right) + \sum_k \left(t_{kR} c_s c_{kR}^\dagger + t_{kR}^* c_{kR} c_s^\dagger \right) + \sum_k \left(t_{kd} c_d c_{kd}^\dagger + t_{kd}^* c_{kL} c_d^\dagger \right) . \tag{5.51}$$

Furthermore, all the junctions are modeled as non-interacting fermions

$$\mathcal{H}_{\mathrm{B}} = \sum_{\nu \in \{L,R,d\}} \sum_k \epsilon_{k\nu} c_{k\nu}^\dagger c_{k\nu} \,. \tag{5.52}$$

Treating the tunneling amplitudes perturbatively and fixing the reservoirs at thermal equilibrium states we derive the standard quantum-optical master equation, compare also Def. 8. Importantly, we do not apply the popular wide-band limit here (which would mean to approximate $\Gamma_\nu(\omega) \approx \Gamma_\nu$). In the energy eigenbasis of $\mathcal{H}_{\mathrm{S}}$ – further-on denoted by $|\rho\sigma\rangle$ where $\rho \in \{E, F\}$ describes the systems dot state and $\sigma \in \{0, 1\}$ denotes the state of the demon dot (both either empty or filled, respectively) – the populations obey a simple rate equation defined by Eq. (2.43). Denoting the populations by $p_{\rho\sigma} = \langle \rho\sigma | \, \rho \, | \rho\sigma \rangle$, the rate equation $\dot{P} = \mathcal{L}P$ in the ordered basis $P = (p_{0E}, p_{1E}, p_{0F}, p_{1F})^T$ decomposes into the contributions due to the different reservoirs

$\mathcal{L} = \mathcal{L}_D + \mathcal{L}_L + \mathcal{L}_R$, which read

$$\begin{aligned}
\mathcal{L}_D &= \begin{pmatrix} -\Gamma_D f_D & +\Gamma_D(1-f_D) & 0 & 0 \\ +\Gamma_D f_D & -\Gamma_D(1-f_D) & 0 & 0 \\ 0 & 0 & -\Gamma_D^U f_D^U & +\Gamma_D^U(1-f_D^U) \\ 0 & 0 & +\Gamma_D^U f_D^U & -\Gamma_D^U(1-f_D^U) \end{pmatrix}, \\
\mathcal{L}_\alpha &= \begin{pmatrix} -\Gamma_\alpha f_\alpha & 0 & +\Gamma_\alpha(1-f_\alpha) & 0 \\ 0 & -\Gamma_\alpha^U f_\alpha^U & 0 & +\Gamma_\alpha^U(1-f_\alpha^U) \\ +\Gamma_\alpha f_\alpha & 0 & -\Gamma_\alpha(1-f_\alpha) & 0 \\ 0 & +\Gamma_\alpha^U f_\alpha^U & 0 & -\Gamma_\alpha^U(1-f_\alpha^U) \end{pmatrix}, \qquad \alpha \in \{L,R\}\,, \qquad (5.53)
\end{aligned}$$

where we have used the abbreviations $\Gamma_\alpha = \Gamma_\alpha(\epsilon_s)$ and $\Gamma_\alpha^U = \Gamma_\alpha(\epsilon_s + U)$ for $\alpha \in \{L, R\}$ and $\Gamma_D = \Gamma_D(\epsilon_d)$ and $\Gamma_D^U = \Gamma_D(\epsilon_d + U)$ for the tunneling rates and similarly for the Fermi functions $f_\alpha = f_\alpha(\epsilon_s)$, $f_\alpha^U = f_\alpha(\epsilon_s + U)$, $f_D = f_D(\epsilon_d)$, and $f_D^U = f_D(\epsilon_d + U)$, respectively. We note that all contributions separately obey local-detailed balance relations. Closer inspection of the rates in Eq. (5.53) reveals that these rates could have been guessed without any microscopic derivation. For example, the transition rate from state $|1E\rangle$ to state $|0E\rangle$ is just given by the bare tunneling rate for the demon junction Γ_D multiplied by the probability to find a free space in the terminal at transition frequency ϵ_d. Similarly, the transition rate from state $|1F\rangle$ to state $|0F\rangle$ corresponds to an electron jumping out of the demon dot to its junction, this time, however, transporting energy of $\epsilon_d + U$. We have ordered our basis such that the upper left block of $\mathcal{L}_D$ describes the dynamics of the demon dot conditioned on an empty system dot, whereas the lower block accounts for the dynamics conditioned on a filled system.

As a whole, the system respects the second law of thermodynamics. We demonstrate this by analyzing the entropy production by means of the Full Counting Statistics. In order to avoid having to trace six counting fields, we note that the system obeys three conservation laws, since the two dots may only exchange energy but not matter

$$I_M^{(L)} + I_M^{(R)} = 0\,, \qquad I_M^{(D)} = 0\,, \qquad I_E^{(L)} + I_E^{(R)} + I_E^{(D)} = 0\,, \qquad (5.54)$$

where $I_E^{(\nu)}$ and $I_M^{(\nu)}$ denote energy and matter currents to terminal ν, respectively. Therefore, three counting fields should in general suffice to completely track the entropy production in the long-term limit. For simplicity however, we compute the entropy production for the more realistic case of equal temperatures at the left and right SET junction $\beta = \beta_L = \beta_R$. Technically, this is conveniently performed by balancing with the entropy flow and using the conservation laws

$$\begin{aligned}
\dot{S}_\mathrm{i} &= -\dot{S}_\mathrm{e} = -\sum_\nu \beta^{(\nu)}(I_E^{(\nu)} - \mu^{(\nu)} I_M^{(\nu)}) \\
&= -\beta(I_E^{(L)} - \mu_L I_M^{(L)} + I_E^{(R)} - \mu_R I_M^{(R)}) - \beta_D I_E^{(D)} \\
&= (\beta - \beta_D) I_E^{(D)} - \beta(\mu_L - \mu_R) I_M^{(R)}\,. \qquad (5.55)
\end{aligned}$$

Thus, we conclude that for equal temperatures left and right it should even suffice to track e.g. only the energy transferred to the demon junction and the particles to the right lead. Therefore, we introduce counting fields for the demon (ξ) and for the particles transferred to the left junctions

(χ), and the counting-field dependent rate equation becomes

$$\begin{aligned}
\mathcal{L}_D(\xi) &= \begin{pmatrix} -\Gamma_D f_D & +\Gamma_D(1-f_D)e^{+\mathrm{i}\xi\epsilon_d} & 0 & 0 \\ +\Gamma_D f_D e^{-\mathrm{i}\xi\epsilon_d} & -\Gamma_D(1-f_D) & 0 & 0 \\ 0 & 0 & -\Gamma_D^U f_D^U & +\Gamma_D^U(1-f_D^U)e^{+\mathrm{i}\xi(\epsilon_d+U)} \\ 0 & 0 & +\Gamma_D^U f_D^U e^{-\mathrm{i}\xi(\epsilon_d+U)} & -\Gamma_D^U(1-f_D^U) \end{pmatrix}, \\
\mathcal{L}_R(\chi) &= \begin{pmatrix} -\Gamma_R f_R & 0 & +\Gamma_R(1-f_R)e^{+\mathrm{i}\chi} & 0 \\ 0 & -\Gamma_R^U f_R^U & 0 & +\Gamma_R^U(1-f_R^U)e^{+\mathrm{i}\chi} \\ +\Gamma_R f_R e^{-\mathrm{i}\chi} & 0 & -\Gamma_R(1-f_R) & 0 \\ 0 & +\Gamma_R^U f_R^U e^{-\mathrm{i}\chi} & 0 & -\Gamma_R^U(1-f_R^U) \end{pmatrix}. \qquad (5.56)
\end{aligned}$$

These counting fields can now be used to reconstruct the statistics of energy and matter transfer. The currents can be obtained by performing suitable derivatives of the rate matrix. For example, the energy current to the demon is given by $I_E^{(D)} = -\mathrm{i}\mathrm{Tr}\left\{\partial_\xi \mathcal{L}(\xi,0)|_{\xi=0}\,\bar{\rho}\right\}$, where $\bar{\rho}$ is the steady state $\mathcal{L}(0,0)\bar{\rho}=0$.

To test the fluctuation theorem, we calculate the characteristic polynomial

$$\begin{aligned}
\mathcal{D}(\xi,\chi) &= |\mathcal{L}(\xi,\chi)-\lambda\mathbf{1}| \\
&= (L_{11}-\lambda)(L_{22}-\lambda)(L_{33}-\lambda)(L_{44}-\lambda) \\
&\quad -(L_{11}-\lambda)(L_{22}-\lambda)L_{34}(\xi)L_{43}(\xi) - (L_{11}-\lambda)(L_{33}-\lambda)L_{24}(\chi)L_{42}(\chi) \\
&\quad -(L_{22}-\lambda)(L_{44}-\lambda)L_{13}(\chi)L_{31}(\chi) - (L_{33}-\lambda)(L_{44}-\lambda)L_{12}(\xi)L_{21}(\xi) \\
&\quad +L_{12}(\xi)L_{21}(\xi)L_{34}(\xi)L_{43}(\xi) + L_{13}(\chi)L_{31}(\chi)L_{24}(\chi)L_{42}(\chi) \\
&\quad -L_{12}(\xi)L_{24}(\chi)L_{31}(\chi)L_{43}(\xi) - L_{13}(\chi)L_{21}(\xi)L_{34}(\xi)L_{42}(\chi) \\
&= (L_{11}-\lambda)(L_{22}-\lambda)(L_{33}-\lambda)(L_{44}-\lambda) \\
&\quad -(L_{11}-\lambda)(L_{22}-\lambda)L_{34}(0)L_{43}(0) - (L_{11}-\lambda)(L_{33}-\lambda)L_{24}(\chi)L_{42}(\chi) \\
&\quad -(L_{22}-\lambda)(L_{44}-\lambda)L_{13}(\chi)L_{31}(\chi) - (L_{33}-\lambda)(L_{44}-\lambda)L_{12}(0)L_{21}(0) \\
&\quad +L_{12}(0)L_{21}(0)L_{34}(0)L_{43}(0) + L_{13}(\chi)L_{31}(\chi)L_{24}(\chi)L_{42}(\chi) \\
&\quad -L_{12}(\xi)L_{24}(\chi)L_{31}(\chi)L_{43}(\xi) - L_{13}(\chi)L_{21}(\xi)L_{34}(\xi)L_{42}(\chi)\,, \qquad (5.57)
\end{aligned}$$

where L_{ij} simply denote the matrix elements of the rate matrix $\mathcal{L}$. We note the symmetries

$$\begin{aligned}
L_{13}(-\chi) &= \frac{1-f_L}{f_L} L_{31}\left(+\chi + \mathrm{i}\ln\frac{f_L(1-f_R)}{(1-f_L)f_R}\right) = \frac{1-f_L}{f_L} L_{31}\left(+\chi + \mathrm{i}\beta(\mu_L-\mu_R)\right), \\
L_{24}(-\chi) &= \frac{1-f_L^U}{f_L^U} L_{42}\left(+\chi + \mathrm{i}\ln\frac{f_L^U(1-f_R^U)}{(1-f_L^U)f_R^U}\right) = \frac{1-f_L^U}{f_L^U} L_{42}\left(+\chi + \mathrm{i}\beta(\mu_L-\mu_R)\right), \\
L_{12}(-\xi) &= L_{21}\left(+\xi + \frac{\mathrm{i}}{\epsilon_d}\ln\frac{1-f_D}{f_D}\right) = L_{21}\left(+\xi + \frac{\mathrm{i}}{\epsilon_d}\beta_D(\epsilon_d-\mu_D)\right), \\
L_{34}(-\xi) &= L_{43}\left(+\xi + \frac{\mathrm{i}}{\epsilon_d+U}\ln\frac{1-f_D^U}{f_D^U}\right) = L_{43}\left(+\xi + \frac{\mathrm{i}}{\epsilon_d+U}\beta_D(\epsilon_d+U-\mu_D)\right), \qquad (5.58)
\end{aligned}$$

which can be used to show that the full characteristic polynomial obeys the symmetry

$$\mathcal{D}(-\xi,-\chi) = \mathcal{D}(\xi + \mathrm{i}(\beta_D-\beta)/U, \chi + \mathrm{i}\beta(\mu_L-\mu_R))\,. \qquad (5.59)$$

This symmetry implies – when monitoring the energy current to the demon e_D and the number of electrons transferred to the right junction n_R – for the corresponding probability distribution the

fluctuation theorem

$$\lim_{t\to\infty}\frac{P_{+\Delta n_S,+\Delta e_D}}{P_{-\Delta n_S,-\Delta e_D}} = e^{(\beta_D-\beta)\Delta e_D+\beta(\mu_L-\mu_R)\Delta n_S}\,. \tag{5.60}$$

Instead of determining the continuous energy emission distribution, we could alternatively have counted the discrete number of electrons entering the demon dot at energy ϵ_D and leaving it at energy ϵ_D+U. Since this process leads to a net energy extraction of energy U from the system, the corresponding matter current is tightly coupled to the energy current across the demon junction, i.e., their number would be related to the energy via $\Delta e_D = n_D U$. Comparing the value in the exponent of Eq. (5.60) with the average expectation value of the entropy production in Eq. (5.55), we can also – roughly speaking – interpret the fluctuation theorem as the ratio of probabilities for trajectories with a positive and negative entropy production.

In addition, we identify $P = (\mu_L-\mu_R)I_M^{(R)} = -(\mu_L-\mu_R)I_M^{(L)}$ as the power generated by the device, which – when the current flows against the bias – may yield a negative contribution βP to the overall entropy production. In these parameter regimes however, the negative contribution $\beta(\mu_L-\mu_R)I_M^{(R)}$ must be over-balanced by the second term $(\beta-\beta_D)I_E^{(D)}$, which clearly requires – when the demon reservoir is colder than the SET reservoirs $\beta_D > \beta_S$ – that the energy current flows out of the demon $I_E^{(D)} < 0$. As a whole, the system therefore just converts a thermal gradient between the two subsystems into power: A fraction of the heat coming from the hot SET leads is converted into power, and the remaining fraction is dissipated as heat at the cold demon junction. The corresponding efficiency for this conversion can be constructed from the output power $P = -(\mu_L-\mu_R)I_M^{(L)}$ and the input heat $\dot{Q}_L+\dot{Q}_R = -I_E^{(D)} - (\mu_L-\mu_R)I_M^{(L)} = \dot{Q}_{\rm diss}+P$, where $\dot{Q}_{\rm diss} = -I_E^{(D)}$ is the heat dissipated into the demon reservoir. Using that $\dot{S}_{\rm i}\geq 0$ we find that the efficiency – which of course is only useful in parameter regimes where the power is positive $\beta(\mu_L-\mu_R)I_M^{(R)} > 0$ – is upper-bounded by Carnot efficiency

$$\eta = \frac{P}{\dot{Q}_{\rm diss}+P} \leq 1-\frac{T_D}{T} = \eta_{\rm Carnot}\,. \tag{5.61}$$

For practical applications a large efficiency is not always sufficient. For example, a maximum efficiency at zero power output would be quite useless. Therefore, it has become common standard to first maximize the power output of the device and then compute the corresponding efficiency at maximum power. Due to the nonlinearity of the underlying equations, this may be a difficult numerical optimization problem. To reduce the number of parameters, we assume that $f_D^U = 1-f_D$ (which is the case when $\epsilon_D = \mu_D - U/2$) and $f_L^U = 1-f_R$ as well as $f_R^U = 1-f_L$ (which for $\beta_L=\beta_R=\beta$ is satisfied when $\epsilon_S = 1/2(\mu_L+\mu_R)-U/2$), see also the left panel of Fig. 5.8. Furthermore, we parametrize the modification of the tunneling rates by a single parameter via

$$\begin{aligned}
\Gamma_L &= \Gamma\frac{e^{+\delta}}{\cosh(\delta)}\,, \qquad \Gamma_L^U = \Gamma\frac{e^{-\delta}}{\cosh(\delta)}\\
\Gamma_R &= \Gamma\frac{e^{-\delta}}{\cosh(\delta)}\,, \qquad \Gamma_R^U = \Gamma\frac{e^{+\delta}}{\cosh(\delta)}
\end{aligned} \tag{5.62}$$

to favor transport in a particular direction. We have inserted the normalization by $\cosh(\delta)$ to keep the tunneling rates finite as the feedback strength δ is increased. Trivially, at $\delta=0$ we recover symmetric unperturbed tunneling rates and when $\delta\to\infty$, transport will be completely rectified. The matter current from left to right in the limit where the demon dot is much faster than the

SET ($\Gamma_D \to \infty$ and $\Gamma_D^U \to \infty$) becomes

$$I_M^{(L)} = \frac{\Gamma}{2}\left[f_L - f_R + \tanh(\delta)\,(f_L + f_R - 2f_D)\right] . \tag{5.63}$$

Similarly, we obtain for the energy current to the demon

$$I_E^{(D)} = \frac{\Gamma U}{2}\left[f_L + f_R - 2f_D + (f_L - f_R)\tanh(\delta)\right] , \tag{5.64}$$

which determines the dissipated heat. These can be converted into an efficiency solely expressed by Fermi functions when we use that

$$\begin{aligned} \beta(\mu_L - \mu_R) &= \ln\left(\frac{f_L(1-f_R)}{(1-f_L)f_R}\right) , \\ \beta U &= \ln\left(\frac{f_R(1-f_R^U)}{(1-f_R)f_R^U}\right) \to \ln\left(\frac{f_R f_L}{(1-f_R)(1-f_L)}\right) , \end{aligned} \tag{5.65}$$

which can be used to write the efficiency of heat to power conversion as

$$\eta = \frac{P}{\dot{Q}_{\rm diss} + P} = \frac{1}{1 + \frac{\beta \dot{Q}_{\rm diss}}{\beta P}} = \frac{1}{1 + \frac{\ln\left(\frac{f_R f_L}{(1-f_R)(1-f_L)}\right)(f_L + f_R - 2f_D + (f_L - f_R)\tanh(\delta))}{\ln\left(\frac{f_L(1-f_R)}{(1-f_L)f_R}\right)(f_L - f_R + (f_L + f_R - 2f_D)\tanh(\delta))}} , \tag{5.66}$$

which is also illustrated in Fig. 5.8.

Beyond these average considerations, the qualitative action of the device may also be understood at the level of single trajectories, see Fig. 5.9. It should be noted that at the trajectory level, all possible trajectories are still allowed, even though ones with positive total entropy production must on average dominate. As a whole, the system thereby merely converts a temperature gradient (cold demon, hot system) into useful power (current times voltage).

5.4.1 Local View: A Feedback-Controlled Device

An experimentalist having access only to the SET circuit would measure a positive generated power, conserved particle currents $I_M^{(L)} + I_M^{(R)} = 0$, but possibly a slight mismatch of left and right energy currents $I_E^{(L)} + I_E^{(R)} = -I_E^{(D)} \neq 0$. This mismatch could not fully account for the generated power, since for any efficiency $\eta > 1/2$ in Fig. 5.9 we have $\left|I_E^{(D)}\right| < P$. Therefore, the experimentalist would conclude that his description of the system by energy and matter flows is not complete and he might suspect Maxwell's demon at work. Here, we will make the reduced dynamics of the SET dot alone more explicit by deriving a reduced rate equation.

We can evidently write the rate equation defined by Eqs. (5.53) as $\dot{P}_{\rho\sigma} = \mathcal{L}_{\rho\sigma,\rho'\sigma'} P_{\rho'\sigma'}$, where ρ and σ label the demon and system degrees of freedom, respectively. If we discard the dynamics of the demon dot by tracing over its degrees of freedom $P_\sigma = \sum_\rho P_{\rho\sigma}$, we formally arrive at a non-Markovian evolution equation for the populations of the SET dot.

$$\dot{P}_\sigma = \sum_{\sigma'} \sum_{\rho\rho'} \mathcal{L}_{\rho\sigma,\rho'\sigma'} P_{\rho'\sigma'} = \sum_{\sigma'} \left[\sum_{\rho\rho'} \mathcal{L}_{\rho\sigma,\rho'\sigma'} \frac{P_{\rho'\sigma'}}{P_{\sigma'}}\right] P_{\sigma'} . \tag{5.67}$$

Here, we may identify $\frac{P_{\rho'\sigma'}}{P_{\sigma'}}$ as the conditional probability of the demon being in state ρ' provided the system is in state σ'.

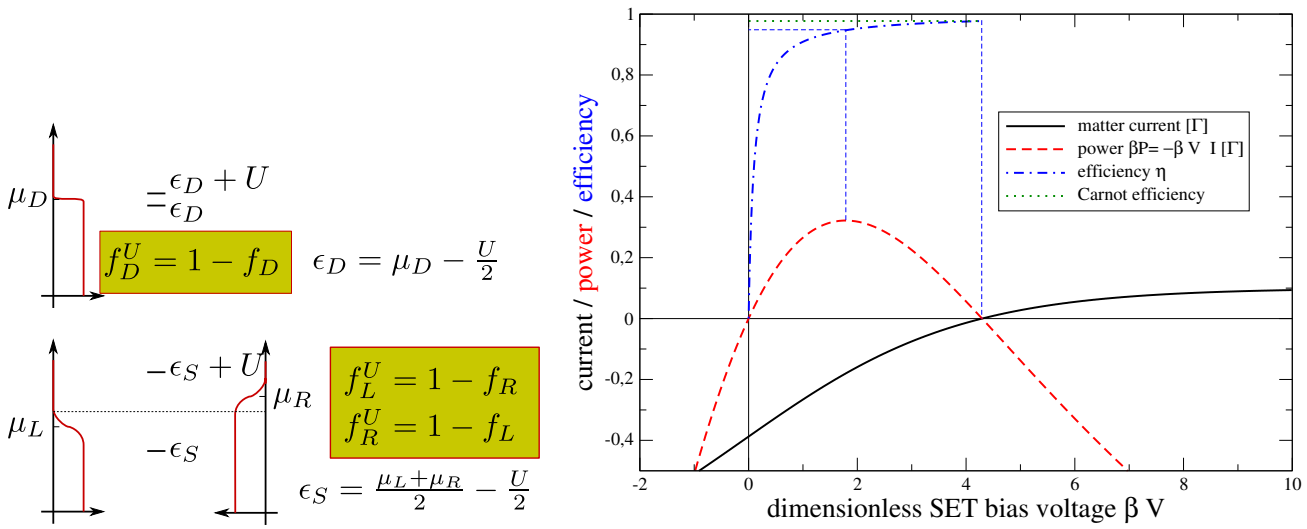

Figure 5.8:
Left: Sketch of the assumed configurations of chemical potentials, which imply at $\beta_L = \beta_R$ relations between the Fermi functions.
Right: Plot of current (solid black, in units of Γ), dimensionless power $\beta V I$ (dashed red, in units of Γ), and efficiency η (dash-dotted blue) versus dimensionless bias voltage. At equilibrated bias (origin), the efficiency vanishes by construction, whereas it reaches Carnot efficiency (dotted green) at the new equilibrium, i.e., at zero power. At maximum power however, the efficiency still closely approaches the Carnot efficiency. Parameters: $\delta = 100$, tunneling rates parametrized as in Eq. (5.62), $f_D = 0.9 = 1 - f_D^U$, $\beta\epsilon_S = -0.05 = -\beta(\epsilon_S + U)$, such that the Carnot efficiency becomes $\eta_{\text{Carnot}} = 1 - (\beta U)/(\beta_D U) \approx 0.977244$.

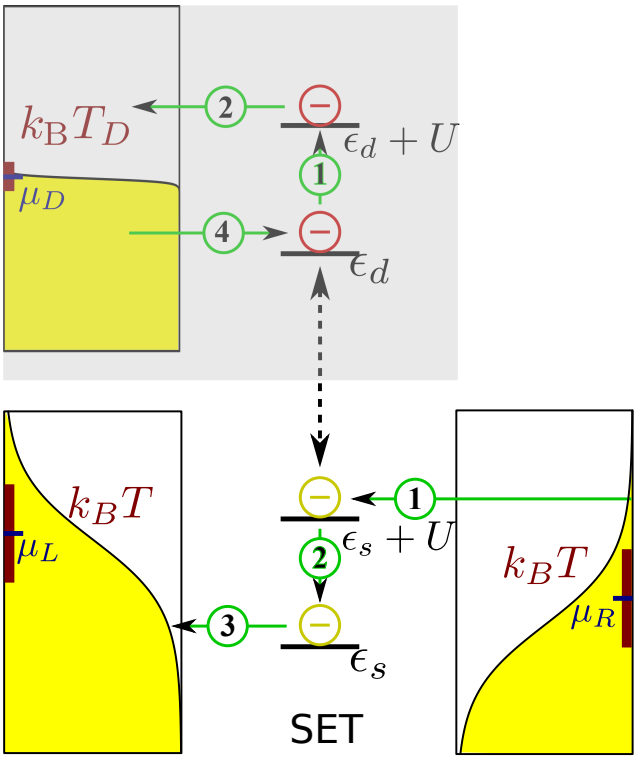

Figure 5.9: Level sketch of the setup. Shaded regions represent occupied levels in the leads with chemical potentials and temperatures indicated. Central horizontal lines represent transition energies of system and demon dot, respectively. When the other dot is occupied, the bare transition frequency of every system is shifted by the Coulomb interaction U. The shown trajectory then becomes likely in the suggested Maxwell-demon mode: Initially, the SET is empty and the demon dot is filled. When $\Gamma_R^U \gg \Gamma_L^U$, the SET dot is most likely first filled from the left lead, which shifts the transition frequency of the demon (1). When the bare tunneling rates of the demon are much larger than that of the SET, the demon dot will rapidly equilibrate by expelling the electron to its associated reservoir (2) before a further electronic jump at the SET may occur. At the new transition frequency, the SET electron is more likely to escape first to the left than to the right when $\Gamma_L \gg \Gamma_R$ (3). Now, the demon dot will equilibrate again by filling with an electron (4) thus restoring the initial state. In essence, an electron is transferred against the bias through the SET circuit while in the demon system an electron enters at energy ϵ_d and leaves at energy $\epsilon_d + U$ leading to a net transfer of U from the demon into its reservoir.

However, direct inspection of the rates suggests that when we assume the limit where the bare rates of the demon system are much larger than the SET tunneling rates, these conditional probabilities will assume their conditioned stationary values much faster than the SET dynamics. In this limit, the dynamics is mainly dominated by transitions between just two mesostates instead of the original four states. These mesostates are associated to either a filled or an empty system quantum dot, respectively. We may hence arrive again at a Markovian description by approximating

$$\frac{P_{\rho'\sigma'}}{P_{\sigma'}} \to \frac{\bar{P}_{\rho'\sigma'}}{\bar{P}_{\sigma'}}\,, \tag{5.68}$$

which yields the coarse-grained rate matrix

$$\mathcal{W}_{\sigma\sigma'} = \sum_{\rho\rho'} \mathcal{L}_{\rho\sigma,\rho'\sigma'} \frac{\bar{P}_{\rho'\sigma'}}{\bar{P}_{\sigma'}}\,. \tag{5.69}$$

For the model at hand, the stationary conditional probabilities become in the limit where $\Gamma_D^{(U)} \gg \Gamma_{L/R}^{(U)}$

$$\begin{aligned} P_{0|E} &= \frac{\bar{P}_{0E}}{\bar{P}_E} = 1 - f_D\,, \qquad P_{1|E} = \frac{\bar{P}_{1E}}{\bar{P}_E} = f_D\,, \\ P_{0|F} &= \frac{\bar{P}_{0F}}{\bar{P}_F} = 1 - f_D^U\,, \qquad P_{1|F} = \frac{\bar{P}_{1F}}{\bar{P}_F} = f_D^U\,, \end{aligned} \tag{5.70}$$

and just describe the fact that – due to the time-scale separation – the demon dot immediately reaches a thermal stationary state that depends on the occupation of the SET dot. The temperature and chemical potential of the demon reservoir determine if and how well the demon dot – which can be envisaged as the demon's memory capable of storing just one bit – captures the actual state of the system dot. For example, for high demon temperatures it will be roughly independent on the system dots occupation as $f_D \approx f_D^U \approx 1/2$. At very low demon temperatures however, and if the chemical potential of the demon dot is adjusted such that $\epsilon_d - \mu_D < 0$ and $\epsilon_d + U - \mu_D > 0$, the demon dot will nearly accurately (more formally when $\beta_D U \gg 1$) track the system occupation, since $f_D \to 1$ and $f_D^U \to 0$. Then, the demon dot will immediately fill when the SET dot is emptied and its electron will leave when the SET dot is filled. It thereby faithfully detects the state of the SET. In the presented model, the demon temperature thereby acts as a source of error in the demon's measurement of the system's state. In addition, the model at hand allows to investigate the detector backaction on the probed system, which is often neglected. Here, this backaction is essential, and we will now investigate it by analyzing the reduced dynamics in detail.

The coarse-grained probabilities P_E and P_F of finding the SET dot empty or filled, respectively, obey the rate equation dynamics

$$\mathcal{L} = \begin{pmatrix} -L_{FE} & +L_{EF} \\ +L_{FE} & -L_{EF} \end{pmatrix} \tag{5.71}$$

with the coarse-grained rates

$$\begin{aligned} L_{EF} &= L_{0E,0F}\frac{\bar{P}_{0F}}{\bar{P}_F} + L_{1E,1F}\frac{\bar{P}_{1F}}{\bar{P}_F} \\ &= (1-f_D^U)\left[\Gamma_L(1-f_L) + \Gamma_R(1-f_R)\right] + f_D^U\left[\Gamma_L^U(1-f_L^U) + \Gamma_R^U(1-f_R^U)\right]\,, \\ L_{FE} &= L_{0F,0E}\frac{\bar{P}_{0E}}{\bar{P}_E} + L_{1F,1E}\frac{\bar{P}_{1E}}{\bar{P}_E} \\ &= (1-f_D)\left[\Gamma_L f_L + \Gamma_R f_R\right] + f_D\left[\Gamma_L^U f_L^U + \Gamma_R^U f_R^U\right]\,. \end{aligned} \tag{5.72}$$

We note that a naive experimenter – not aware of the demon interacting with the SET circuit – would attribute the rates in the coarse-grained dynamics to just two reservoirs: $\mathcal{L} = \mathcal{L}_L + \mathcal{L}_R$ with the rates $\mathcal{L}^{(\alpha)}_{EF} = (1 - f^U_D)\Gamma_\alpha(1 - f_\alpha) + f^U_D\Gamma^U_\alpha(1 - f^U_\alpha)$ and $\mathcal{L}^{(\alpha)}_{FE} = (1 - f_D)\Gamma_\alpha f_\alpha + f_D\Gamma^U_\alpha f^U_\alpha$. Thus, when the SET is not sensitive to the demon state $\Gamma^U_{L/R} \approx \Gamma_{L/R}$ and $f^U_{L/R} \approx f_{L/R}$, local detailed balance is restored, and we recover the conventional SET rate equation.

We note that the matter current

$$I^{(\nu)}_M = L^{(\nu)}_{EF}\bar{P}_F - \mathcal{L}^{(\nu)}_{FE}\bar{P}_E \tag{5.73}$$

is conserved $I^{(L)}_M = -I^{(R)}_M$, such that the entropy production becomes

$$\begin{aligned}
\dot{S}_\mathrm{i} &= \sum_{\nu\in\{L,R\}} L^{(\nu)}_{EF}\bar{P}_F \ln\left(\frac{\mathcal{L}^{(\nu)}_{EF}\bar{P}_F}{\mathcal{L}^{(\nu)}_{FE}\bar{P}_E}\right) + \mathcal{L}^{(\nu)}_{FE}\bar{P}_E \ln\left(\frac{\mathcal{L}^{(\nu)}_{FE}\bar{P}_E}{\mathcal{L}^{(\nu)}_{EF}\bar{P}_F}\right) \\
&= \sum_{\nu\in\{L,R\}} \left(L^{(\nu)}_{EF}\bar{P}_F - \mathcal{L}^{(\nu)}_{FE}\bar{P}_E\right) \ln\left(\frac{\mathcal{L}^{(\nu)}_{EF}\bar{P}_F}{\mathcal{L}^{(\nu)}_{FE}\bar{P}_E}\right) \\
&= I^{(L)}_M \ln\left(\frac{\mathcal{L}^{(L)}_{EF}\mathcal{L}^{(R)}_{FE}}{\mathcal{L}^{(L)}_{FE}\mathcal{L}^{(R)}_{EF}}\right) = I^{(L)}_M \mathcal{A}\,,
\end{aligned} \tag{5.74}$$

and is thus representable in a simple flux-affinity form. Similarly, we note that if we would count particle transfers from the left to the right reservoir, the following fluctuation theorem would hold

$$\frac{P_{+n}}{P_{-n}} = e^{n\mathcal{A}}\,, \tag{5.75}$$

and the fact that these fluctuations could in principle be resolved demonstrates that the affinity in the entropy production is a meaningful and measurable quantity. Without the demon dot, the conventional affinity of the SET would simply be given by

$$\mathcal{A}_0 = \ln\left(\frac{(1 - f_L)f_R}{f_L(1 - f_R)}\right) = \beta_L(\epsilon - \mu_L) - \beta_R(\epsilon - \mu_R)\,, \tag{5.76}$$

and ignoring the physical implementation of the demon, we can interpret the modification of the entropy production due to the demon as an additional information current that is tightly coupled to the particle current

$$\dot{S}_\mathrm{i} = I^{(L)}_M\mathcal{A}_0 + I^{(L)}_M(\mathcal{A} - \mathcal{A}_0) = \dot{S}^{(0)}_\mathrm{i} + \mathcal{I}\,. \tag{5.77}$$

When the demon temperature is lowered such that $\beta_D U \gg 1$ and its chemical potential is adjusted such that $f_D \to 1$ and $f^U_D \to 0$, the affinity becomes

$$\mathcal{A} = \ln\left(\frac{\Gamma_L(1 - f_L)\Gamma^U_R f^U_R}{\Gamma^U_L f^U_L \Gamma_R(1 - f_R)}\right) = \ln\left(\frac{\Gamma_L\Gamma^U_R}{\Gamma^U_L\Gamma_R}\right) + \ln\left(\frac{f_L f^U_R}{f^U_L f_R}\right) + \mathcal{A}_0\,. \tag{5.78}$$

The last term on the right-hand side is simply the affinity without the demon dot. The first two terms quantify the modification of the affinity. The pure limit of a Maxwell demon is reached, when the energetic backaction of the demon on the SET is negligible, i.e., when $f^U_L \approx f_L$ and $f^U_R \approx f_R$, which requires comparably large SET temperatures $\beta_{L/R}U \ll 1$. Of course, to obtain any nontrivial effect, it is still necessary to keep non-flat tunneling rates $\Gamma^U_{L/R} \neq \Gamma_{L/R}$, and in this case one recovers the case discussed in the previous section – identifying Γ^E_α with Γ_α and Γ^F_α with Γ^U_α.

5.5 Qubit stabilization

Qubits – any quantum-mechanical two-level system that can be prepared in a superposition of its two states $|0\rangle$ and $|1\rangle$ – are at the heart of quantum computers with great technological promises. The major obstacle to be overcome to build a quantum computer is decoherence: Qubits prepared in pure superposition states (as required for performing quantum computation) tend to decay into a statistical mixture when coupled to a destabilizing reservoir (of which there is an abundance in the real world). Here, we will approach the decoherence with a quantum master equation and use feedback control to act against the decay of coherences.

The system is described by

$$\begin{aligned} \mathcal{H}_{\rm S} &= \frac{\Omega}{2}\sigma^z\,, \qquad \mathcal{H}_{\rm B}^1 = \sum_k \omega_k^1 (b_k^1)^\dagger b_k^1\,, \qquad \mathcal{H}_{\rm B}^2 = \sum_k \omega_k^2 (b_k^2)^\dagger b_k^2 \\ \mathcal{H}_{\rm I}^1 &= \sigma^z \otimes \sum_k \left[h_k^1 b_k^1 + (h_k^1)^* (b_k^1)^\dagger\right]\,, \qquad \mathcal{H}_{\rm I}^2 = \sigma^x \otimes \sum_k \left[h_k^2 b_k^2 + (h_k^2)^* (b_k^2)^\dagger\right]\,, \end{aligned} \tag{5.79}$$

where σ^α represent the Pauli matrices and b_k bosonic annihilation operators. We assume that the two bosonic baths are independent, such that we can calculate the dissipators separately. We have already calculated the Fourier-transform of the bath correlation function for such coupling operators. When we analytically continue the spectral coupling density to negative frequencies as $J(-\omega) = -J(+\omega)$, it can also be written as

$$\gamma(\omega) = J(\omega)\left[1 + n(\omega)\right]\,. \tag{5.80}$$

Since it obeys the KMS condition we may expect thermalization of the qubits density matrix with the bath temperature. Note that due to the divergence of $n(\omega)$ at $\omega \to 0$, it is favorable to use an Ohmic spectral density such as e.g.

$$J(\omega) = J_0 \omega e^{-\omega/\omega_c}\,, \tag{5.81}$$

which grants an existing limit $\gamma(0)$. For the two interaction Hamiltonians chosen, we can make the corresponding coefficients explicit

coefficient	A: pure dephasing $A = \sigma^z$	B: dissipation $A = \sigma^x$
$\gamma_{00,00}$	$+\gamma(0)$	0
$\gamma_{00,11}$	$-\gamma(0)$	0
$\gamma_{11,00}$	$-\gamma(0)$	0
$\gamma_{11,11}$	$+\gamma(0)$	0
$\gamma_{01,01}$	0	$\gamma(+\Omega)$
$\gamma_{10,10}$	0	$\gamma(-\Omega)$
σ_{00}	$\frac{\sigma(0)}{2\mathrm{i}}$	$\frac{\sigma(-\Omega)}{2\mathrm{i}}$
σ_{11}	$\frac{\sigma(0)}{2\mathrm{i}}$	$\frac{\sigma(+\Omega)}{2\mathrm{i}}$

and rewrite the corresponding Liouvillian in the ordering $\rho_{00}, \rho_{11}, \rho_{01}, \rho_{10}$ as a superoperator (fur-

ther abbreviating $\gamma_{0/\pm} = \gamma(0/\pm\Omega)$, $\Sigma = \sigma_{00} - \sigma_{11}$)

$$\begin{aligned}
\mathcal{L}_A &= \begin{pmatrix} 0 & 0 & 0 & 0 \\ 0 & 0 & 0 & 0 \\ 0 & 0 & -2\gamma_0 - \mathrm{i}\Omega & 0 \\ 0 & 0 & 0 & -2\gamma_0 + \mathrm{i}\Omega \end{pmatrix} \\
\mathcal{L}_B &= \begin{pmatrix} -\gamma_- & +\gamma_+ & 0 & 0 \\ +\gamma_- & -\gamma_+ & 0 & 0 \\ 0 & 0 & -\frac{\gamma_- + \gamma_+}{2} - \mathrm{i}(\Omega + \Sigma) & 0 \\ 0 & 0 & 0 & -\frac{\gamma_- + \gamma_+}{2} + \mathrm{i}(\Omega + \Sigma) \end{pmatrix} .
\end{aligned} \tag{5.82}$$

Both Liouvillians lead to a decay of coherences with a rate (we assume $\Omega > 0$)

$$\begin{aligned}
\gamma_A &= 2\gamma_0 = 2 \lim_{\omega \to 0} J(\omega)\,[1 + n(\omega)] = 2\frac{J_0}{\beta} = 2J_0 k_\mathrm{B} T\,, \\
\gamma_B &= \frac{\gamma_- + \gamma_+}{2} = \frac{1}{2}\left[J(\Omega)[1 + n(\Omega)] + J(-\Omega)[1 + n(-\Omega)]\right] = \frac{1}{2}\left[J(\Omega)[1 + n(\Omega)] + J(\Omega) n(\Omega)\right] \\
&= \frac{1}{2} J(\Omega) \coth\left[\frac{\Omega}{2k_\mathrm{B}T}\right] ,
\end{aligned} \tag{5.83}$$

which both scale proportional to T for large bath temperatures. Therefore, the application of either Liouvillian or a superposition of both will in the high-temperature limit simply lead to rapid decoherence. The same can be expected from a turnstyle (open-loop control), where the Liouvillians act one at a time following a pre-defined protocol.

The situation changes however, when measurement results are used to determine which Liouvillian is acting. We choose to act with Liouvillian $\mathcal{L}_A$ throughout and to turn on Liouvillian $\mathcal{L}_B$ in addition – multiplied by a dimensionless feedback parameter $\alpha \geq 0$ – when a certain measurement result is obtained. Given a measurement with just two outcomes, the effective propagator is then given by

$$\mathcal{W}(\Delta t) = e^{\mathcal{L}_A \Delta t} \mathcal{M}_1 + e^{(\mathcal{L}_A + \alpha \mathcal{L}_B)\Delta t} \mathcal{M}_2\,, \tag{5.84}$$

where $\mathcal{M}_i$ are the superoperators corresponding to the action of the measurement operators $M_i \rho M_i^\dagger$ on the density matrix. First, to obtain any nontrivial effect (coupling between coherences and populations), the measurement superoperators should not have the same block structure as the Liouvillians. Therefore, we consider a projective measurement of the σ^x expectation value

$$M_1 = \frac{1}{2}\left[\mathbf{1} + \sigma^x\right] , \qquad M_2 = \frac{1}{2}\left[\mathbf{1} - \sigma^x\right] . \tag{5.85}$$

These projection operators obviously fulfil the completeness relation $M_1^\dagger M_1 + M_2^\dagger M_2 = \mathbf{1}$. The superoperators corresponding to $M_i \rho M_i^\dagger$ are also orthogonal projectors

$$\mathcal{M}_1 = \frac{1}{4}\begin{pmatrix} 1 & 1 & 1 & 1 \\ 1 & 1 & 1 & 1 \\ 1 & 1 & 1 & 1 \\ 1 & 1 & 1 & 1 \end{pmatrix} , \qquad \mathcal{M}_2 = \frac{1}{4}\begin{pmatrix} 1 & 1 & -1 & -1 \\ 1 & 1 & -1 & -1 \\ -1 & -1 & 1 & 1 \\ -1 & -1 & 1 & 1 \end{pmatrix} . \tag{5.86}$$

Exercise 47 (Measurement superoperators) *(1 points)*
Show the correspondence between M_i and $\mathcal{M}_i$ in the above equations.

However, they are not complete in this higher-dimensional space $\mathcal{M}_1 + \mathcal{M}_2 \neq \mathbf{1}$. Since the measurement superoperators do not have the same block structure as the Liouvillians, we cannot expect a simple rate equation description to hold anymore.

Without feedback ($\alpha = 0$), it is easy to see that the measurements still have an effect in contrast to an evolution without measurements

$$\frac{1}{2}\begin{pmatrix} 1 & 1 & 0 & 0 \\ 1 & 1 & 0 & 0 \\ 0 & 0 & e^{-(2\gamma_0+\mathrm{i}\Omega)\Delta t} & e^{-(2\gamma_0+\mathrm{i}\Omega)\Delta t} \\ 0 & 0 & e^{-(2\gamma_0-\mathrm{i}\Omega)\Delta t} & e^{-(2\gamma_0-\mathrm{i}\Omega)\Delta t} \end{pmatrix} = e^{\mathcal{L}_A \Delta t}\left(\mathcal{M}_1 + \mathcal{M}_2\right) \neq$$

$$e^{\mathcal{L}_A \Delta t} = \begin{pmatrix} 1 & 0 & 0 & 0 \\ 0 & 1 & 0 & 0 \\ 0 & 0 & e^{-(2\gamma_0+\mathrm{i}\Omega)\Delta t} & 0 \\ 0 & 0 & 0 & e^{-(2\gamma_0-\mathrm{i}\Omega)\Delta t} \end{pmatrix}. \tag{5.87}$$

This may have significant consequences – even without dissipation ($\gamma_0 = 0$) and without feedback ($\alpha = 0$): The repeated application of the propagator for measurement without feedback ($\gamma_0 = 0$ and $\alpha = 0$) yields

$$\left[e^{\mathcal{L}_A \Delta t}\left(\mathcal{M}_1 + \mathcal{M}_2\right)\right]^n = \frac{1}{2}\begin{pmatrix} 1 & 1 & 0 & 0 \\ 1 & 1 & 0 & 0 \\ 0 & 0 & e^{-\mathrm{i}\Omega\Delta t}\cos^{n-1}(\Omega\Delta t) & e^{-\mathrm{i}\Omega\Delta t}\cos^{n-1}(\Omega\Delta t) \\ 0 & 0 & e^{+\mathrm{i}\Omega\Delta t}\cos^{n-1}(\Omega\Delta t) & e^{+\mathrm{i}\Omega\Delta t}\cos^{n-1}(\Omega\Delta t) \end{pmatrix}. \tag{5.88}$$

Exercise 48 (Repeated measurements) *(1 points)*
Show the validity of the above equation.

In contrast, without the measurements we have for repeated application of the propagator simply

$$\left[e^{\mathcal{L}_A \Delta t}\right]^n = e^{\mathcal{L}_A n \Delta t}. \tag{5.89}$$

When we now consider the limit $n \to \infty$ and $\Delta t \to 0$ but $n\Delta t = t$ remaining finite, it becomes obvious that the no-measurement propagator for $\gamma_0 = 0$ simply describes coherent evolution. In contrast, when the measurement frequency becomes large enough, the measurement propagator in Eq. (5.87) approaches

$$\left[e^{\mathcal{L}_A \Delta t}\left(\mathcal{M}_1 + \mathcal{M}_2\right)\right]^n = \frac{1}{2}\begin{pmatrix} 1 & 1 & 0 & 0 \\ 1 & 1 & 0 & 0 \\ 0 & 0 & 1 & 1 \\ 0 & 0 & 1 & 1 \end{pmatrix} \tag{5.90}$$

and thereby freezes the eigenstates of the measurement superoperators, e.g. $\bar{\rho} = \frac{1}{2}\left[|0\rangle + |1\rangle\right]\left[\langle 0| + \langle 1|\right]$. This effect is known as Quantum-Zeno effect (a watched pot never boils) and occurs when measurement operators and system Hamiltonian do not commute and the evolution between measurements is unitary (here $\gamma_0 = 0$). When the evolution between measurements is an open one ($\gamma_0 > 0$), the Quantum-Zeno effect cannot be used to stabilize the coherences, which becomes evident from the propagator in Eq. (5.87).

With feedback ($\alpha > 0$) however, the effective propagator $\mathcal{W}(\Delta t)$ does not have the Block structure anymore. It can be used to obtain a fixed-point iteration for the density matrix

$$\rho(t + \Delta t) = \mathcal{W}(\Delta t)\rho(t)\,. \tag{5.91}$$

Here, we cannot even for small Δt approximate the evolution by another effective Liouvillian, since $\lim_{\Delta t \to 0} \mathcal{W}(\Delta t) \neq \mathbf{1}$. Instead, one can analyze the eigenvector of $\mathcal{W}(\Delta t)$ with eigenvalue 1 as the (in a stroboscopic sense) stationary state. It is more convenient however to consider the expectation values of $\langle \sigma^i \rangle_t$ that fully characterize the density matrix via

$$\rho_{00} = \frac{1 + \langle \sigma^z \rangle}{2}\,, \qquad \rho_{11} = \frac{1 - \langle \sigma^z \rangle}{2}\,, \qquad \rho_{01} = \frac{\langle \sigma^x \rangle - \mathrm{i}\,\langle \sigma^y \rangle}{2}\,, \qquad \rho_{10} = \frac{\langle \sigma^x \rangle + \mathrm{i}\,\langle \sigma^y \rangle}{2}\,. \tag{5.92}$$

Note that decoherence therefore implies vanishing expectation values of $\langle \sigma^x \rangle \to 0$ and $\langle \sigma^y \rangle \to 0$ in our setup. Converting the iteration equation for the density matrix into an iteration equation for the expectation values of Pauli matrices we obtain

$$\begin{aligned}
\langle \sigma^x \rangle_{t+\Delta t} &= \frac{e^{-2\gamma_0 \Delta t}}{2}\left\{(1 + \langle \sigma^x \rangle_t)\cos(\Omega \Delta t) - (1 - \langle \sigma^x \rangle_t)\, e^{-(\gamma_- + \gamma_+)\alpha \Delta t/2} \cos\left[(\Omega + \alpha(\Omega + \Sigma))\,\Delta t\right]\right\} \\
\langle \sigma^y \rangle_{t+\Delta t} &= \frac{e^{-2\gamma_0 \Delta t}}{2}\left\{(1 + \langle \sigma^x \rangle_t)\sin(\Omega \Delta t) - (1 - \langle \sigma^x \rangle_t)\, e^{-(\gamma_- + \gamma_+)\alpha \Delta t/2} \sin\left[(\Omega + \alpha(\Omega + \Sigma))\,\Delta t\right]\right\} \\
\langle \sigma^z \rangle_{t+\Delta t} &= \frac{(\gamma_+ - \gamma_-)\,(1 - \langle \sigma^x \rangle_t)}{2(\gamma_- + \gamma_+)}\left(1 - e^{-(\gamma_- + \gamma_+)\alpha \Delta t}\right)\,,
\end{aligned} \tag{5.93}$$

which (surprisingly) follow just the expectation values $\langle \sigma^x \rangle_t$ on the r.h.s. The first of the above equations can be expanded for small Δt to yield

$$\frac{\langle \sigma^x \rangle_{t+\Delta t} - \langle \sigma^x \rangle_t}{\Delta t} = -\frac{1}{4}\left[8\gamma_0 + \alpha\,(\gamma_- + \gamma_+)\right]\langle \sigma^x \rangle_t + \frac{1}{4}\alpha\,(\gamma_- + \gamma_+) + \mathcal{O}\{\Delta t\}\,. \tag{5.94}$$

When $\Delta t \to 0$, this becomes a differential equation with the stationary state

$$\langle \bar{\sigma}^x \rangle = \frac{\alpha(\gamma_- + \gamma_+)}{8\gamma_0 + \alpha(\gamma_- + \gamma_+)}\,, \tag{5.95}$$

which approaches 1 for large values of α. Taking into account the large-temperature expansions for the dampening coefficients

$$\gamma_0 = J_0 k_\mathrm{B} T\,, \qquad \gamma_- + \gamma_+ \approx 2J_0 e^{-\Omega/\omega_c} k_\mathrm{B} T\,, \tag{5.96}$$

we see that this stabilization effect also holds at large temperatures – a sufficiently strong (and perfect) feedback provided. An initially coherent superposition is thus not only stabilized, but also emerges when the scheme is initialized in a completely mixed state. Also for finite Δt, the fixed-point iteration yields sensible evolution for the expectation values of the Pauli matrices, see Fig. 5.10.

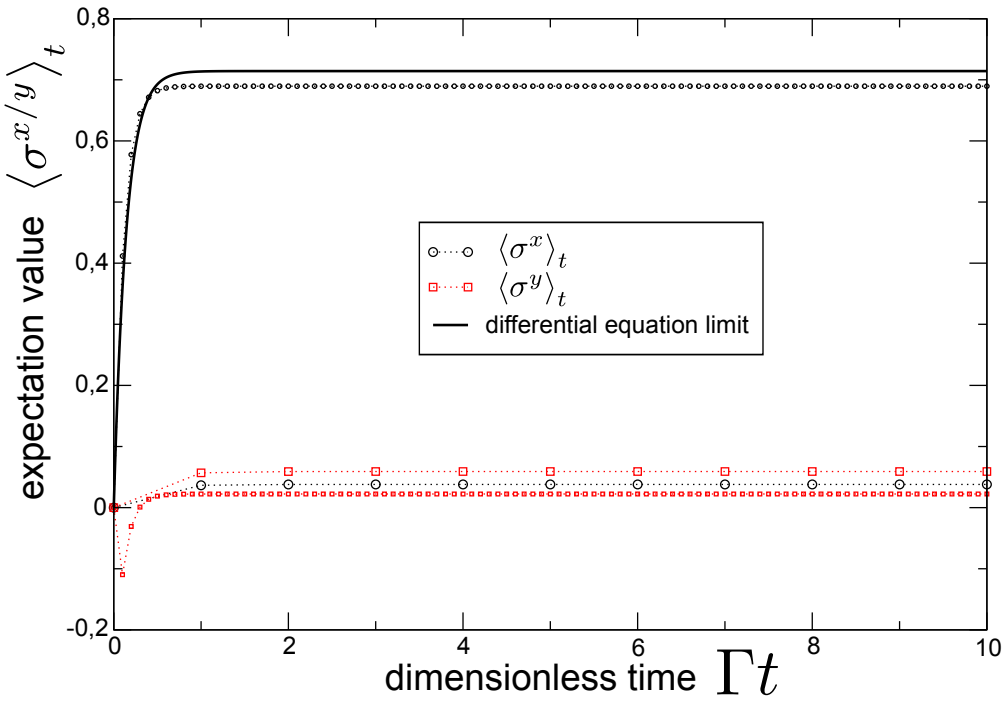

Figure 5.10: Expectation values of the Pauli matrices for finite feedback strength $\alpha = 10$ and finite stepsize Δt (spacing given by symbols). For large Δt, the fixed point is nearly completely mixed. For small Δt, the curve for $\langle \sigma^x \rangle_t$ approaches the differential equation limit (solid line), but the curve for $\langle \sigma^y \rangle_t$ approaches 0. For $\gamma_- = \gamma_+$, the iteration for $\langle \sigma^z \rangle_t$ vanishes throughout. Parameters: $\gamma_- = \gamma_+ = \gamma_0 = \Gamma$, $\Omega \Delta t = \in \{1, 0.1\}$, and $\Sigma \Delta t \in \{0.5, 0.05\}$.

5.6 Relaxation Dynamics

So far, control has only affected the interaction (e.g. tunneling rates) or the system (projective measurements or time-dependent system parameters). A direct change of the reservoir parameters would normally be hard to describe (and to achieve experimentally), since here fast changes would usually drive the reservoir out of equilibrium. A third possibility that is usually not explored is to force the reservoirs into a maximum entropy state subject to the side constraint of varying energy and matter content. In our master equation, this would simply mean that the reservoir inverse temperature β_α and chemical potential μ_α are allowed to be time-dependent and are consistently calculated from the energy and matter currents between system and reservoir α.

For a thermal reservoir state, the total particle number in the reservoir α is represented as

$$N_\alpha = \sum_k \left\langle c_{k\alpha}^\dagger c_{k\alpha} \right\rangle = \sum_k f(\omega_{k\alpha}) = \int \mathcal{D}_\alpha(\omega) f_\alpha(\omega) d\omega \,, \tag{5.97}$$

where $f_\alpha(\omega)$ (depending implicitly on inverse temperature β_α and chemical potential μ_α) can be a Fermi or Bose distribution – depending on the type of the reservoir. Furthermore, $\mathcal{D}_\alpha(\omega) = \sum_k \delta(\omega - \omega_{k\alpha})$ is the spectral density of the reservoir. In an analogous fashion we can obtain the energy contained in the reservoir

$$E_\alpha = \int \mathcal{D}_\alpha(\omega) \omega f_\alpha(\omega) d\omega \,. \tag{5.98}$$

Total conservation of charge and energy implies that given charge and energy currents into the reservoir

$$\begin{aligned}\dot{N}_\alpha &= -I_M^{(\alpha)} = \frac{\partial N_\alpha}{\partial \mu_\alpha}\dot{\mu}_\alpha + \frac{\partial N_\alpha}{\partial \beta_\alpha}\frac{d\beta_\alpha}{dT_\alpha}\dot{T}_\alpha\,,\\ \dot{E}_\alpha &= -I_E^{(\alpha)} = \frac{\partial E_\alpha}{\partial \mu_\alpha}\dot{\mu}_\alpha + \frac{\partial E_\alpha}{\partial \beta_\alpha}\frac{d\beta_\alpha}{dT_\alpha}\dot{T}_\alpha\end{aligned} \tag{5.99}$$

one can calculate the change of reservoir charge and energy. Here however, we will be interested in the change of reservoir temperature and chemical potential, for which we can obtain a differential equation by solving the above equations for $\dot{\mu}_\alpha$ and $\dot{T}_\alpha$. For example, in case of fermions, we can first solve for

$$\begin{aligned}\frac{\partial N_\alpha}{\partial \mu_\alpha} &= \int \mathcal{D}_\alpha(\omega) f_\alpha(\omega)[1-f_\alpha(\omega)]d\omega\beta_\alpha = \mathcal{I}_1\beta_\alpha\,,\\ \frac{\partial N_\alpha}{\partial \beta_\alpha} &= -\int \mathcal{D}_\alpha(\omega) f_\alpha(\omega)[1-f_\alpha(\omega)](\omega-\mu_\alpha)d\omega = -\mathcal{I}_2\,,\\ \frac{\partial E_\alpha}{\partial \mu_\alpha} &= \int \mathcal{D}_\alpha(\omega)\omega f_\alpha(\omega)[1-f_\alpha(\omega)]d\omega\beta_\alpha = (\mathcal{I}_2+\mu_\alpha\mathcal{I}_1)\beta_\alpha\,,\\ \frac{\partial E_\alpha}{\partial \beta_\alpha} &= -\int \mathcal{D}_\alpha(\omega)\omega f_\alpha(\omega)[1-f_\alpha(\omega)](\omega-\mu_\alpha)d\omega = -\mathcal{I}_3-\mu_\alpha\mathcal{I}_2\,.\end{aligned} \tag{5.100}$$

Here, we have defined three integrals

$$\begin{aligned}\mathcal{I}_1 &= \int \mathcal{D}_\alpha(\omega) f(\omega)[1-f_\alpha(\omega)]d\omega\,, \qquad \mathcal{I}_2 = \int \mathcal{D}_\alpha(\omega)(\omega-\mu_\alpha) f_\alpha(\omega)[1-f_\alpha(\omega)]d\omega\,,\\ \mathcal{I}_3 &= \int \mathcal{D}_\alpha(\omega)(\omega-\mu_\alpha)^2 f_\alpha(\omega)[1-f_\alpha(\omega)]d\omega\,,\end{aligned} \tag{5.101}$$

which in the wide-band limit $\mathcal{D}_\alpha(\omega) = D_\alpha$ can be solved exactly

$$\mathcal{I}_1 = \frac{D_\alpha}{\beta_\alpha} = D_\alpha T_\alpha\,, \qquad \mathcal{I}_2 = 0\,, \qquad \mathcal{I}_3 = \frac{\pi^2}{3}\frac{D_\alpha}{\beta_\alpha^3} = \frac{\pi^2}{3}D_\alpha T_\alpha^3\,. \tag{5.102}$$

Exercise 49 (Fermi integrals) *Show validity of Eq. (5.102). You might want to use that*

$$\int_0^\infty \frac{\ln^2(x)}{(x+1)^2} = \frac{\pi^2}{3}\,. \tag{5.103}$$

From these, we obtain a simple relation between currents and thermodynamic parameters

$$\begin{pmatrix} -I_M^{(\alpha)} \\ -I_E^{(\alpha)} \end{pmatrix} = D_\alpha \begin{pmatrix} 1 & 0 \\ \mu & \frac{\pi^2}{3}T_\alpha \end{pmatrix} \begin{pmatrix} \dot{\mu}_\alpha \\ \dot{T}_\alpha \end{pmatrix}\,. \tag{5.104}$$

We can directly invert the matrix containing the heat and charge capacities to solve for the first derivatives

$$\begin{pmatrix} \dot{\mu}_\alpha \\ \dot{T}_\alpha \end{pmatrix} = \frac{1}{D_\alpha} \begin{pmatrix} 1 & 0 \\ -\frac{3}{\pi^2}\frac{\mu_\alpha}{T_\alpha} & \frac{3}{\pi^2}\frac{1}{T_\alpha} \end{pmatrix} \begin{pmatrix} -I_M^{(\alpha)} \\ -I_E^{(\alpha)} \end{pmatrix}\,. \tag{5.105}$$

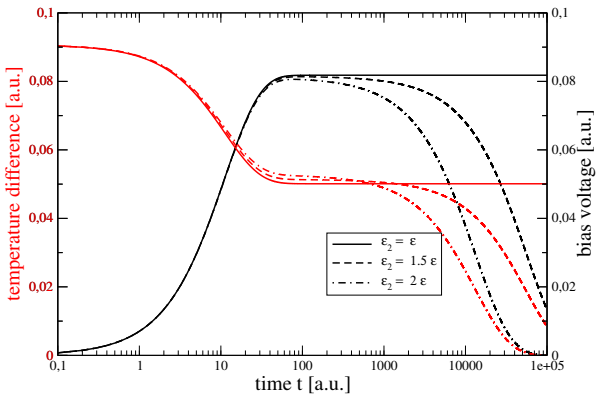

Figure 5.11: Temporal evolution of the bias voltage $V(t)$ (black) and the temperature difference $T_L - T_R$ (red) for different ratios of channel energies $\epsilon_2 = \alpha\epsilon = \epsilon_1$ (solid, dashed, and dash-dotted, respectively). After an initial evolution phase the system reaches a pseudo-equilibrium that is persistent only for $\epsilon_1 = \epsilon_2$ (solid curves). Whenever the channel energies are different, the pseudo-equilibrium eventually relaxes to thermal equilibrium. During the pseudo-equilibrium phase (intermediate plateaus), part of the initial temperature gradient has been converted into a voltage.

Although we have represented this using a matrix, we stress that the resulting ODE is highly nonlinear, since the currents may themselves depend in a highly nonlinear fashion on the reservoir temperature. Any reasonable two-terminal setup should realistically obey particle conservation $I_M^R + I_M^L = 0$ and also energy conservation $I_E^R + I_E^L = 0$. This will in general lead to conserved quantities respected by the system of coupled differential equations.

A useful example is the single-electron transistor that has been treated previously. Here, we have two reservoirs with temperatures T_L, T_R and chemical potentials μ_L and μ_R, respecively. When these are connected via a single quantum dot, the current (counting positive if directed from left to right) reads

$$J_M = \gamma \left[f_L(\epsilon) - f_R(\epsilon) \right] , \qquad J_E = \epsilon J_M , \tag{5.106}$$

where γ encodes details of the coupling strength to the respective reservoirs into a single factor and where ϵ was the on-site energy of the quantum dot. The so-called tight-coupling property $J_E = \epsilon J_M$ follows from the fact that a single quantum dot only has a single transition frequency ϵ. This can be compared with a more complicated structure, e.g. two quantum dots connecting the two reservoirs in parallel without direct interaction. Then, the currents have the structure

$$\begin{aligned} J_M &= \gamma_1 \left[f_L(\epsilon_1) - f_R(\epsilon_1) \right] + \gamma_2 \left[f_L(\epsilon_2) - f_R(\epsilon_2) \right] , \\ J_E &= \epsilon_1 \gamma_1 \left[f_L(\epsilon_1) - f_R(\epsilon_1) \right] + \epsilon_2 \gamma_2 \left[f_L(\epsilon_2) - f_R(\epsilon_2) \right] . \end{aligned} \tag{5.107}$$

These do not exhibit the tight-coupling property $J_E \neq \epsilon J_M$ – unless the ϵ_i are equal. Nevertheless, also here global equilibrium $\mu_L = \mu_R$ and $\beta_L = \beta_R$ will evidently lead to vanishing currents and therefore to fixed points. Now, by initializing the system e.g. with a temperature gradient in the absence of a charge gradient it is possible to generate (at least temporally) a voltage, i.e., to extract work. The temporal evolution of such a system is depicted in Fig. 5.11. It is visible that in the tight-coupling limit, it is possible to convert e.g. an initial temperature gradient into work (a persistent voltage). However, it should realistically be kept in mind that the tight-coupling property is never exactly fulfilled and relaxation into final equilibrium may thus be expected. Nevertheless, even these more realistic systems show a distinct timescale separation between initial charge separation and discharging of the system.